

LOS ALAMOS
SCIENTIFIC LABORATORY
OF THE UNIVERSITY OF CALIFORNIA
LOS ALAMOS, NEW MEXICO

CONTRACT W-7405-ENG.36 WITH THE
U.S. ATOMIC ENERGY COMMISSION

FOR REFERENCE

UNCLASSIFIED

NOT TO BE TAKEN FROM THIS ROOM

CAT. NO. 1935

LIBRARY BUREAU

LOS ALAMOS NATIONAL LABORATORY



3 9338 00191 3689

~~SECRET~~

UNCLASSIFIED

LOS ALAMOS SCIENTIFIC LABORATORY

of the

UNIVERSITY OF CALIFORNIA PUBLICLY RELEASABLE

Per *E.M. Johnson* FSS-16 Date: *6-18-85*

By *Marvin Bell* CIC-14 Date: *2-12-96*

Report written:
May 1954

Classification changed to UNCLASSIFIED
by authority of the U. S. Atomic Energy Commission,

Per *C. S. Marshall* 9-1-60

By REPORT LIBRARY *V. Marting*

LA-1664

This document consists of 140 pages,
~~SECRET~~ of 50 copies, Series A.

HEIGHT OF BURST FOR ATOMIC BOMBS, 1954

PART I. THE FREE AIR CURVE
This material contains information affecting
the national defense of the United States
within the meaning of the Espionage Laws,
Title 18, U.S.C., Sections 793 and 794,
and the transmission or revelation of
information in any manner to an unauthorized person is pro-
hibited by law.

by
F. B. Porzel

~~SECRET~~
authorities 2-14-59
C. S. Marshall
BY REPORT LIBRARY 2-14-59

LOS ALAMOS NATL LAB LIBS
3 9338 00191 3689

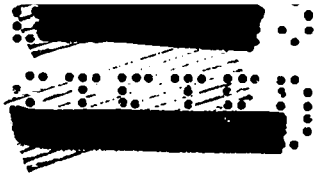
~~SECRET~~
Marvin Bell

~~SECRET~~

~~SECRET~~

~~SECRET~~

UNCLASSIFIED



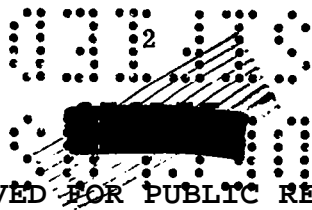
UNCLASSIFIED

Report distributed: JUN 29 1955

AEC Classified Technical Library
University of California Radiation Laboratory, Livermore
Los Alamos Report Library

LA-1664

1-7
8
9-50



UNCLASSIFIED

UNCLASSIFIED

ABSTRACT

This paper is issued in two volumes: LA-1664 and LA-1665.

In LA-1664, the fundamental properties of a shock in free air are described, including the reasons for failure of similarity scaling. The results of an analytic solution for strong shocks are presented, which permit a determination of the energy in a shock wave from its rate of growth without recourse to similarity assumptions; from it the scaling laws for both homogeneous and inhomogeneous atmospheres are explicitly shown. The total energy is evaluated in a machine calculation for the blast wave and from this evaluation, the free air wave form for all hydrodynamic variables is presented. The general nature of the laws governing thermal radiation from atomic bombs is deduced, a new figure of merit for thermal radiation is suggested to replace the concepts of "thermal energy" and "critical calories," which are considered ambiguous. Partition of energy is considered negligible in most cases of interest; the waste heat concept is reconsidered and the failures of scaling to TNT are regarded primarily as a failure of the ideal gas law.

LA-1665 is concerned with preparation of height of burst curves. In the reflection process over ideal surfaces, the usual subdivision into regions of regular and Mach reflection is considered inadequate, and the reflection process is subdivided into five zones: regular reflection, transition reflection, low stem height Mach reflection, high stem height Mach reflection, and hemispherical reflection. On the basis of these concepts, the reflected static pressures and dynamic pressures are deduced as a function of free air pressure and angle of incidence, from which the height of burst curve applicable to an ideal surface is deduced and drawn.

A theory of surface effects is postulated in two parts for reduction in peak pressure over real surfaces. The first is categorized as mechanical effects, which include dust loading, surface viscosity and roughness, turbulence, flow effects, shielding, and ground shock. Based on these concepts, the height of burst curves which are applicable in the presence of mechanical effects are deduced. The category of thermal effect is postulated in two parts: the radiation from a bomb is sufficiently strong and violent so that the ground surface may literally blow up prior to shock arrival

UNCLASSIFIED


011
0110

UNCLASSIFIED

but at least creates a layer of dust or smoke-laden air near the surface in which subsequent radiation is absorbed, thus forming a layer of hot air near the surface. The second part of the postulate is that once such a layer is formed, the hydrodynamics of the wave entering it are violently altered by mechanisms described as strong precursor action and weak precursor action. Based on these concepts, the thermal height of burst curves are drawn for 1 kt and shown to be appropriate over a fair range of scaling.

0114
0110

UNCLASSIFIED


 3170

UNCLASSIFIED

AUTHOR'S NOTE


The present paper suffers from a number of deficiencies which the author wishes to acknowledge. These are due, in part, to a lack of time for preparation because the author is presently transferring from the Los Alamos Scientific Laboratory.

In some respects the paper is too long. Many of its sections are more appropriately parts of separate papers. For emphasis, it is usually worthwhile to present only one new theory for a method of approach in a single paper; the present paper probably contains too many.

No library search has been made to check whether the material in the present paper has been published previously. The author wishes to apologize if any such oversights have been made, because they are certainly unintentional. He has tried to exercise extreme care in what is considered common knowledge and in acknowledging the source of information when it has come from someone else.

Much of the discussion is sketchy and should be carried to logical completion. Even in its present length only the principal results for many of the derivations are given. If time and opportunity permit, the author intends to carry these projects to their logical completion, but it would require at least a man year of work, and could appropriately be parts of a dozen or more papers.

The author has had the benefit of excellent editing by members of his own group at Los Alamos, and by Bergen R. Suydam of the Los Alamos Scientific Laboratory, but it is recognized that many parts could be rewritten. Despite the deficiencies of the paper, it is being issued at the present time with the hope that the methods it suggests and the approach to the problems may furnish sufficient "food for thought" to offset its deficiencies.

0115

 3170

UNCLASSIFIED



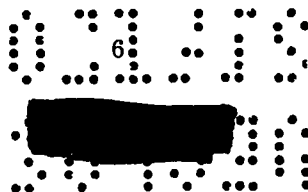
UNCLASSIFIED

ACKNOWLEDGMENT

The author wishes to thank the Commanding General and other members of AFSWP, Sandia Base, for their cooperation in the preparation of the work. In particular, Commander Carl A. Schweikert, USN, Major Thomas Carew, USA, Captain Robert E. Babb, USAF, and Lieutenant Graham D. Stewart, USN, participated directly in the preparation of the derived curves from the IBM Run.

The author wishes also to thank Major General Stanley Mikkelsen, Commanding General, and Colonel Jesse F. Thomas, Chief of Weapons Division, both of Ft. Bliss, Texas for their encouragement. In particular, Lt. Colonel Raymond I. Schnittke, USA, and Corporal Joseph Bukowski spent several weeks at Los Alamos assisting directly with the preparation of the thermal height of burst curves.

The author wishes to acknowledge the assistance and many useful comments in discussions with Bergen R. Suydam of Los Alamos Scientific Laboratory, who was also kind enough to read and comment on parts of this paper.



UNCLASSIFIED

SECRET

UNCLASSIFIED



CONTENTS

PART I. THE FREE-AIR CURVE

	Page
ABSTRACT	3
AUTHOR'S NOTE	5
ACKNOWLEDGMENT	6
DEFINITIONS	10
SYMBOLS.	17
FUNDAMENTAL LAWS	21
CHAPTER 1 INTRODUCTION	24
1.1 Purpose	24
1.2 History of the Problem	25
1.3 Present Approach to the Problem	26
CHAPTER 2 THE SHOCK WAVE FROM A NUCLEAR EXPLOSION IN FREE AIR	27
2.1 Definitions and Basic Principles	27
2.1.1 Statement of Problem	27
2.1.2 Shock Process—Rankine-Hugoniot Equations	28
2.1.3 Hydrodynamic Relationships on the Interior of a Shock Wave	35
2.1.4 Entropy Change Across the Shock Front	37
2.1.5 Similarity Solutions for Strong Shocks	38
2.2 Analytic Solution for Strong Shock	41
2.2.1 Definition of the Hydrodynamic Kiloton	42
2.2.2 Variable Gamma Theory.	43
2.2.3 Wave Forms Behind the Shock Front	44
2.2.4 Energy Expression for the Shock Wave	47
2.2.5 Scaling Laws	50
2.3 IBM Machine Calculation of the Blast Wave	56
2.3.1 Original Derivation	56
2.3.2 Energy Integration of IBM Run	57
2.3.3 Analytic Solution on the IBM Run	59

SECRET

UNCLASSIFIED



 CONTENTS (continued)

UNCLASSIFIED

	Page
2.4 Derived Curves for Free Air	61
2.4.1 Variables at the Shock Front	61
2.4.2 Hydrodynamic Variables on the Interior of a Wave	63
2.5 Thermal Radiation	65
2.5.1 Total Thermal Energy of the Bomb	65
2.5.2 Black Body Model for Thermal Radiation	70
2.5.3 Radiation in Depth	71
2.5.4 Absorption External to Sphere of Effective Radiation	75
2.5.5 Effective Thermal Radiation from Space and Time Dependence	83
2.5.6 Scaling Laws for Thermal Radiation	88
2.6 Efficiency of a Nuclear Explosion	90
2.6.1 Waste Heat Concept	90
2.6.2 Efficiency with Respect to TNT	91
2.6.3 Partition of Energy	92
2.7 The Shock Front in Free Air	94
2.7.1 Proofs for the Existence of a Sharp Shock	94
2.7.2 Possible Perturbation to Sharp Shocks	96
APPENDIX A. SHOCK CONDITIONS FOR 1 KT IN FREE AIR	122

PART II. THEORY OF SURFACE EFFECTS (LA-1665)



TABLE

Table I. Some Results from the Analytic Solution Applied to IBM Problem M	60
---	----

LIST OF ILLUSTRATIONS

CHAPTER 2 THE SHOCK WAVE FROM A NUCLEAR EXPLOSION IN FREE AIR

2.1.2a The Process of a "Shocking Up"	98
2.1.2b Definitions for Deriving the Rankine-Hugoniot Equations	99
2.1.3-1 The Unit Volume for Differential Conservation of Mass	100
2.1.3-2 The r-t Plot for a Shock	101
2.2.2-1 Thermodynamic Properties of Air Along the Hugoniot	102
2.2.2-2 Thermodynamic Properties of Air Showing the Hugoniot and Its Branches	103
2.2.2-3 Thermodynamic Properties of Air Showing the Hugoniot and Its Branches	104
2.2.2-4 Thermodynamic Properties of Air Showing the Hugoniot and Its Branches	105
2.2.5-1 Illustrates the Cross-over Point Where Changes in the Equation of State Compensate for Changes in (W/P_0) Scaling	106
2.2.5-2 Lateral Feeding of Energy Near Shock Front	107
2.2.5-3 Growth of a Shock Front in an Inhomogeneous Medium	108
2.4.1-1 Free Air Peak Overpressure vs Distance	109
2.4.1-2 Peak Pressure Efficiency IBM at 11.5 kt Compared with Kirkwood- Brinkley at 1 kt	110

UNCLASSIFIED

SECRET

UNCLASSIFIED

SECRET


LIST OF ILLUSTRATIONS (continued)

	Page
2.4.2-1 Isobars in Space-time	111
2.4.2-2 Particle Position in Space-time	112
2.4.2-3 Density in Space-time	113
2.4.2-4 Material Velocity in Space-time	114
2.4.2-5 Dynamic Pressure in Space-time	115
2.5.1-1 Thermal Radiation Function vs Time	116
2.5.3-1 Qualitative Presentation of Thermal Yield vs Total Yield	117
2.5.3-2 Absorption Coefficient of Air vs Wave Length	118
2.5.4-1 Cloud Chamber Effect on Total Thermal Radiation for Various Humidities	119
2.5.5-1 Residual Heat from Space Dependence $R^2 \Delta T$ vs R	120
2.5.5-2 Dependence of the Thermal Pulse Shape on Yield	121

SECRET

SECRET

UNCLASSIFIED


 3:10:00

UNCLASSIFIED

1. DEFINITIONS

A partial list of definitions used in this paper is given below, arranged according to subject headings. Those definitions which deal with the origin of thermal radiation in the bomb are included under the heading of "Free Air"; those dealing with the effects of thermal radiation are under the heading of "Thermal Effects."

DAMAGE CRITERIA

Dynamic Pressure: The quantity $\frac{\rho u^2}{2}$; it has the dimensions of pressure.

Peak Overpressure: The maximum value of pressure above ambient behind the shock wave, in the absence of isolated, locally reflecting surfaces.

Peak Pressure Damage Level: The damage occurring from a blast wave specified by the peak overpressure of a free air wave form. It includes the contribution to damage from dynamic pressures, the thermal shock or precursor action. It applies to objects in which the damage is not seriously affected by the duration of the wave.


Total Pressure Head: The sum of the peak static overpressure plus the dynamic pressure behind the shock. As used in this paper, the total pressure head characterizes the peak pressure damage level, but the peak pressure damage level is labeled by the peak static pressure alone.

FREE AIR

Absolute Yield: An energy release determined without reference to scaling from other bombs.

Analytic Solution: The evaluation of the total hydrodynamic yield as derived by the author from a measurement of the growth of the shock front, including the first and second derivatives of radius with respect to time, on an absolute basis, without the assumptions of similarity scaling.

Breakaway: The time during which the shock front ceases to be luminescent and becomes detached from the fireball. This time marks the division between early and late fireball. It is close in time, but not necessarily identical with the light minimum.

10

 3:10:00

UNCLASSIFIED

UNCLASSIFIED

Early Fireball: That period of the growth of a nuclear explosion during which the shock front is luminescent, and identified with the fireball on a photographic plate.

Effective Thermal Radiation: The thermal energy radiated from a bomb up to some arbitrary time when it is no longer effective in raising the temperature of irradiated objects. This term is to be distinguished from the term "Thermal Yield," which is considered ambiguous.

Free Air Pressure: The pressures achieved by an explosion burst in the absence of any large reflecting medium. This is to be distinguished from "Free Stream" pressures.

Free Steam Pressures: The pressures locally achieved by an explosion which may be burst over a large reflecting medium such as the earth's surface, but in the absence of a locally reflecting structure. It is used to compare the enhancement of pressure of the local structure with the pressure in the absence of this structure.

Hydrodynamic Invariants: These are derived ratios of the state variables in dimensionless form which can be held constant in comparing explosions in different media, or yields. One self-consistent scheme comprises

Pressure	P/P_0
Density	ρ/ρ_0
Shock Velocity	U/c_0
Material Velocity	u/c_0
Sound Velocity	c/c_0
Temperature	T/T_0

Hydrodynamic Kiloton: $\left(\frac{4\pi}{3}\right) \times 10^{18}$ ergs, or approximately 10^{12} calories.

Hydrodynamic Transport Velocity: The sum of local material velocity plus local sound velocity, which gives the velocity of a signal in a moving fluid.

Hydrodynamic Variables: These refer to quantities like pressure, density, temperature, material velocity, sound velocity, entropy, or other quantities which describe the condition of a moving fluid.

Hydrodynamic Yield: The integrated total of internal and kinetic energy per unit volume on the interior of the shock. In part, this concept is intended to replace the concept of blast efficiency, which is considered ambiguous. The hydrodynamic yield is practically 100% of the total energy release, when measured prior to breakaway.

Ideal Gas Law: The approximation that the equation of state of a gas may be represented by $PV/T = \text{constant}$.

UNCLASSIFIED

UNCLASSIFIED

Inhomogeneity Effects: The perturbation of a blast wave which is propagating in non-uniform air as a result of the local lapse rate of temperature and pressure with altitude. It includes refraction effects as well as differences in scaling because of the local ambient conditions.

Late Fireball: That period of the growth of a nuclear explosion in which the shock front is too cool to be luminescent, and the visible fireball is well within the shock front.

Light Minimum: The time near breakaway at which the radiation rate from the fireball reaches a minimum value; it does not necessarily exist on all bombs.

Mass Effect: The perturbation on the growth of a shock front and the wave form behind it due to the finite mass of bomb parts or adjacent materials other than air.

Partition of Energy: The division of nuclear energy from the bomb, from energy released prior to breakaway, which is not later involved in a conversion from hydrodynamic to thermal energy or vice versa. For most bombs fired near the earth's surface, this involves only a small fraction of the nuclear yield, less than 1%, which escapes the fireball to large distances prior to breakaway. By custom, neither the analytic solution nor the radiochemical yield includes the energy from fission decay products or neutrons after breakaway. The definition here is to be carefully distinguished from the usual concept of "partition of energy" which represents the situation as if the blast yield, thermal yield, and residual nuclear radiation were supposed to total 100% of the "total" yield.

Radiative Phase: The very early period of fireball growth in which the energy at the edge of the fireball is transmitted by radiative transport instead of hydrodynamic transport as in shocks.

Radiative Transport: The mechanism by which energy is transferred by photons. It is distinguished from hydrodynamic transport of energy associated with material and sound velocities.

Refraction: The mechanism by which acoustic signals travel along curved paths because of the variation in sound velocity in the medium.

Second Maximum: The time during the late fireball stage at which the thermal radiation rate from the fireball reaches a maximum value. It does not necessarily exist on all bombs.

Shock Front Yield: A yield which is based on comparison by similarity scaling from conditions at the shock front alone. It is to be distinguished from the analytic solution which, in principle, determines conditions on the interior from the growth of the shock front, without assuming similarity of wave forms on the interior.

Similarity Scaling: The assumption that the hydrodynamic variables can be expressed in dimensionless units in such a way that in a comparison between bombs of two different yields, the same

0112
 0112

UNCLASSIFIED

UNCLASSIFIED

values of hydrodynamic invariants will occur at distances which are proportional to $(W/P_0)^{1/3}$ and at times proportional to $1/c_0 (W/P_0)^{1/3}$.

Space Time Invariants: These are derived ratios of space and time which are held constant in the scaling process to compare different explosions in different media. One self-consistent scheme states that the same values of hydrodynamic invariants are achieved at the same values of

$$\begin{aligned} \text{space:} & \quad R (P_0/W)^{1/3} \\ \text{time:} & \quad t c_0 (P_0/W)^{1/3} \end{aligned}$$

Strong Shock: A shock in which all points behind the shock front satisfy the condition that the hydrodynamic transport velocity is greater than the shock velocity, i.e., $u + c > U$. This concept replaces the condition sometimes demanded that $\xi \gg 1$. As defined herein, the strong shock region extends down to approximately 3 atmospheres peak overpressure.

Taylor Similarity: The condition that, for sufficiently strong shocks, the shock pressure is inversely proportional to the cube of the distance. The assumptions leading to this solution are not made in this paper because the result is shown to be only an approximation.

Total Thermal Energy: The energy represented by air at temperatures above ambient left behind the shock after a long time. The temperatures are due to irreversible changes occurring when the shock passes over the air, and due to departures from the ideal gas law. This term is to be distinguished from "thermal yield," which is considered ambiguous. At a very late stage the total thermal energy is nearly 100% of the total energy release.

Variable Gamma Theory: The system of hydrodynamics based on the fundamental definition of gamma as $E_m = PV/\gamma - 1$, where E_m is the internal energy per unit mass, P is the absolute pressure, and V is the specific volume.

Weak Shock: A shock in which some point behind the shock front has a hydrodynamic transport velocity which is less than the shock velocity, i.e., $u + c < U$.

IDEAL SURFACES

Hemispherical Reflection: The late phase in the reflection process when the Mach stem is effectively closed so that the wave forms at or near the surface can be described by free air wave forms with a reflection factor which is constant in space and time.

High Stem Height - Mach Reflection: The phase in the reflection process following low stem height Mach reflection, in which the Mach stem rises rapidly. The boundary between low stem height and high stem height Mach reflection is somewhat arbitrary. High stem height Mach reflection represents the transition between earlier phases of the reflection process in which the peak

0113
0113

UNCLASSIFIED

UNCLASSIFIED

pressure and wave forms are strongly controlled by conditions at or near the shock front, and the late phase when the stem approaches a hemisphere.

Ideal Surface: A smooth, rigid, thermally reflecting surface. In practice, it means any surface approximated by these conditions such as water, in which the thermal and mechanical effects, as defined later, are small.

Low Stem Height -Mach Reflection: The early phase of Mach reflection following transition reflection in which the growth of the Mach stem is slow, and the triple point path remains essentially parallel to the ground.

Pressure Multiplication: The ratio of the reflected pressure to the free air pressure at the same distance and angle from the bomb. It is to be distinguished from the reflection factor.

Principle of Least Possible Pressures: The assumption in this paper that in a shock process, the shock front and wave forms will always achieve that configuration which requires the least pressure out of all possible configurations which can satisfy the boundary conditions.

$P_R - \theta$ Plot: A graph which specifies the relationship between reflected pressures, incident pressures, and angles of incidence, based on the fundamental assumption in this and in earlier papers that the reflected pressure is a function only of the incident pressure and the angle of incidence, if the yield and the type of surface are held constant.

Reflection Factor: The ratio of the yield required to obtain the same pressure in free air at the same distance as the reflected pressure obtained from the enhancement due to the reflection process itself. The reflection factor of 2 applies only during hemispherical reflection. At other times, the reflection factor may vary from 2 to 8 or, in complex situations, go as high as 27. The reflection factor is uniquely related to the pressure multiplication but usually has a different numerical value.

Regular Reflection: The phase of the reflection process in which the incident and reflected shocks intersect at the ground surface according to the theory by J. von Neumann. As used in this paper, regular reflection is restricted to that period in which the strength of the reflected shock and the reflected angle are uniquely determined by the conditions at the shock front without being affected by past history of the shock.

Sonic Line: The line of points in regular reflection on a $P_R - \theta$ plot where the sum of material and sound velocity behind the shock become equal to the velocity of the intersection of the reflected and incident waves along the ground. It is to be distinguished from the customary "end of regular reflection" where regular reflection solutions become imaginary. The sonic line occurs shortly before this time and in this paper it delineates the boundary between regular reflection and transition reflection.

0 1 1 4
 0 1 1 4
 0 1 1 4

UNCLASSIFIED

UNCLASSIFIED

Transition Reflection: The phase of the reflection process following regular reflection in which the incident and reflected shock intersect at the ground, but the reflected angle and reflected shock depend upon the past history of the shock, and cannot be uniquely determined from the incident shock strength and the incident angle alone.

MECHANICAL EFFECTS

Dust Loading: The addition of solids (dust, smoke, etc.) to the air, when their mass per unit volume is appreciable relative to the density of air.

Dust Loading Factor: The ratio of the solids per unit volume to the density of air in dust-laden air.

Flow Effects: The general category of pressure reduction due to the familiar Bernoulli effect.

Mechanical Surface: A real surface which is non-rigid, rough, and/or dusty but not productive of a thermal layer.

Surface Viscosity: The mechanism by which the material velocity near the ground is slowed in comparison with the velocities obtained over an ideal surface in a layer whose depth is of practical interest for damage. It is distinguished from the usual concept of gas viscosity which is a phenomenon of molecular dimension.

Turbulence: The phenomenon in which the flow behind the shock is violently perturbed in direction by the surface roughness, not in conformity with the flow pattern demanded by the reflection process over an ideal surface.

THERMAL EFFECTS

Conduction Coefficient: The value of the expression $\frac{a}{\sqrt{\pi h \rho \sigma}}$. It is a property of the surface composition in determining the surface temperature for a thick slab when exposed to thermal radiation. The product of the conduction coefficient and the thermal intensity give the surface temperature at a given time. It partially replaces the concept of a critical number of cal/cm², which is usually ambiguous in determining the effect of thermal radiation on materials.

Maximum Thermal Intensity: The maximum value of I (t). (See "Thermal Intensity").

Partial Shock: A wave form in which the initial rise is fairly sharp and is followed by a rounded-off peak due to the main shock; it characterizes weak precursor action.

Precursor: A marked change in outward curvature of a main shock as a result of strong or weak precursor action. In practice, it usually means the result of precursor action plus the thermal shock, if any, together with their mutual reinforcement.

0140 15
 0140 15

UNCLASSIFIED

UNCLASSIFIED

Rise Time: The period of time from the initial rise of the pressure to its maximum value behind the wave. In weak precursor action it is the interval between the time the shock front is rounded off and the time when it reaches its maximum. In strong precursor action, the rise time includes the entire time length of the precursor, plus whatever rounding occurs within the main wave.

Slow Rise: A wave form in which the pressure rises gradually from ambient; it characterizes strong precursor action.

Strong Precursor Action: The perturbation occurring in a shock wave in a region in which the ambient sound velocity at or near a surface exceeds the projection of the shock velocity on the ground. It is marked by a slow rise in pressure, separated by an appreciable distance in time and space from the main wave.

Thermal Blow-Up: The postulate in this paper that the thermal radiation from a bomb is sufficiently violent to generate a dust or smoke-laden layer of air near ground surface.

Thermal Intensity: An integral quantity which expresses the effect of the bomb in producing a rise in surface temperatures. It is defined by $I(t) = \int_0^t \left[\left(\frac{dQ}{dt} \right) d\tau \right] / \sqrt{\tau - t}$. It replaces the usual concept of thermal yield which is considered ambiguous for determination of surface temperatures.

Thermal Shock: A thermal blow-up of sufficient violence that a finite pressure pulse could be observed as a result of the impact of thermal radiation.

Thermal Surface: A real surface which absorbs thermal radiation from the bomb but might otherwise be smooth and rigid so that the mechanical effects would be at a minimum.

Thermal Threshold: The postulate in this paper that the surface blow-up may not occur until a critical temperature is reached. It usually means a temperature at which the surface begins to decompose in such a way as to give a marked rise in the volume of the decomposition products.

Weak Precursor Action: The perturbation in a shock wave which occurs in a thermal layer in which the sound velocity in the layer is above ambient but less than the shock velocity or its projection along the ground. It is marked by a partial shock front followed by a rounding off of the peak pressure spike.

UNCLASSIFIED

. . . : [REDACTED]
 . . . : [REDACTED]
 . . . : [REDACTED]

UNCLASSIFIED

ii. SYMBOLS

- a - The thermal absorptivity of a surface. In this paper it is meant to be the average over all wave lengths, and integrated over the normal components of all radiation within 90° of the normal to the surface.
- A - Sometimes used as the incident angle of a shot.
- b - Stefan-Boltzmann constant.
- B - Sometimes used as the reflected angle of a shock.
- c - Local sound velocity.
- P_0, ρ_0, T_0, c_0 - The quantities - pressure, density, temperature, and sound velocity, respectively, in the medium ahead of a shock.
- P^*, T^*, U^*, c_0^* , etc. - The superscript denotes the hydrodynamic variables in a thermal layer.
- P_B, ρ_B, c_B , etc. - The subscript refers to the peak value immediately behind the shock in an ideal wave form.
- C_p - Specific heat at constant pressure.
- C_v - Specific heat at constant volume.
- d - Thickness of a thermal layer.
- E_i - Internal energy.
- E_k - Kinetic energy.
- E_m - Internal energy per unit mass.
- E_v - Internal energy per unit volume.
- f - A general symbol reserved for an arbitrary function of several variables denoted as $f(x_1, x_2, \dots)$.
- g - The universal gravity constant.
- h - Specific heat.
- i - A running index.
- $I(t)$ - The thermal intensity (see definition).

. . . : 17 . . .
 . . . : [REDACTED]
 . . . : [REDACTED]

UNCLASSIFIED

UNCLASSIFIED

- k - The description of a parameter which describes the pressure behind a shock front of a strong shock in which $1 - k$ represents the ratio of the limiting value of the absolute pressure on the interior of the wave to the peak pressure at the shock front.
- m - The approximation that the path of the mass particles behind the shock front may be described in the form that $r \sim t^m$. It is rigorously defined by $m = \frac{d \ln r}{d \ln t}$.
- n - The coefficient which approximates the rate of growth of the shock coordinate R and the time t , as $R \sim t^n$. It is rigorously defined by $n = \frac{d \ln R}{d \ln t}$.
- P - An absolute pressure.
- P_D - Dynamic pressure = $\frac{1}{2} \rho u^2$.
- P_f - The peak overpressure behind an incident shock, or free air shock.
- P_m - The reflected peak overpressure over a mechanical surface.
- P_R - The reflected peak overpressure behind the shock, $P - P_0$.
- P_s - The subscript refers to the peak value immediately behind the shock in an ideal wave form.
- P_{th} - The reflected peak overpressure over a thermal surface.
- q - The coefficient in the power law which approximates the density distribution behind the strong shock: $\rho = \rho_s \left(\frac{r}{R} \right)^q$.
- $Q(t)$ - Total thermal radiation incident on a surface up to time t .
- Q_N - Arbitrary value of calories used to normalize the thermal intensity. It should not be confused with the total integrated cal/cm².
- r - The space coordinate of a particle behind the shock.
- R - The radius of a shock front.
- S - Entropy.
- t - Time.
- T - Temperature.
- T_c - Temperature of a surface, considering conduction process alone.
- T_0 - Temperature in the medium ahead of a shock.
- T_R - Temperature of a surface exposed to thermal radiation in which the phenomenon of re-radiation has been taken into account.
- u - Local material velocity.
- U - Shock velocity.
- U^* - Shock velocity in a thermal layer.
- V - Specific volume.

01110
18
01110

UNCLASSIFIED

UNCLASSIFIED

- V_0 - An ambient specific volume.
- V_f - The specific volume of a gram of air initially shocked, but now returned to ambient pressure.
- V_s - The specific volume directly behind the shock.
- W - Hydrodynamic yield.
- Y - Thermal yield.

GREEK SYMBOLS

- α - Sometimes used as an angle of incidence; corresponds to θ or A .
- γ - Defined here by $E_m = PV/(\gamma - 1)$; to be distinguished from the customary definition of $\gamma = C_p/C_v$.
- Δ - General function denoting an increment.
- ϵ - $1/(\gamma - 1)$.
- ϵ_0 - $1/(\gamma_0 - 1) = 2.5$.
- $\bar{\epsilon}$ - The average value of ϵ on the interior of a shock wave, defined by

$$\bar{\epsilon} = \frac{\int_{\text{volume}} \left[\frac{P}{(\gamma - 1)} \right] dV}{\int_{\text{volume}} PdV}$$

- η - The density ratio across the shock, given by ρ/ρ_0 .
- θ - The angle between an incident shock and the ground.
- θ' - The angle between a reflected shock and the ground.
- λ - Absorption coefficient for thermal radiation. In this paper it means the average overall wave lengths.
- μ - $\frac{\gamma + 1}{\gamma - 1}$.
- ν - A frequency, usually of light.
- ξ - The ratio of absolute pressure to the ambient pressure just in front of the shock, i.e., P/P_0 .
- ξ_s - The ratio of absolute pressures at the shock front.
- ξ' - The pressure ratio across the reflected shock.
- ξ_1 - The incident shock pressure ratio.
- ξ_2 - The pressure ratio across the reflected shock.

01110
19
00000

UNCLASSIFIED

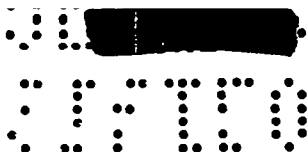
0110
0110

UNCLASSIFIED

- ρ - Density.
- ρ_0 - Density in the medium ahead of a shock.
- ρ_s - Density at the shock front.
- σ - Thermal conductivity.
- τ - A dummy variable for time.
- $\phi(t)$ - The normalized value of $I(t)$.
- ψ^5 - Equals $\frac{R^5}{t^2}$.
- dQ/dt - The rate of energy transport due to thermal radiation. In practice it refers to the average value from the normal component of all angles of incidence integrated over the entire spectrum of wave lengths.

0110²⁰
0110

UNCLASSIFIED



UNCLASSIFIED

iii. FUNDAMENTAL LAWS

This paper is based on the development of certain well known physical laws which are part of the standard literature. The symbols are defined in the previous section.

Adiabatic Law: A result of the principle of conservation of energy from the first law of thermodynamics. When gamma is constant it can be expressed in the form:

$$P = \rho^\gamma \text{ const.}$$

Continuity of Mass: A fundamental law of hydrodynamics which demands that there be no source or sink of mass within the blast wave. It is given by the condition that:

$$\frac{\partial \rho}{\partial t} + \text{div} (\rho u) = 0$$

For a plane wave this reduces to:

$$u \frac{\partial \rho}{\partial r} + \frac{\partial \rho}{\partial t} + \rho \frac{\partial u}{\partial r} = 0$$

Conservation of Momentum: A fundamental law of hydrodynamics which is essentially the expression of Newton's law:

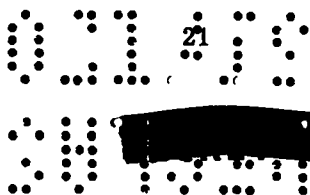
$$\text{Grad } P + \frac{1}{\rho} \left(\frac{d u}{d t} \right) = 0$$

Conservation of Energy: A fundamental law of hydrodynamics which demands that there be no source or sink of energy within the blast wave at the time it is considered. In its most simple form, it is given by the first law of thermodynamics:

$$dq = dE_i + PdV$$

In practice, it is expressed by the condition that:

$$u \frac{\partial S}{\partial r} + \frac{\partial S}{\partial t} = 0$$



UNCLASSIFIED

UNCLASSIFIED

Conservation of Mass - Rankine-Hugoniot Condition: A special form of the continuity of mass which demands that across a shock moving into still air

$$\rho_0 U = \rho(U - u)$$

Conservation of Momentum - Rankine-Hugoniot Condition: A derived law which demands that across a shock moving into still air

$$(P - P_0) = \rho_0 u U$$

Conservation of Energy - Rankine-Hugoniot Condition: A special case of the conservation of energy which demands that across a shock:

$$\frac{1}{2} (P + P_0)(V_0 - V) = \frac{PV}{(\gamma - 1)} - \frac{P_0 V_0}{(\gamma_0 - 1)}$$

Conduction or Diffusion Equation: The general law that the space-time variation of temperature within a substance is given by:

$$K \nabla^2 T + \frac{\partial T}{\partial t} = 0$$

For a thick slab of infinite extent in which the depth into the surface is expressed by x, this law reduces to:

$$K \frac{\partial^2 T}{\partial x^2} + \frac{\partial T}{\partial t} = 0$$

Inverse R²-cosine Law: A law which expresses the thermal intensity from a point source as

$$Q(R) \sim (\cos \theta / R^2) e^{-\text{constant time } R}$$

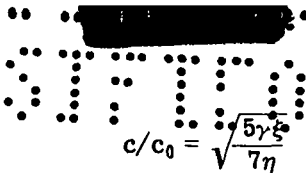
The Rankine-Hugoniot conditions across the shock uniquely determine the relationship between the peak hydrodynamic variables behind the shock when specified by one of the hydrodynamic variables. These relationships are exceedingly useful and for convenience are tabulated as follows:

Density Compression Ratio: $\eta = \frac{\mu \xi + 1}{\xi + 6}$

Shock Velocity: $U/c_0 = \sqrt{\frac{5(\mu \xi + 1)(\xi - 1)}{7[\xi(\mu - 1) - 5]}}$

Material Velocity: $u/c_0 = \sqrt{\frac{5(\xi - 1)[\xi(\mu - 1) - 5]}{7(\mu \xi + 1)}}$

UNCLASSIFIED



UNCLASSIFIED

Sound Velocity:

$$c/c_0 = \sqrt{\frac{5\gamma\xi}{7\eta}}$$

Temperature:

$$T/T_0 = \frac{5\gamma\xi}{7\eta}$$

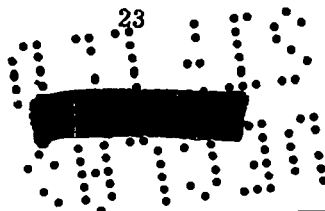
Excess Energy per Unit

Volume at Shock:

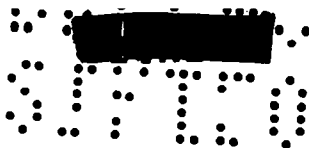
$$E_v = P_s[(V_0/V) - 1] = P_0\xi(\eta - 1)$$

Stefan-Boltzmann Law: Law giving the rate of radiation from a black body as

$$dQ/dt = bT^4$$



UNCLASSIFIED



UNCLASSIFIED

Chapter 1

INTRODUCTION

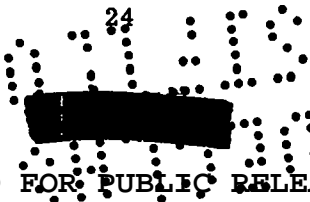
1.1 PURPOSE

The primary purpose of this paper is to provide, as a function of height of burst and horizontal distance, reasonable estimates for the pattern of static and dynamic pressures achieved from a nuclear explosion burst over both ideal and real surfaces.

The paper has a number of secondary purposes. The first of these is broad: to define the problems connected with height of burst for atomic bombs, and to suggest methods for their solution by actually carrying the problem from fundamental principles through reasonable completion.

Another purpose is to suggest a number of new theories. A principal one is the theory of surface effects, which refers to the reduction in peak pressure due to effects over real surfaces, categorized as "mechanical" and "thermal" effects. To define the free air curve results of an analytic solution for strong shocks is presented. The problem of thermal radiation from an atomic bomb is considered in some detail and this suggests marked revisions of previous concepts. The reflection process over ideal surfaces is described in a different fashion. Finally, certain phenomena associated with nuclear explosions are explained. These studies are by no means complete, but at least show separate parts of the whole problem.

From the point of view of security classification, a requirement seems to exist for a study to delineate between the types of information which must be considered as Restricted Data, and the type which can be considered common knowledge, since they can be readily deduced from fundamental principles. Another secondary purpose of this paper is to show the great extent to which the phenomenology from nuclear explosions may be deduced in quantitative detail without recourse to Restricted Data, and the extent to which information affecting the security of the United States may be deduced from apparently trivial scattered information concerning actual tests.



UNCLASSIFIED

UNCLASSIFIED

In order to provide reasonably reliable data for purposes of Civil Defense, it is clear that Restricted Data from real bombs should not generally be released. This paper provides data entirely from non-classified sources. It is the author's hope that the paper will satisfy a need for fairly realistic, but unclassified material.

1.2 HISTORY OF THE PROBLEM

During World War II, and even prior to the development of the atomic bomb, an immense amount of work had been done on blast from small charges by many investigators. J. von Neumann¹ pointed out the fundamental fact that the peak pressure could be enhanced by raising the height of burst, and he provided the theory of regular reflection to describe part of the process. Calculations for regular reflection were carried out in detail by Polachek and Seeger.² Taub³ and Smith⁴ correlated the theory of regular reflection with results from small-charge and shock-tube tests, and investigated Mach reflection to provide the pattern of reflected pressures on the ground from small charges over an ideal surface. Pertinent data were also obtained by Halvorsen⁵ and Kennedy⁶ in the region above the ground and over different surfaces.

Many of these results are contained in Summary Technical Report, OSRD-Div. 2. During the past few years, Bleakney has made fundamental contributions; he provided perhaps the first satisfactory empirical free-air curve for small charges; and later conducted a large number of shock-tube studies which are basic to the understanding of blast phenomena.

This paper is an extension and revision of a number of previous papers by the author, dating from 1949, and many of the contents have been hitherto unpublished. Very active work on the theory of surface effects was pursued by the author from the summer of 1951 through the summer and fall of 1952. At that time policy changes at the Los Alamos Scientific Laboratory no longer permitted primary interest in this field, and since then the work has proceeded on a part-time basis. The principal parts of the theory of surface effects date from the summer of 1951. The theory of variable gamma and the analytic solution date from 1950; the detailed use of the analytic solution and application to IBM problem M was done during the fall of 1952 and up to the spring of 1953. The theory concerning thermal radiation was done principally during the same period, although parts of it in its present definite form were done as late as the fall of 1953.

This paper is a logical extension of a previous paper, LA-1406, "Height of Burst for Atomic Bombs," which was completed in March 1952 but was issued only recently. An author's note in that paper contains a comparison with the present paper.

UNCLASSIFIED

UNCLASSIFIED



1.3 PRESENT APPROACH TO THE PROBLEM

The present paper may be considered entirely theoretical, and the reason deserves some amplification. No use is made nor reference given to either full-scale or small-charge tests in the preparation of the theory and results for this paper. IBM problem M supplies the bulk of the details for the free air wave forms but this was deduced from straightforward hydrodynamic principles.

The reason for the theoretical approach is partly for security reasons as mentioned above, but there is a stronger reason in that it divorces the results from subsequent changes and revisions in the data as they occur. The theoretical approach has a number of other advantages. If one professes to know and understand the phenomena, it ought to be possible to carry it through completion without recourse to data, and the theoretical approach is useful in forcing one to define all the problems which exist. Understanding is also clearer if no recourse is made to the semi-empirical approach of pegging the theory to the data; once empirical data are used, it becomes extremely difficult to separate the rightness or wrongness of the data from the rightness or wrongness of the theory. The theory describes the rules which ought to apply in all cases, especially the ability to extrapolate to new situations. One does not ask if the data fit the theory, but, fully expecting that the data will depart from the theory, he finds the most interesting aspect to be the magnitude of the discrepancies which do occur, because their magnitude then furnishes fruitful suggestions for further work.

REFERENCES

1. J. von Neumann, "Oblique Reflection of Shocks," AM-251, Explosives Research Report No. 12, Navy Department, Washington, D. C.
2. H. Polachek and R. J. Seeger, "Regular Reflection of Shocks in Ideal Gases," February 12, 1944, Explosives Res. Report No. 13, Navy Department, Bu. Ord., Washington, D. C.
3. A. H. Taub, "Peak Pressure Dependence on Height of Detonation," NDRC Div. 2 Interim Report No. 1, OSRC-A-4076. See also OSRC-6660.
4. L. G. Smith, "The Reflection of Shock Waves in Air," Air and Earth Shock, Interim Report No. 1, August 1944, NDRC, Div. 2, OSRC-4076.
5. R. R. Halvorsen, "The Effect of Air Burst on the Blast from Bombs and Charges. II. Analysis of Experimental Results," OSRD-4899.
6. W. D. Kennedy, "The Effect of Air Burst on the Blast from Bomb and Small Charges. I. Experimental Results," OSRD-4246, September 1944.

UNCLASSIFIED

UNCLASSIFIED

UNCLASSIFIED

Chapter 2

THE SHOCK WAVE FROM A NUCLEAR EXPLOSION IN FREE AIR

2.1 DEFINITIONS AND BASIC PRINCIPLES

2.1.1 Statement of Problem.

The purpose of this chapter is to derive and describe the nature of a shock wave from a nuclear explosion in free air using only well known principles of classical physics.

The derivation is independent of either small-charge tests or tests on nuclear explosions. It is a fair statement that considerably more is known about the fundamental behavior of nuclear explosions than about TNT explosions. While comparisons with TNT are useful, they are often misleading, if not treacherous, and it is no exaggeration that such comparisons have probably done more harm than good in the attempt to understand nuclear explosions during the past few years. Insofar as it appears possible to do so, probably the best procedure is to describe the nuclear explosion on its own merits without besetting the problem with the vastly more complex phenomenology of a TNT explosion.

By "free air" is meant the description of a spherically symmetrical explosion in the absence of any large reflecting surface. The term is not to be confused with the term "free stream pressures," which is usually used to mean the pressures in a blast wave without the presence of a locally reflecting surface such as a structure, as distinguished from the locally reflected pressures near such a structure.

The description and specification of the free air curve is a prerequisite to a discussion of further problems. It is the basic framework upon which rest

- (1) The reflection pattern on the ground
- (2) Scaling of bombs to different energies and atmospheres
- (3) Thermal radiation from the bomb

UNCLASSIFIED

UNCLASSIFIED

UNCLASSIFIED

2.1.2 Shock Process - Rankine-Hugoniot Equations.

The steep shock front in the conventional picture of a shock wave intrinsically follows from the thermodynamic properties of air. Later portions of this paper will deal with the reasons why a slow rise is obtained instead, and it is useful to consider first the strong requirement for a sharp shock in an ideal situation.

The process of "shocking up" has been adequately described by various authors, but the following exposition may be satisfactory. Consider an arbitrary pressure disturbance moving to the right as shown by the left hand full line in Fig. 2.1.2a. The conditions to the right of this pressure disturbance are a pressure, P_0 , and an ambient sound velocity, c_0 . Conditions to the left of the disturbance are specified by the variables, P , c , and u , each regarded as a function of space and time. By definition, sound velocity is given by

$$c = \sqrt{\left(\frac{\partial P}{\partial \rho}\right)_S}$$

where the subscript S denotes that the entropy is held constant, and usually one speaks of this as an adiabatic change of state. A fundamental property of nearly all materials, and air in particular, is that the quantity $\partial P/\partial \rho$ increases with pressure, which is simply the observation that it becomes increasingly difficult to compress materials the more they are compressed. The sound velocity is therefore an increasing function with pressure. In the pressure disturbance of Fig. 2.1.2a, we may regard the pressure wave as composed of pressure signals of infinitesimal amplitudes dP propagating in the field of pressure P as shown in the figure. During the next instant of time the pressure signals at high pressures will be propagated forward with greater local sound velocity, c , and hence over greater distances, than the low pressure signals will be carried. The wave form is steepened as the pressure front moves to the right, as indicated by the dashed line A in the figure.

Superimposed on this process is another which contributes to the steepening. A small volume of air in the pressure field is subject to a pressure gradient, specified as $\partial P/\partial r$ which, by Newton's law, will accelerate the air to the right and impart material velocity to it, according to

$$\partial P/\partial r = - (1/\rho) du/dt$$

The velocity of air particles to the right increases as long as the gradient is negative (as shown) and the longer the time; that is

$$u = \int \left(\frac{du}{dt}\right) dt$$

UNCLASSIFIED

UNCLASSIFIED

Sound signals from within the medium are propagated forward with the velocity, $u + c$, which we call the hydrodynamic transport velocity. The added component of material velocity, u , again contributes to the steepening, as shown by position B.

This argument for steepening of the pressure wave must continue until the "thickness of the shock" is of molecular dimensions, when the various definitions for c and u become ambiguous, and the problem passes from hydrodynamics into the realm of kinetic theory. Because the steep shock front follows from such fundamental properties of air, it is reasonable to expect that only strong perturbations could alter the shock front to a slow rise in pressure.

Given a shock front propagating in space, relationships between the various hydrodynamic variables across this shock front were derived many years ago by Rankine and by Hugoniot, independently and with different methods. These derivations are considered well known. It is also known that the pressure difference across a true shock is one of the sharpest discontinuities in nature and the shock "thickness" is only a few molecular free mean paths of air. But this sharpness, together with the usual derivations for the Rankine-Hugoniot conditions, has led to the supposition that a sharp shock front is a necessary condition for the validity of the Rankine-Hugoniot equations. In the remainder of this section the Rankine-Hugoniot relations will be deduced in a manner intended to emphasize the fundamental validity of the equations, whether the shock is "perfectly" sharp or not.

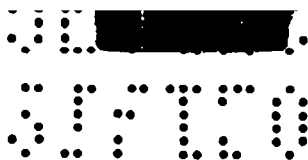
We first apply conservation of mass to the arbitrary pressure disturbance shown in Fig. 2.1.2b. To the right of the dashed lines, ambient conditions are specified by subscripts zero. To the left of the dashed lines the state variables are as shown without subscripts. The middle band labeled "the shock front" will be a loosely defined region of transition from the hydrodynamic variables on the right to the hydrodynamic variables on the left, caused by the "shock front" as it passes through the air. We impose two restrictions on this shock front: that the decay of pressure in the pressure wave to the left of the dashed lines be sufficiently slow so that there is some meaning to peak values of u , P , V , c and T ; next, that this shock front be sufficiently stable in time or sufficiently thin in space so the mass within it does not change appreciably in time. The material engulfed by the shock front in unit time across unit cross section is a column of air u cm long and of density ρ_0 , with mass $\rho_0 u$. After unit time the front edge of the disturbance will be a distance U to the right, but the trailing edge of the material engulfed will have been carried forward a distance, u , compressing the column to a length, $U - u$, with a density, ρ . Since the mass of the column is unchanged, we write

29

UNCLASSIFIED

UNCLASSIFIED

$$\rho (U - u) = \rho_0 U$$



(2.1.2-1)

and speak of this as the Rankine-Hugoniot condition for conservation of mass.

The conservation of momentum is applied to this system with similar restrictions that momenta stored within the "shock front" do not change appreciably in time. The fundamental statement of Newton's law is

$$F = \frac{d}{dt} (mu)$$

During the passage of the shock over the material, the column of air is initially U cm long, and 1 cm^2 in area; it is subject to a force P on the left and force P_0 on the right, and the difference is $P - P_0$. According to Newton's law, the time rate of change of momentum is equal to this applied force. The mass of this material is given by either side of the equation for conservation of mass, and we take it as $\rho_0 U$. Its initial velocity was zero and its final velocity is u so that the change in momentum per unit time is simply

$$\rho_0 U u$$

By Newton's law, we have

$$P - P_0 = \rho_0 U u \quad (2.1.2-2)$$

and speak of this as the Rankine-Hugoniot condition for the conservation of momentum.

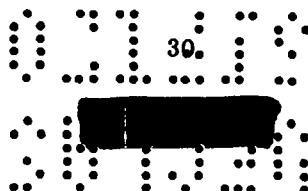
The conservation of energy is applied to this system with a similar assumption that no appreciable change occurs in the energy stored in the shock front. Before proceeding directly we will use an expression for u which is obtained directly from Equations 2.1.2-1 and 2.1.2-2, by eliminating U ; that is,

$$u^2 = (P - P_0)(V_0 - V).$$

Consider the work done on a unit mass of gas as it is shocked. The material to the left acts on this unit mass with a pressure, P , and regarding this unit mass as contained in a column 1 cm^2 , this unit mass is compressed from length V_0 to length V . Quite independent of the details in the shock process, the total work done on the gas by the material to the left of the shock is just

$$P (V_0 - V)$$

The work is distributed between the kinetic energy and change in internal energy of the air presently being shocked. Since we are dealing with unit mass, its kinetic energy is simply $1/2 u^2$. Substituting for u^2 we have



UNCLASSIFIED

UNCLASSIFIED

●●●●●
●●●●●
●●●●●
●●●●●
●●●●●

Total Work Done = Change in Internal Energy + Kinetic Energy

$$P(V_0 - V) = \Delta E_i + \frac{(P - P_0)(V_0 - V)}{2}$$

The change in internal energy of the air as it is shocked is then given by

$$\Delta E_i = 1/2 (P + P_0)(V_0 - V)$$

It is a fundamental property of thermodynamics that the state of a material can be specified by only two independent hydrodynamic variables. In this case we mean that the equation of state must regard E_i , P , and V as connected in some fashion so that E_i may be eliminated from the above equation. Now it is well known that in an ideal gas

$$E_i = PV/(\gamma - 1)$$

where γ is the ratio of the specific heat at constant pressure to the specific heat at constant volume. Based on this clue, we suspect that in real gases, γ is a slowly varying function of P and V . Let us do more and simply say we will define a γ such that

$$E_i = PV/(\gamma - 1)^*$$

Based on this definition, the internal energy per unit mass before the shock is $P_0V_0/(\gamma_0 - 1)$ and after the shock it is $PV/(\gamma - 1)$. Equating the change in internal energy to the relationships obtained, we find that

$$PV/(\gamma - 1) - P_0V_0/(\gamma_0 - 1) = 1/2 (P + P_0)(V_0 - V) \quad (2.1.2-3)$$

and speak of this as the Rankine-Hugoniot condition for conservation of energy.

In the preceding derivations there is surprisingly little requirement for a sharp shock for the validity of the Rankine-Hugoniot conditions. The equations for conservation of mass and momentum are independent of any equation of state, and applicable to any medium. Even Equation 2.1.2-3 applies so long as we define γ as we have. From these three conditions a number of exceedingly useful relationships are readily derived. These specify the value of any of the state variables, provided the shock strength is specified by only one of them. Usually it is convenient to specify the

*This relationship is, of course, well known for ideal gases. The author has independently extended this formalism and its implications as used in this and in succeeding sections. It is tantamount to the construction of a hydrodynamic system to exploit this fundamental definition of γ , which is often referred to as "variable gamma theory."

UNCLASSIFIED

●●●●● 31 ●●●●●
●●●●●
●●●●●
●●●●●
●●●●●

UNCLASSIFIED

shock strength in terms of the pressure, or, more generally, by the ratio of pressures, $\xi = P/P_0$ across the shock front.

The density ratio is obtained by suitable algebraic transformation of Equation 2.1.2-3 to give,

$$V_0/V = \frac{(\gamma + 1) P + (\gamma - 1) P_0}{(\gamma_0 - 1) P + (\gamma_0 + 1) P_0} \cdot \frac{(\gamma_0 - 1)}{(\gamma - 1)} \quad (2.1.2-4)$$

It is convenient to express these in the non-dimensional form by defining a density compression ratio as η , and

$$\eta = \frac{V_0}{V} = \frac{\rho}{\rho_0} = \frac{\left(\frac{\gamma + 1}{\gamma - 1}\right) \xi + 1}{\xi + \frac{\gamma_0 + 1}{\gamma_0 - 1}}$$

The equation for η has certain interesting properties. For low pressures, i.e., $\xi \rightarrow 1$, this equation passes into the ordinary adiabatic law for ideal gases, namely: $PV^\gamma = \text{constant}$. However, at extremely high pressures, namely, $\xi \rightarrow \infty$, the compression ratio does not increase without limit, as indicated in the adiabatic law, but reaches a constant limit given by

$$\mu = (\gamma + 1)/(\gamma - 1)$$

The implications of this fact are perhaps the most important of any in the hydrodynamic of strong shocks for nuclear explosions.

The shock velocity of the pressure disturbance is specified by U and follows immediately from conservation of mass and momentum. By eliminating the material velocity u from Equations 2.1.2-1 and 2.1.2-2 we obtain

$$U^2 = \frac{P - P_0}{V_0 - V} V_0^2 = \frac{P_0 V_0 (P/P_0 - 1)}{1 - V/V_0} = P_0 V_0 \frac{(\xi - 1)\eta}{\eta - 1}$$

In this form the Rankine-Hugoniot shock velocity equation is applicable to any medium, because it does not depend on the equation of state, and can be regarded to be as fundamentally sound as the principles of the conservation of mass and momentum. If we are dealing with air and define the sound velocity as

$$c_0 = \sqrt{(\partial P / \partial \rho)_S}$$

then

$$c_0^2 = \gamma P_0 V_0$$

UNCLASSIFIED

UNCLASSIFIED

UNCLASSIFIED

The Mach number of the shock is the dimensionless quantity U/c_0 relative to the ambient sound velocity ahead of the shock, and related to ξ and η by

$$(U/c_0)^2 = \frac{\eta(\xi - 1)}{\gamma_0(\eta - 1)}$$

For low pressures in air $\gamma \cong 7/5$ and a useful relationship is that

$$U/c_0 = \sqrt{(6\xi + 1)/7}$$

Some properties of this equation are of interest. At low pressures $\xi \rightarrow 1$, and the shock velocity degrades into sound velocity as $U/c_0 \rightarrow 1$. At high pressures the shock velocity is roughly proportional to $\xi^{1/2}$. As long as the shock pressure is finite the shock velocity is supersonic, and it would be hazardous to apply the adiabatic law to a finite shock wave as is occasionally done in attempting to describe the "slow rise." Some further insight may now be gained into the process of "shocking up." Consider the shock front as extremely broad and, if the very front of the wave were of infinitesimal amplitude, it would travel with ambient sound velocity. As derived previously, the shock velocity equation describes the velocity of the pressure disturbance at the point of pressure, P ; this maximum pressure will travel with supersonic velocities and clearly overtake any acoustic signal ahead of it, provided the medium is homogeneous and no energy losses are occurring within the shock front.

The material velocity of the flow immediately behind the shock follows from Equations 2.1.2-1 and 2.1.2-2 as

$$u^2 = (P - P_0)(V_0 - V) = P_0 V_0 (\xi - 1)(\eta - 1)/\eta$$

As stated in this form, the material velocity equation is independent of the equation of state and is applicable to any medium. Using the relationship for sound velocity as before, we find the ratio of material velocity to the sound velocity ahead of the shock is a dimensionless number given by

$$(u/c_0)^2 = \frac{(\eta - 1)(\xi - 1)}{\gamma_0 \eta}$$

In the special case of air at low pressures, where $\gamma = 7/5$,

$$u/c_0 = \frac{5(\xi - 1)}{\sqrt{7}(6\xi + 1)}$$

This equation has several interesting properties. At low pressures, as $\xi \rightarrow 1$, the material velocity

UNCLASSIFIED

UNCLASSIFIED

approaches zero. At high pressures, where $\xi \rightarrow \xi_0$, the material velocity is roughly proportional to $\xi^{1/2}$. At high pressures the material velocity is only slightly smaller than the shock velocity, and the ratio between them is specified by

$$u/U = \frac{\eta - 1}{\eta} = \frac{\mu - 1}{\mu} = \frac{2}{\gamma + 1}$$

We have used the relationship for sound velocity a number of times and, while it is not intrinsically part of the Rankine-Hugoniot equations, some remarks are in order regarding its application. By definition, we speak of

$$c = \sqrt{(\partial P / \partial \rho)_S}$$

which is rigorous as a definition whether c is the actual sound velocity or not. Following this definition and using the relationship that the slope of an adiabat on $\log P - \log \rho$ coordinates is k ,

$$k = d \ln P / d \ln \rho = (\rho / P) dP / d\rho$$

It follows that

$$c = \sqrt{(kP / \rho)}$$

which is an equally rigorous expression. If c is to be used in the Rankine-Hugoniot equations, it will be more accurate to calculate it from this equation than to use a measured value of actual sound velocity, or to calculate it from the temperature. The usual derivation for sound velocity is from elementary thermodynamics, with the assumption that the ideal gas law holds in the form $PV = RT$, and that

$$\gamma = \frac{C_p}{C_v} = k$$

Under these conditions, one finds that

$$c = \sqrt{\gamma RT}$$

or

$$c/c_0 = \sqrt{T/T_0}$$

This expression relating temperature to sound velocity is actually a special case, applicable only where the ideal gas law applies, and less general than

$$c = \sqrt{kP/\rho}.$$

UNCLASSIFIED

UNCLASSIFIED

2.1.3 Hydrodynamic Relationships on the Interior of a Shock Wave

The relationships between pressure, density, and material velocity on the interior of a shock wave are obtained by straightforward application of the principles of conservation of mass, momentum, and energy. These are expressed in differential form rather than the direct form as it is possible to do by the Rankine-Hugoniot relations across the shock front.

The differential equation for conservation of mass is obtained by considering unit volume of gas as indicated in Fig. 2.1.3-1. The net flow of mass across any of the boundaries is the vector quantity $\rho \vec{u}$. The net flow per unit time across all surfaces is given by $\text{div}(\rho \vec{u})$. In unit time the average density of this curve must increase or decrease according to the net flow, and we write the conservation of mass as

$$\partial \rho / \partial t = - \text{div}(\rho \vec{u}) \quad (2.1.3-1)$$

In the special case where the symmetry of the wave permits a description in terms of a single space variable, r , the conservation of mass is simply portrayed by use of a radius-time graph on which the path of the shock front and the mass particles may be plotted, as shown in Fig. 2.1.3-2. The slope of the particle paths in this r - t plane, with linear coordinates is, by definition, the local material velocity. The spacing between adjacent mass lines graphically portrays the specific volume of the air.

Some insight into the broad validity of the Rankine-Hugoniot equations may be gained immediately from such a plot. Consider the parcel of air originally bound within the spatial limits labeled V_0 on the graph. After time Δt , when the shock has passed over this material, it will be compressed in some manner, indicated as arbitrary. Before the shock arrived, this mass occupied the volume which is proportional to V_0 ; just after the shock has passed over it, the front of this layer remains in the same position, but the rear of the layer has been moved forward to occupy the volume V . Before the shock V_0 is proportional to $\bar{U} \Delta t$. After the shock is passed the same material now occupies a volume proportional to $(\bar{U} - \bar{u}) \Delta t$. Setting the mass equal, and using the proportionality

$$\frac{\bar{U} \Delta t}{V_0} = \frac{(\bar{U} - \bar{u}) \Delta t}{V}$$

we have

$$\rho_0 \bar{U} = \rho(\bar{U} - \bar{u})$$

UNCLASSIFIED

UNCLASSIFIED

which is nearly identical to the expression previously derived from Rankine-Hugoniot relations alone. Note that variations in shock or material velocity during Δt do not deny the validity of the expressions for conservation of mass, provided we interpret both U and u as average values during the time in question.

In the special case of a wave of spherical symmetry, conservation of mass can again be expressed simply. From the r - t plot, we regard the band indicated by V_0 as specifying the thickness of a shell with a volume initially proportional to $4\pi r^2$. In this case, a general expression for conservation of mass can be written as

$$\rho r^2 dr = \text{constant}$$

where dr means the thickness of the mass shell as measured by the distance between two adjacent mass point lines.

Conservation of momentum is applied by the application of Newton's law to a particle. In any type of wave, it is readily shown that such a unit volume is subject to a net force of $\text{grad } P$. By Newton's law this is equal to the time rate of change of momentum for unit volume of gas:

$$\text{Grad } P = -\rho \, du/dt$$

The equation applies along a particle path u , so by du/dt we will mean

$$du/dt = u \cdot \partial u / \partial r + \partial u / \partial t$$

This expression for du/dt is readily visualized on the r - t plot as the curvature of a mass line. If the pressure gradients are high the curvature is great; when the pressure gradient is low the curvature is small, and the mass motion lines are effectively straight on a linear plot.

The conservation of energy is applied on the interior of a wave through a customary assumption that after the passage of the shock the subsequent changes are adiabatic, and the entropy remains constant. This is sometimes written as

$$\frac{dS}{dt} = u \frac{\partial S}{\partial r} + \frac{\partial S}{\partial t} = 0$$

meaning that the entropy is constant along a particle path u . The alternate form of this expression, namely, $P = \rho^k \cdot \text{constant}$, is an equally valid expression along this path. It will be observed in the preceding equations that the form of the equation for conservation of energy is the only expression which is not valid when radiative transport occurs. If either pressure P or density ρ are specified on the interior of the wave, the other value is determined by

UNCLASSIFIED

SECRET
 0110
 0110

UNCLASSIFIED

$$P/P_S = (\rho/\rho_S)^k$$

where k is the slope of the adiabat in the equation of state (usually γ) and P_S and ρ_S are the shock values for the mass particle in question.

2.1.4 Entropy Change Across the Shock Front

The entropy change across the shock front, as demanded by the Rankine-Hugoniot relationships, has important implications when coupled with the adiabatic expansion of the same material after the shock has passed.

The compression at the shock front is given by

$$\eta_S = \frac{\mu \xi_S + 1}{\xi_S + \mu_0} \quad (2.1.4-1)$$

During the subsequent expansion the adiabatic law is assumed to hold, so the final pressure and density can be written in terms of the shock front values by

$$\frac{P_{\text{final}}}{P_{\text{shock}}} = \left(\frac{\rho_{\text{final}}}{\rho_{\text{shock}}} \right)^\gamma \quad (2.1.4-2)$$

or

$$\eta_f = \eta_S (\xi_f / \xi_S)^{1/\gamma} \quad (2.1.4-3)$$

If the final pressure returns to P_0 , $\xi_f = 1$, and inserting the relationship for η_S we obtain

$$\eta_f = \frac{\mu \xi_S + 1}{\xi_S + \mu_0} (1/\xi_S)^{1/\gamma} \quad (2.1.4-4)$$

For air shocked at low pressure, recall that η_S approaches $\xi_S^{1/\gamma}$, meaning that $\eta_f \rightarrow 1$, and the material returns to its pre-shock density. At high pressures, however, $\eta_f \sim \mu(1/\xi_S)^{1/\gamma}$. This means that if the particle was originally shocked to a high pressure, even though the material finally returns to ambient pressure, the final density is very much smaller than the initial density. It follows from this that the final temperatures of such air are very high even though it returns to normal pressure.

By an expansion of the adiabatic law and the Rankine-Hugoniot energy relationship it can be shown that the difference between them is only a third-order difference. As a consequence, the hydrodynamics of weak shocks, like those of TNT, are not seriously altered by the entropy change across the shock front. Once the pressures become high enough, as in a nuclear explosion, the changes rapidly become profound.

SECRET
 0110
 0110

UNCLASSIFIED

████████████████████

████████████████████

UNCLASSIFIED

It is this entropy change across the shock front which gives rise to the most spectacular feature of a nuclear explosion, namely, the fireball itself. Because of the presence of such a fireball one knows without further experimentation that a non-adiabatic change such as the Rankine-Hugoniot relationship must indeed have occurred at the shock front during its strong shock phases. It is this violent residual heat which gives rise to a principal effect from a nuclear explosion, namely, the thermal radiation. As the author delights in telling his colleagues who specialize in thermal radiation, the thermal radiation from a bomb is only the garbage left behind the shock wave.

Fuchs applied the concept of "waste heat" to this phenomenon, and for many years it has been taken for granted that this "waste heat" accounted for a presumably reduced blast efficiency from atomic bombs in comparison with TNT, and a large-scale "partition of energy." As will be shown in detail, this heat is not entirely wasted, even to the blast wave. Because of the high final temperatures and correspondingly larger final volume of the late fireball, conservation of mass would demand a greater average compression, and higher average pressure, for the air between the fireball and the shock than from a cool inner core. One could then argue with equal plausibility that the shock front pressures are enhanced by the fireball. When the failure of the ideal gas law is taken into account it is found that a greater total hydrodynamic energy is actually required for an explosion in air to give the same shock front yield as an explosion in gas of $\gamma = 1.4$, but this is not waste heat per se. The energy per unit volume is $P/(\gamma - 1)$ and it happens that the air in the late fireball has values of γ like 1.18, so the energy density is more than twice that for the ideal case. In other words, the failure of the ideal gas law involves as much energy in the fireball region as an overpressure of more than 1 atm of ideal air.

2.1.5 Similarity Solutions for Strong Shocks

An approximate solution for the propagation of a strong shock in air has previously been given by a number of authors, such as Taylor, von Neumann, and Bethe.

The details of their derivations will not be repeated here but an essential feature involves the constancy of the compression ratio η in the limit as $\xi \rightarrow \infty$. Under these conditions certain similarities exist in the expressions for the hydrodynamics which in turn permit a Taylor similarity condition usually specified by the statement that for strong shocks

$$P \sim 1/R^3$$

18

████████████████████

████████████████████

UNCLASSIFIED

UNCLASSIFIED

On the basis of this similarity condition, Be the pointed out a fundamental characteristic of the radius vs time curve for a strong shock, sometimes referred to as the 0.4 power law. The derivation was based on simple, dimensional considerations as in the following five steps. By the shock velocity relationship in Section 2.1.2, observe that

$$1. \quad U \sim P^{1/2}$$

From the similarity condition, we have

$$2. \quad P \sim 1/R^3$$

Since by definition, $U = dR/dt$ it follows that

$$3. \quad U = dR/dt \sim 1/R^{3/2}$$

Multiply through by $R^{3/2}$ to obtain

$$4. \quad R^{3/2} dR \sim dt$$

This is readily integrated (the constant of integration is zero because $R = 0$ when $t = 0$) to yield

$$5. \quad R^{5/2} \sim t \text{ or } R \sim t^{2/5}$$

In other words, if the log of the shock front radius is plotted against the log of the time, the shock front would appear as a straight line of slope 0.4.

The author has shown previously in a number of papers that this derivation is not exact for strong shocks for a variety of reasons. With regard to the first step in the derivation, the variable gamma theory shows that the relationship is more exactly

$$1' \quad U \sim \left(\frac{\gamma + 1}{2\gamma} P \right)^{1/2}$$


In this case there is a slight dependency of the shock velocity on γ as well as P so that the variation of U with P is close to, but not quite like, the $1/2$ power.

The similarity condition which yielded the dependence of the pressure on the cube of the radius is not strictly applicable. If there is any quantity which ought to decrease with volume in a point source explosion it will be the energy density per unit volume rather than the pressure. By the definition of γ in this paper it follows that if we regard γ as some sort of average value at a given shock radius,

$$E_i \sim P/(\gamma - 1) \sim 1/R^3$$

39

UNCLASSIFIED


 3170

and

UNCLASSIFIED

$$2' \quad P \sim (\gamma - 1)/R^3$$

Upon combining this relation with Step 1, the third step is replaced by

$$3' \quad dR/dt \sim \left(\frac{\gamma^2 - 1}{2\gamma} \right)^{1/2} \cdot \frac{1}{R^{3/2}}$$


Now the dependence of shock velocity on γ is considerably more serious because of the presence of the term $\gamma^2 - 1$, especially because γ is a number usually not far different from 1.

A further difficulty is now recognized in Step 4. If γ is not a constant, then the preceding expression cannot be integrated directly but must be performed in some complex fashion, depending upon the variation of γ with R at the particular state of the air being shocked.

The fifth step has a further difficulty, stated as follows: One cannot profess to know the function $R = R(t)$ unless one knows the entire history of dR/dt starting from zero time. As it turns out, the growth of the shock wave is such that the dependence of R on t from zero time is not governed entirely by the Rankine-Hugoniot equations, and the dimensional arguments leading to the 0.4 law are not applicable.

During a very early stage of growth, Hirschfelder pointed out (see Effects of Atomic Weapons (EAW)) that above a temperature of approximately 300,000°K the energy propagates outward by diffusion of radiation faster than it can be propagated by shock hydrodynamics. Several years ago, the author showed the consequences of this fact that during very early times the shock radius is considerably larger than it would have been had it propagated by shock hydrodynamics alone. This effect might be conceived simply as adding a constant increment to R during later stages of fireball growth. It decreases the slope of the radius-time curve on logarithmic coordinates to values like 0.1 during the radiative phase. This perturbation persists for a remarkably long time until the increment in R is small compared with R itself and extends well into those times when the shock front is no longer luminous, around 100 atmospheres.

As will be discussed later, similar mechanisms of radiative transport persist on the interior of the shock long after the shock front itself has ceased to propagate by radiative expansion. This additional mechanism for energy transport will perturb the shock hydrodynamics on the interior, and will transmit energy to the shock front in a different way from bomb to bomb; this partially negates the simplicity which might have resulted from simple scaling in the absence of such radiative transport.

40


UNCLASSIFIED

UNCLASSIFIED

Finally, in all explosions, especially those from TNT, there is a period during which the mass of the bomb parts or surrounding material is not small in comparison with the mass engulfed by the shock. Since the energy density or the temperatures on the interior of the shock are strongly governed by the mass engulfed rather than simple volume considerations alone, the result is that the average pressure in the fireball and at the shock does not scale like $1/R^3$ even apart from the considerations of variable γ or radiative transport. Under the conditions of large mass effect the slope of the shock front will be approximately 1.0 if radiative transport is also present.

The purpose in discussing these perturbations here is to show that the departures from similarity are too great to be neglected in the attempt to compare different explosions at high pressures. Radiative transport, mass effect, and variable gamma represent competing mechanisms, which differ from one explosion to another, so there is never a region in which the slope n can be regarded as constant, or in which $P \sim 1/R^3$ strictly applies. It requires, of course, a long and difficult process to predict how long these effects persist, but the best procedure seems to be to derive, if possible, the rate of growth of a strong shock without recourse to similarity assumptions or scaling laws. This is done in the following section.

2.2 ANALYTIC SOLUTION FOR STRONG SHOCK

This section describes briefly the results of a derivation which expresses the total hydrodynamic energy of a blast wave in an analytic form from a measurement of the radius of the shock front at various times, together with its time derivatives, but without recourse to similarity assumptions.

The purposes of presenting the results here are fourfold. First, they provide some insight into the general nature of wave forms behind the shock front. Second, they provide the basis for scaling laws to transpose results from one homogeneous atmosphere into another and, to a limited extent, some insight into the perturbations to scaling which will result when an explosion occurs in an inhomogeneous atmosphere. While these laws have been derived previously from dimensional considerations, the derivation here is more explicit. The third point is this: from theoretical considerations one expects a definite failure of the ordinary simple cube root scaling laws at high pressures and this failure may persist on some bombs down to pressures low enough to be considered of practical importance. These failures in scaling are believed to be too serious to neglect in an exposition of shock hydrodynamics, because of the shock's "memory" of its early and very different history, not only from TNT explosions but among nuclear explosions as well. Finally, we

41

UNCLASSIFIED

UNCLASSIFIED

will use this solution to evaluate the energy in a machine solution to the blast wave, and thereby establish the "free air curve" for an atomic bomb, which in turn is the basic framework upon which are based all the reflected pressure patterns of widespread practical importance.

2.2.1 Definition of the Hydrodynamic Kiloton

We define

$$1 \text{ hydrodynamic kiloton} = (4\pi/3) 10^{19} \text{ ergs}$$

since

$$4\pi/3 = 4.1888$$

and the mechanical equivalent of heat is such that

$$1 \text{ cal} = 4.185 \text{ joules}$$

It follows that the hydrodynamic kiloton is effectively 10^{12} cal, which is identical to the radiochemical kiloton of 4.185×10^{19} ergs, quoted in "Effects of Atomic Weapons."

The hydrodynamic or radiochemical kiloton is equivalent to the supposed energy release of a kiloton of TNT in only a very rough way because the energy release of high explosives under these or other conditions may not be known with sufficient precision. So far as the author can determine from the folklore at Los Alamos concerning the origin of the "kiloton," it seems that the energy release of TNT was taken, in round numbers, to be 1000 cal/gm. Under this very rough assumption the kiloton of 10^{12} cal is 1000 metric tons of TNT and not 2,000,000 lb of TNT. However, the radiochemical kiloton was always defined by an energy release in ergs, and never dependent on the actual energy release of high explosive.

By hydrodynamic energy we mean the energy which is determined from the state variables of the air and bomb material within the shock front, namely, pressure, density, temperature, and material velocity. When so determined, the hydrodynamic yield is close, but not necessarily identical, to the radiochemical yield. The radiochemical yield should pertain more nearly to the energy release of the nuclear components of the bomb from known nuclear reactions, and the translation of these numbers into blast phenomenology requires a long train of intermediate calculations and estimates which involve the energy per fission, the processes by which nuclear energy is first transformed into radiant energy, and then into hydrodynamic energy. There is no guarantee that these processes are exactly similar for all sizes and types of weapons, so it appears preferable to describe the blast wave on the basis of the total hydrodynamic energy present after these transformations have occurred.

42

UNCLASSIFIED

SECRET

UNCLASSIFIED

2.2.2 Variable Gamma Theory

As a prerequisite to the derivations in the analytic solution, we require a formalism which is adequate to treat air in which the ideal gas law does not hold. We refer to this treatment as variable gamma theory.

The whole of the variable gamma theory rests on exploiting a simple definition for gamma. We define a gamma such that the internal energy per gram is

$$E_i = PV/(\gamma - 1)$$

For the moment we will assume no properties of gamma other than this definition, although it is clear enough that at standard conditions it will be, as usual, the ratio of specific heats. The details of the derivations in the Rankine-Hugoniot equations using this formalism will not be repeated here and only the salient results are given.

The adiabatic law becomes:

$$dP/P + \gamma dV/V - d\gamma (\gamma - 1) = 0$$

which can be integrated for small changes as:

$$PV^\gamma = (\gamma - 1) \text{ constant}$$

instead of the usual expression for constant γ :

$$PV^\gamma = \text{constant}$$

The compression ratio across the shock front is related to the pressure by

$$\eta = \frac{\left(\frac{\gamma + 1}{\gamma - 1}\right) \frac{P}{P_0} + 1}{\frac{P}{P_0} + \frac{\gamma_0 + 1}{\gamma_0 - 1}} = \frac{\mu\xi + 1}{\xi + \mu_0}$$

Here it will be observed that in the limit $\xi \gg 1$, the expression is identical algebraically to that in which γ is a constant. Of particular importance is the fact that, as γ approaches values like 1.18 for strong shocks, compression ratios as high as 12 are achieved where one might have expected a maximum value of 6 under the assumption that $\gamma = 1.4$.

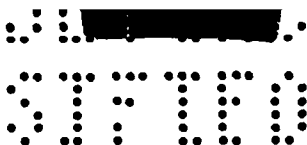
The equation for shock velocity becomes

$$(U/c_0)^2 = \frac{(\xi - 1)(\mu\xi + 1)}{2\gamma_0[\xi/(\gamma - 1) - 1/(\gamma_0 - 1)]}$$

43

SECRET

UNCLASSIFIED



UNCLASSIFIED

For $\xi \gg 1$, this reduces to

$$(U/c_0)^2 = \left[\frac{(\gamma + 1)}{2\gamma_0} \right] \xi$$

The equation for material velocity becomes

$$(u/c_0)^2 = \frac{2(\xi - 1) \left[\xi/(\gamma - 1) - 1/(\gamma_0 - 1) \right]}{\gamma_0 \frac{\gamma + 1}{\gamma - 1} \xi + 1}$$

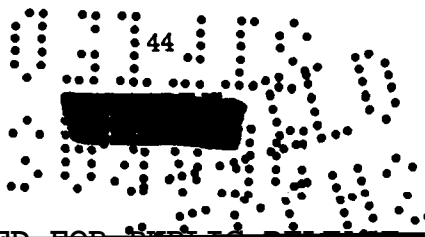
This formalism has found wide application for a number of years since its first appearance in LA-1214. On the basis of lengthy theoretical calculations by a number of authors, it is possible to calculate the effective values of γ for air for large changes of the state variables. These results were correlated by the author and are presented graphically in Figs. 2.2.2-1 through 2.2.2-4. It is of particular interest to note that despite the changes in the equation of state, the appearance of these graphs is not markedly different from what would have resulted from the assumption of constant γ . The adiabats are nearly straight lines with slope of nearly γ , instead of being parallel lines of slope 1.4. The isotherms are not straight lines of slope 1 but do not depart very strongly from that condition. Note now a feature of these graphs which will be of importance later. Near normal atmospheric pressures, γ decreases markedly as the density decreases (and the temperature increases). This means that much larger quantities of energy are contained in unit volume at normal pressure but small density than would be required if the ideal gas law held and $\gamma = 1.4$.

2.2.3 Wave Forms Behind the Shock Front

The details of the analytic solution will not be repeated here but the main outlines for the derivation are as follows:

An intrinsic property of a strong spherical shock is a sharp density gradient behind it, for associated with the high shock pressure is a material velocity entirely comparable in magnitude to the shock velocity. Because of spherical divergence, the rapid movement of material outward from the center causes an enormous drop in density, and a corresponding drop in pressure because of the adiabatic expansion of each air parcel. Any reasonable mathematical description of the wave form will show this characteristic high pressure and also density gradients near the shock front.

As we now look at material successively closer to the center, the initial shock pressure associated with each particle rapidly increases and, because of this, had a higher entropy change initially and has greater residual temperatures now. This in turn leads rapidly to states of gas in



UNCLASSIFIED

UNCLASSIFIED

which radiative transport of energy quickly overrides hydrodynamic transport, for, apart from details, the mean free path for radiation goes roughly as T^3 and inversely as ρ . The hydrodynamics alone will almost guarantee that pressures will be fairly uniform on the interior of the wave, because once the violence of the initial shock has passed, pressure is a self-leveling variable in the sense that pressure signals always propagate from regions of high pressure to regions of low pressure. If the pressure wave form is somewhat flat, near the center, the ideal gas law would require the density to be inversely proportional to the temperature, and an overall dependence of mean free path would be something like the inverse fourth power of the density. Toward the interior of the fireball, the ratio of radiative transport to hydrodynamic transport has an enormous power dependence on the radius, and will almost guarantee that pressure, density, and temperature will be uniform at a given time within this region.

It is this radiative transport on the interior of a strong shock which strongly controls the propagation at the shock front, guarantees a sort of uniformity in the core (which may be very close to the shock front), and constitutes a "pusher" behind the shock by sending hydrodynamic signals across the relatively short distance from the isothermal sphere to the shock front.

As a result of this radiative transport on the interior and the likelihood of fairly uniform density near the center, it can be shown that the material velocity wave form is of the form

$$u \sim r$$

and to the extent that the isothermal sphere is close to the shock front

$$u = u_s (r/R)$$

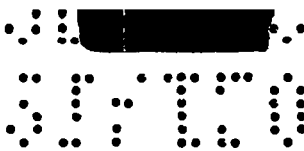
Given a shock at radius R , conservation of mass over the entire fireball places a restriction on the density distribution of material within it. One knows the density at the shock front from the Rankine-Hugoniot equations which we specify as ρ_s . From the entropy considerations discussed in Section 2.1.4, we know also that the density at the origin should be effectively zero. To a first approximation we will specify a power law dependence such that the density ρ at a position coordinate r is given by:

$$\rho = \rho_s (r/R)^q$$

By applying conservation of mass to the entire shock, one obtains the result that the exponent q is given by:

UNCLASSIFIED

$$q = 3 \left[\frac{\eta_s}{1 + M/M'} - 1 \right]$$



UNCLASSIFIED

where M is the mass of the bomb and M' is the mass of air engulfed. Since it is no secret that atomic bombs are carried by aircraft, it is easily verified that $M/M' \cong 0$ for nuclear explosions at almost all pressures of interest. Rigorously, q varies with r , but the expression obtained gives the correct average value of q . The simplicity of the equations and the accuracy of the final energy expression depend greatly on the fact that q has high values, ranging from 15 to 33.

As a consequence of radiative transport and the density distribution on the interior of the shock, the relation between material velocity and distance is

$$u = u_s (r/R)$$

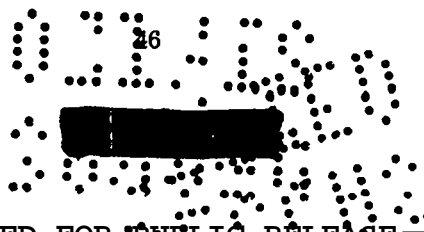
By hydrodynamic transport of energy alone, this relation would not strictly hold, but the presence of radiative transport on the interior of the shock appears to perturb the hydrodynamics in such a way that this equation does hold. Moreover, the final energy expression is not sensitive to the exact form of the velocity distribution. If a body of gas is allowed to expand in such a way that the pressure, density, and temperature at any time are uniform, then this direct proportionality of velocity with radial distance necessarily follows. It is of interest to note that this velocity distribution is precisely the same as is given in the concept of an expanding universe: At the reference point all other points appear to diverge from it with a velocity proportional to the distance from the reference point.

One can now do more. With the observation that the compression ratio across the shock front is not strongly dependent on the shock pressure one can conserve mass locally in the regions near the shock front. Under these conditions the density gradient at the shock front is again specified by a power law with exponent q which is identical to the expression previously derived for conservation of mass over the shock front as a whole, namely

$$q = 3 (\eta_s - 1), \frac{M}{M'} \cong 0$$

It is this coincidence that gives credibility to the density distribution assumed, namely, that the density is correct at $r = 0$, at $r = R$, that its integrated value is correct, and that its first derivative is correct at the shock front.

The pressure gradient behind the shock front is then derived from the relationship



UNCLASSIFIED

$$dP/dr = \rho \, du/dt$$

$$\rho = \rho_s (r/R)^q$$

$$u = dr/dt = mr/t$$

$$m(t) = d \ln r / d \ln t$$

$$n(t) = d \ln R / d \ln t$$

After integration,

$$P = \int \frac{\partial P}{\partial r} dr$$

and evaluation of the integration constant by $\xi = \xi_s$ at $r = R$, the pressure wave form is given by

$$\xi = \xi_s \left[(1 - k) + \left(\frac{r}{R} \right)^{q+2} \right]$$

where k is the expression

$$k = \frac{\eta_s - 1}{q + 2} \left[\frac{1}{m} \left(1 - \frac{d \ln m}{d \ln t} \right) - 1 \right]$$

$$m = n \left(\frac{\eta_s}{\eta_s - 1} \right)$$

This pressure variation is of considerable interest because it shows that the pressure drops very sharply behind the shock, because of the power $q + 2$. It rapidly settles down to a constant fraction of the pressure at the shock front given by $1 - k$. It will be observed that the value of $1 - k$ depends on η_s , M/M' , n , and $d \ln m / d \ln t$ at the shock front. It is this fundamental variation in the shape of the wave on the interior, through the dependencies, which prohibits the assumption of simple similarity scaling in the hydrodynamics of strong shocks.

2.2.4 Energy Expression for the Shock Wave

Given the variation in pressure, density, and material velocity as specified in the previous section, one writes the energy in the wave as

$$W = \int (E_i + E_k) dV$$

where E_i is the internal energy per unit volume and E_k is the kinetic energy per unit volume and the integration is performed over the entire volume of the blast wave. After these operations have been performed, an expression for the energy is obtained in terms of the shock strength ξ_s , and the radius R

UNCLASSIFIED

UNCLASSIFIED

$$W = (4/3 \pi) R^3 \rho_0 (\xi_s - 1) \Sigma$$

UNCLASSIFIED

Here Σ is a function of n , η_s , and $\bar{\epsilon}$ given by

$$\Sigma = \bar{\epsilon} (1 - k) + \frac{3\bar{\epsilon}k}{q + 5} + \frac{3(\eta_s - 1)}{2(q + 5)} + \frac{\bar{\epsilon} - \epsilon_0}{\xi_s - 1}$$

where $\bar{\epsilon}$ is the average value of $1(\gamma - 1)$ on the interior of the wave, and Σ is the sum of all the constants resulting from the integration of energy over the volume of the blast wave. The significance of the various terms in Σ is as follows. The first term involving $1 - k$ is the energy represented by the flat portion of the pressure wave on the interior of the fireball. The next term involving $3\bar{\epsilon}k$ is the internal energy in the pressure peak near the shock front which is above the flat portion of the portion of the pressure wave. The third term involving $\eta_s - 1$ is the contribution by the kinetic energy to the total energy within the shock front. The final term involving $\bar{\epsilon} - \epsilon_0$ is a small correction resulting from the fact that the equation of state of air has been modified from that which applied under ambient conditions, and this term rigorously allows for the difference in energy involved by subtracting out the initial energy density $P_0/(\gamma_0 - 1)$.

The expression for the energy can be numerically improved by removing the strong variation of both R^3 and ξ_s since their product varies slowly. One performs the transformations necessary to relate shock velocity to shock pressure and uses the relationship

$$U = nR/t$$

The energy can now be expressed solely in terms of the radius-time curve, by

$$W = \rho_0 \left[\frac{n^2 R^5}{t^2} \right] F = \rho_0 n^2 \psi^5 F$$

$$\psi = R/t^{2/5}$$

$$F = \left(\frac{\eta_s - 1}{\eta_s} \right) \Sigma$$

The first logarithmic derivative of R is contained in n and F and implies the second derivative as well.

It should be pointed out that in the expressions, as they stand, no explicit use was made of the Rankine-Hugoniot energy equation in the final expressions of the analytic solution. The transformation from shock pressure to shock velocity is the same expression given in Section 2.2.2 and involves only the conservation of mass and momentum. In a practical case, one can resort to the Rankine-Hugoniot energy relationship to specify the dependence of η_s on ξ_s . In principle, however,

UNCLASSIFIED

UNCLASSIFIED

this dependence could also be determined by measuring the density compression ratio concurrently with a measurement of radius and time. This measurement is easily accomplished by a measurement of the material velocity behind the shock concurrently with the shock velocity. Then, in turn, η_s is specified directly by the ratio of material velocity to the shock velocity through

$$u/U = \frac{\eta_s - 1}{\eta_s}$$

without use of the equation of state.

If an approximation is desired for expressing the radius-time curve of a strong shock, one suspects from dimensional considerations that instead of $n = 0.4$, it would be better to use $m = 1/3$, whence

$$n = \frac{1}{3} \left(\frac{\eta_s}{\eta_s - 1} \right)$$

In such a case, n would vary from

$$n = 0.36 \quad \text{where} \quad \eta_s = 12$$

through

$$n = 0.4 \quad \text{where} \quad \eta_s = 6$$

and

$$n = 0.5 \quad \text{where} \quad \eta_s = 3$$

This is apart from the early radiative growth, where we expect an early dependence like $n \cong 0.1$ and mass effects where the early dependence is like $n = 1$.

We can now explicitly tabulate the failure of the similarity condition $P \sim 1/R^3$ by the observations that

(1) n and hence ψ are not constant with time;

n can vary from $\cong 0.1$ to $\cong 1.0$.

(2) η_s is not independent of the pressure but varies from 12 to less than 4, because of changes in the equation of state.

(3) $\bar{\epsilon}$ is not independent of the pressure but varies from 2.5 at low pressures where $\gamma = 1.4$, to a maximum value of $\cong 5.5$ near several hundred atmospheres.

(4) There is only the suspicion, but no rigorous proof, that $d \ln m / d \ln t$ is zero.

UNCLASSIFIED

SECRET

SECRET

SECRET

2.2.5 Scaling Laws

The $W^{1/3}$ scaling law is perhaps the most widely known law in blast hydrodynamics. The basis for the law lies in strong shocks and its limitations are explicit in the energy expression in the analytic solution.

The form of the equation which relates pressure and radius to yield is the direct evidence that it is possible to separate the variables into groups of dimensionless numbers, ξ_s and F , as separate from the space dimension R^3 . This means, if we regard ξ_s as an invariant in describing different bombs of different yields, and if F were also uniquely related to ξ_s on all bombs, then in the same atmosphere, W/R^3 is also an invariant. This simple scaling law does not apply solely to pressures; through the hydrodynamic equations the other hydrodynamic quantities can also be expressed in terms of ξ_s as the invariants, ρ_s/ρ_0 , c/c_0 , u/c_0 , T/T_0 . These latter expressions are equally valid as hydrodynamic invariants in the scaling law. Because velocities are invariant, it follows that time should also scale like $W^{1/3}$. The complete statement for the scaling law is as follows: Given bombs of different yields in the same atmosphere, all details of the wave forms both in space and time, will scale like $W^{1/3}$.

In transposing the results of an explosion in one homogeneous atmosphere to another homogeneous atmosphere, the pressure is also introduced in the scaling. The dependence of this result on pressure is now well known; it was derived independently by Suydam and Sachs. Their conclusions were based essentially on dimensional considerations of the invariance of the hydrodynamic equations under certain transformations of the state variables. The analytic solution expresses the same relationship somewhat more explicitly. If two explosions are similar in all respects, including the variations in n , γ , and $d \ln m / d \ln t$, the F 's will be identical at the same given value of ξ_s . This means that the quantity $(W/P_0 R^3)$ is also invariant. The rule is best applied by regarding the quantity $(W/P_0)^{1/3}$ as the energy invariant with P_0 expressed in bars if the original curve is in bars. By the same token, if the quantity ξ_s is an invariant, we mean that the overpressure expressed in local atmospheres is also an invariant. In scaling from a high pressure atmosphere to a lower pressure atmosphere it follows that distances will be increased, but pressures will be reduced. It is easily verified that the result of these transformations makes no difference in the overpressure vs distance curves in those regions where $P \sim 1/R^3$, but makes substantial difference when $P \sim 1/R$. In the limits as $P_0 \rightarrow 0$, it is easily verified that, while a given pressure ratio occurs, at infinite distance, the actual overpressure anywhere is zero; this is consistent with the intuitive judgment that no blast wave can occur in a vacuum. In such a different atmosphere the velocities are

SECRET

UNCLASSIFIED

invariant if they are expressed in ratios to ambient sound velocity or to a similar quantity such as $\sqrt{P_0 V_0}$. This means that the quantity t/c_0 scales like $(W/P_0)^{1/3}$ or that, in comparing different explosives with different atmospheres, times will scale like $1/c_0 (W/P_0)^{1/3}$. In a very cold atmosphere the time durations will be considerably longer than those obtained solely from $(W/P_0)^{1/3}$ correction.

There are further difficulties, however, in scaling to very different atmospheres. These are occasioned by changes in the equation of state, and the dependence of the energy expression on n and F . The temperature invariant is T/T_0 , so all temperatures behind the shock are reduced as T_0 is reduced. This changes the value of γ in the shocked air, at similar ratios of ξ_s , with corresponding changes in n and $\bar{\epsilon}$. For a cold enough atmosphere, γ might remain near 1.4, and the changes in $\bar{\epsilon}$ would alone make a difference of more than 2 in F , and give the same scaled peak pressure-distance curve with only half the total energy. Moreover, the effect of radiative transport in supporting the strong shock is likely to be quite different in, say, a cold but very rare atmosphere, and will result in corresponding changes in n .

These effects will persist down to pressures of practical interest, for once the shock becomes weak ($\xi_s \cong 3$), the region near the shock front becomes hydrodynamically independent of the interior. Even if two explosions scale by (W/P_0) to the same curve at sea level over a range of weak shock pressures, this is by no means a guarantee that the hydrodynamic energy is the same.

The facts that W/P_0 scaling alone does not lower the overpressure at altitude for strong shocks, and that changes in the equation of state can raise the overpressure, for a given energy content, suggest that a change to a rarer, but very much colder atmosphere, would actually raise the overpressure vs distance curve. At long distances, of course, W/P_0 scaling demands a lowering of the overpressure vs distance curve. Hence, one says there is a region of high enough pressures where the overpressure curve at altitude is higher than at sea level; there is a cross-over point at some pressure level, and below this the overpressure curve lies below the sea level curve.

Without recourse to detailed calculation, one can estimate the point at which the overpressures at altitude cease to be higher than those at sea level, from a plot of $\log P_f$ vs $\log R$ plot, as in Fig. 2.2.5-1. Assume that the equation of state at altitude increases by the factor $F_s/F_a \cong \frac{\bar{\epsilon}_{\text{altitude}}}{\bar{\epsilon}_{\text{sea level}}}$ because W and F are roughly proportional to $\bar{\epsilon}$ this is simply a horizontal shift by $(F_s/F_a)^{1/3}$. At the same time, W/P_0 scaling will move points downward by P_s/P_a and to the right by $(P_s/P_a)^{1/3}$. In general, high altitudes are also cold and, since $\bar{\epsilon}$ is largely a function of temperature, $(F_s/F_a)^{1/3}$ is expected to be a shift to the right. Over a region in which the overpressure could be described as

UNCLASSIFIED




UNCLASSIFIED

$$P \sim 1 R^n$$

the geometry now gives the cross-over point as occurring where

$$n = \frac{\log P_s/P_a}{\log (F_s/F_a)^{1/3} + \log (P_s/P_a)^{1/3}}$$

which yields

$$\frac{\log F_s/F_a}{\log P_s/P_a} = \frac{3-n}{n}$$

While great detail is required to relate F , P_s/P_a , and n to satisfy these equations, some features are clear. For high pressures, $n \cong 3$, (W/P_0) scaling transforms points along the curve itself, but a subsequent shift to the right of F increases the distance at which a given overpressure occurs. Hence we say that at high pressures the distance at which a given pressure occurs will be $(F_s/F_a)^{1/3}$ times larger, and the pressure-distance curve is raised. At low pressure, $n < 3$, the net decrease due to (W/P_0) quickly overrides the net increase due to $F^{1/3}$. A cursory examination of the equation of state in Figs. 2.2.2-1 to 2.2.2-4 shows that F increases in the order of 5% for $(P_s/P_a) = 10$ or at 0.1 standard atm. Insertion of these values gives

$$\frac{\log 1.05}{\log 10} = 3/(n-1)$$

or



$$n = 2.93$$

Now $n = 2.93$ corresponds to high pressures like 100 atm, near the sea level fireball stage, and to this extent one expects the pressure-distance curve to lie below the corresponding sea level curve, below a pressure ratio of 100 or, for $P_a = 0.1 P_s$, at 145 psi overpressure. To choose an extreme in which $\gamma = 1.4$ throughout, the ratio of F has a limiting value of about 2. At very low pressures $n \cong 1$, whence

$$\frac{\log 2}{\log P_s/P_a} = 2$$

$$P_a/P_s = \sqrt{2}$$

and for all such atmospheres in which $P_a > 0.707 P_s$, the pressure-distance curve will lie above the standard curve. From these considerations we conclude that, in general, the shift to a rarer

UNCLASSIFIED

UNCLASSIFIED

atmosphere will raise pressures slightly at high pressures, and decrease pressures at low pressures. Unusual ambient conditions can be assumed in which the pressure-distance curve lies above the corresponding curve at high shock strengths, but for homogeneous standard atmospheres, the cross-over point from highness to lowness probably occurs well above pressures of practical interest.

In an inhomogeneous atmosphere the problems of scaling are very much more complex and it is doubtful that any simple analytic expression can ever be derived which is universally applicable.

The problem has been treated previously by Fuchs, but he assumed no angular flow of energy and has treated the problem at best semiacoustically. The neglect of refraction effects and early history are fundamental limitations on the method, and in general it predicts lower pressures at high altitudes. Occasionally the problem has been treated by acoustic refraction methods; the difficulty here is that the hydrodynamic transport of energy is quite different from the propagation of acoustic signals; this method leads generally to pressures "higher than expected" at altitude.

Rigorously, each case ought to be treated separately, and this probably requires a difficult and at least two-dimensional integration to derive the wave form as a function of the atmospheric parameters at different angles as well as the distance from the bomb. Even an approximate derivation is too lengthy to present here in detail and is more properly the subject of a separate paper. The general features of such an estimate are indicated below, where a solution is suggested which does not require a detailed machine integration.

During the strong shock phase of an inhomogeneous atmosphere, the absolute pressure at the shock front strongly tends to be constant at the same time, for, if a pressure gradient existed along the shock, this pressure gradient would in itself accelerate a flow of material in a direction to relieve that pressure. The mechanism of radiative transport extending in close proximity to the shock front also guarantees a uniformity of temperature within the fireball, and this is the "pusher" or flow of energy necessary to support high pressures at altitude. This strong tendency to equalize the absolute pressure means that the overpressure in the rarified portion of the atmosphere could actually be higher at a given time than the overpressures in the denser portions of the atmosphere. But the gravity head at altitude will limit the pressures to the statement that "at least the overpressure" will be constant at a given time. In either case, because of the higher pressure ratio in the rarified atmosphere at altitude, the shock velocity there will be correspondingly higher and usually will exceed the shock velocity in a denser, but hotter, medium near the surface through

$$U = c_0 \sqrt{\frac{(6 P_f/P_0) + 7}{7}} = c_0 \sqrt{[6/7(P_f/P_0)] + 1}$$

UNCLASSIFIED

UNCLASSIFIED

For an adiabatic lapse rate, with $\gamma = 1.4$, $c_0 \sim P_0^{1/7}$. To the extent that $6P_f/P_0 \gg 1$, this means

$$U \sim P_0^{1/7}, P_0^{-1/2} \sim P_0^{-5/14}$$

Therefore, for strong shocks, shock velocity increases with altitude, despite the lower sound velocity. Along any ray, $R = \int_0^t U dt$, and this means that the shock radii are greater at altitude than on the surface. The shape of the shock front can be carried forward in integrated steps along different rays as long as the condition for equality of overpressure is valid.

Similarly, the rate of work per unit area by the shock is $\dot{W} = Pu$, and by similar arguments on u , as used for U , it will follow that \dot{W} is higher at altitudes than at the surface.

This constitutes a preferential flow of energy towards the regions of lightest density, just as it does at any interface, like the ground. The concept should not be thought of as "blowing a hole in the earth's atmosphere" with a sufficiently large bomb, because such a dire phenomenon would require an explosion of such magnitude that the material velocities at, say, 200 miles altitude would exceed the escape velocity from the earth, which is in the order of 7 miles/sec. In such a case it is doubtful if there would be much further earthly interest in the validity of scaling laws in an inhomogeneous atmosphere.

Eventually, at low enough pressure, shock velocity becomes sonic, $(6/7)(P_f/P_0) \rightarrow 0$. We reach a pressure level where the low value of c_0 overrides the higher pressure ratio, and not until then does the shock at altitude slow down to give the same radius at the same time and overpressure.

Once the shock ceases to be strong, the region near the shock front becomes detached hydrodynamically from the interior and by this time the fireball is no longer a mechanism for keeping the pressure uniform behind the shock. There is still sidefeeding of energy which persists for some time, because $u + c > U$ at the shock, and some idea of its importance is gained from considering the lateral angular spread for which hydrodynamic transport velocity can influence the shock. Figure 2.2.5-2 shows the construction and this lateral angle. From these results one judges that lateral feeding persists down to fairly low pressures like 0.05 atm. with a corresponding tendency to keep overpressures fairly uniform. This is the concept which replaces the concept of acoustic refraction.

Once the possible angle for lateral feeding becomes small, the shock can propagate without the requirement for uniform overpressure along the shock front. The subsequent decay of the shock can then be calculated by a method using the integrated results of the ordinary spherical problem. Since the shock front is locally detached both radially and angularly, it should decay like a small

UNCLASSIFIED

UNCLASSIFIED

part of the spherical wave at these conditions, if we take R to mean the local radius of curvature instead of the true distance from the origin of the bomb. From the integration of the spherically symmetric wave the rate of decay of a shock with distance is found to be related to the radius by:

$$(\xi_s - 1) \sim 1/R^i$$

where, by similarity arguments, i is a function only of the shock strength $\xi_s - 1$. Intuitively one knows also that this rate of decay is connected directly to the shape of the wave form behind the shock. From the shape of the shock front as it developed during strong shock growth, the radii of curvature can be calculated at several angles. With these values of radius of curvature, and the i , which corresponds to the local value of ξ_s , the pressure at a new time can be calculated by a short reiterative process, using the average velocity in this range. After this is done at several angles, the new shock front path can be plotted. The radii of curvature for the next step can then be calculated.

Without presenting the details of the calculation, one can readily infer the general nature of the results shown qualitatively in Fig. 2.2.5-3, in which the shapes are greatly exaggerated. At early times the strong shock conditions make the wave propagate faster at altitude than at the ground, as in A. During this period, at least, the overpressure is constant at a given time, so the pressure-distance curve at altitude lies above the pressure-distance curve for the surface. If we were to demand that the average shock front energy be the same as the true total hydrodynamic yield, some point on the shock front has the "ideal" pressure for its distance, as shown by the line I; above this line pressures would be above "ideal," and below it the pressure would be below "ideal." Radii of curvature are smaller at altitude than at the ground. As the shock becomes weak, the shock at altitude slows down relative to the shock at the surface, partly because all velocities become sonic, and partly because of the smaller radii of curvature, thus greater divergence is introduced. The shock front distance at altitude and surface become more nearly alike, as indicated by the semi-circle B, although it would be fortuitous if the circular shape held for all angles. At still later times, indicated by C, the shock velocity is nearly sonic, and the growth of the shock is faster and the distance from zero is larger at the surface than at altitude. This implies, however, that the radii of curvature at the surface are smaller, and the surface peak pressure-distance curve decays more rapidly than one would expect for the same yield and horizontal distance. This implies that the pressure-distance curve at the surface continues to diverge from the ideal curve; it was already below ideal during the strong shock phase.

UNCLASSIFIED

SECRET

UNCLASSIFIED

The method presented above has been done several times by members of Group J-10 at Los Alamos by hand integration, and requires about one man week for each special case once the techniques are learned. The extension of the method to a burst at high altitudes is clear.

2.3 IBM MACHINE CALCULATION OF THE BLAST WAVE

2.3.1 Original Derivation

A machine integration of the hydrodynamic equations for a shock wave was carried out at LASL in 1944 under the direction of Fuchs, von Neumann, and others.

The calculation started with the assumption of an isothermal and isobaric sphere of radius 10 meters, and supposedly containing 10 KT of energy. This calculation was carried forward to a radius of 80 meters by hand calculation, using $(\gamma - 1)$ theory. At that time the wave form was put into the machine as the boundary condition for the start of the machine problem. The machine solution is an integration of the hydrodynamic equations as indicated in Section 2.1.3. An equation of state was used which provided for variations in γ through a fitted equation; it was probably valid, at least near the shock front. It was felt that whatever reasonable errors in wave form were present at the start of the run would not seriously affect the shape and growth of the wave at some time later when the hydrodynamic equations had literally "taken over."

After the run was completed, the energy in it was said to have been integrated (in a manner unknown to the author) and found to be as high as 13.4 KT instead of the supposed 10 KT it originally contained. For a number of years this problem lay untouched, in part, because of the uncertainty of its yield and, in part (which now seems ironical), because it did not agree with the data on nuclear explosions which were considered most reliable during the late 1940's and early 1950's. Some three or four years ago the author, as well as Bergen Suydam of LASL, began to use the results of this problem, accepting its supposed uncertainty in yield for the sake of its general utility.

Having the variable gamma theory and the analytic solution available, one now reasonably asks two questions: First, whether 10 KT of energy was actually put in the blast wave at a radius of 10 meters, because this is a matter of knowing the correct values of γ at pressure levels where it was known less reliably than at lower pressures. The second question is whether the evaluation of 13.4 KT was based on reliable values of γ at late times for the "bookkeeping."

Whatever the initial conditions of the IBM Run were, or the specific equation of state used, we now propose that the IBM Run specifies P , ρ , and u in its listings at separate times. This configuration of hydrodynamic variables is sufficient to define an energy content. If one then applies any

SECRET

UNCLASSIFIED

UNCLASSIFIED

equation of state, the energy in the wave may be integrated simply as a matter of bookkeeping. If it turns out that this energy content is reasonably constant over a range of pressures, then the IBM results are useful, particularly in view of the insensitivity of the most interesting parameters near the shock front to the energy content of the wave as a whole, and because the starting conditions and equation of state were not in great error.

The remainder of this section is devoted to this energy evaluation, which was done in two ways, followed by a presentation of the results of the IBM calculations in a usable form.

2.3.2 Energy Integration of IBM Run

Despite the uncertainties regarding the values of γ used in the IBM Run, the existing entries specify the state of the material by giving specific values of P , ρ , and u , which are sufficient to prescribe the internal energy, using whatever energy is given by modern values in the equation of state.

The energy evaluation of the IBM Run was first integrated directly as follows. By definition, the hydrodynamic energy is given by the expression

$$W = \int (E_i + E_k) dV$$

$$= 4\pi \int_0^R \left[\frac{P}{(\gamma-1)} - \frac{P_0}{(\gamma_0-1)} + \frac{1}{2} \rho u^2 \right] r^2 dr$$

At pressures of interest (below 3000 atm) the contribution of radiation energy density to the integral is negligible. To facilitate the numerical integration, transform this equation as follows

$$W = 4\pi P_0 \int_0^R \left[\frac{\xi}{(\gamma-1)} - \frac{1}{(\gamma_0-1)} + \frac{1}{2} \frac{\rho u^2}{P_0} \right] r^2 dr$$

$$= 4\pi P_0 \int_0^R \left[\frac{\xi}{(\gamma-1)} - \frac{1}{(\gamma_0-1)} + \frac{1}{2} \left(\frac{\rho}{P_0 V_0} u^2 \right) \right] r^2 dr$$

Upon conversion of material velocity in IBM units, u' , to cgs units, u , and with $\rho_0 = 1.1613 \times 10^{-3}$ gm/cm³, $P_0 = 10^6$ ergs/cm³,

$$\frac{\eta u^2}{2 P_0 V_0} = \frac{\eta u'^2 (1.1613 \times 10^{-3})}{2 \cdot 10^6} \left(\frac{2.0}{2.5} \right)^2 = 74.32 \frac{\eta}{2} u'^2$$

Observe that

$$r^2 dr = 1/3 d(r^3)$$

UNCLASSIFIED

UNCLASSIFIED



The integration is facilitated by plotting the energy density against r^3 and then integrating directly.

Because the distances in the IBM Run are expressed in units of 20 meters, and with $1 \text{ KT} = 4.19 \times 10^{19} \text{ ergs} = \left(\frac{4}{3} \pi\right) \times 10^{19} \text{ ergs}$,

$$W \text{ (KT)} = 8 \times 10^{-4} \int_0^R \left[\frac{\xi}{(\gamma - 1)} - \frac{1}{(\gamma_0 - 1)} + \frac{\eta}{2} \frac{u'^2}{P_0 V_0} \right] d(r^3)$$

The average density $\bar{\eta}$ between mass points may be calculated directly from entries in the IBM Run. Denoting the initial position of the mass points by r_{0i} and the present position by r_i , conservation of mass requires that

$$\bar{\eta} = \frac{r_{0i}^3 - r_{0i-1}^3}{r_i^3 - r_{i-1}^3}$$

It is convenient to integrate this equation in numerical form as

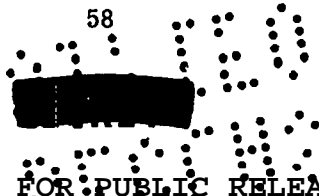
$$W = 8 \times 10^{-4} \sum_{i=1}^{\text{shock}} \left[\frac{\xi}{(\gamma - 1)} - \frac{1}{(\gamma_0 - 1)} + \frac{\eta}{2} \frac{u'^2}{P_0 V_0} \right] (r_i^3 - r_{i-1}^3)$$

Both η and ξ are specified by the IBM Run. Figures 2.2.2-1 through 2.2.2-4 give the value of γ to use through the definition $E_i = PV/(\gamma - 1)$.

In some cases the IBM Run does not extend sufficiently far into the interior to specify pressures completely to the origin. For strong shocks this difficulty is overcome by use of the relationships from the analytic solution. The tabulated results of the integration are as follows:

Radius (IBM Units)	Times (IBM Units)	Pressure (Bars)	Yield (KT)
4.0	0	77.25	11.7
5.1	38	40.02	11.4
8.37	222	11.58	11.1
23.28	2164	2.007	11.5
79.62	13,652	1.1375	11.6
Average			11.5

In view of the consistency of these results, the modicum of effort which could be devoted to this study, the uncertainties in the equation of state in Figs. 2.2.2-1 through 2.2.2-4, and the meager requirement for accuracy in energy, it seems clear enough that the energy in the IBM Run over the entire range is $11.5 + 0.5 \text{ KT}$ for practical purposes.



UNCLASSIFIED

UNCLASSIFIED

There is one additional interesting conclusion from this study. At low pressures there is a strong temptation to specify γ as 1.4, which is certainly correct near the shock front, even at substantial pressures like 50 psi, and the interior of the wave has long since decayed to normal atmospheric pressures. An examination of the lines of constant γ in Figs. 2.2.2-1 through 2.2.2-4 shows, however, that this is not the case; despite the fact the air near the center has returned to ambient pressure, it is at the very high temperatures induced by the original entropy change, and the departures are large from the ideal equation of state with $\gamma = 1.4$. If the energy integration is performed at low pressures with $\gamma = 1.4$ over the entire wave the remarkable result is that the apparent energy of the blast wave at low pressures drops to 5.5 KT. The ratio of this number to the average value of 11.5 KT is surprisingly close to the so-called blast efficiency of a nuclear explosion, in comparison with TNT. This means further that the entropy change itself does not "waste heat" as such, but that the final configuration of pressure and density on the interior of the wave requires a greater energy by virtue of low values of $\gamma - 1$ than would be required for $\gamma = 1.4$.

2.3.3 Analytic Solution on the IBM Run

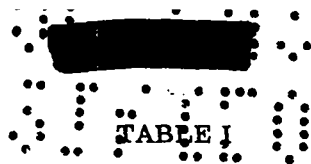
The analytic solution was applied to the IBM Problem M for several purposes: (1) to find the pressure level at which the analytic solution is no longer valid because it is a strong shock solution; (2) to give an independent determination of the IBM yield; and (3) to test the validity of the second derivative terms involved in $d \ln m / d \ln t$ by applying the solution in a region where the logarithmic slopes n and m are known to be changing rapidly.

Some pertinent points in the procedure follow. A zero time correction is necessary and zero time for the IBM run was arbitrarily set to make the slope of the $\log r$ vs $\log t$ plot exactly 0.4 at the first listing at 80 meters. This may or may not correspond to a real bomb but the procedure is reasonable because this assumption of slope was current at the time the work was done. Second, the values of η_g are tabulated listings and these were used directly rather than those from Figs. 2.2.2-1 through 2.2.2-4. The values of $\bar{\epsilon}$ were obtained from the tabulated values of ξ_g for a given time. Third, the tabulated values of pressure and velocity at the shock front were used since these are specified directly by the run. Finally, no attempt was made to smooth out variations in yield by an iteration of the solution to correct for variations in the plotting and calculating procedure.

The tabulated results of this study appear in the following table.

UNCLASSIFIED

UNCLASSIFIED



SOME RESULTS FROM THE ANALYTIC SOLUTION APPLIED TO IBM PROBLEM M

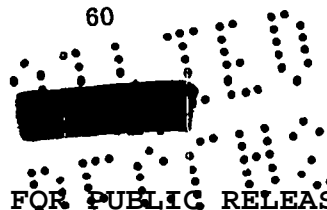
Time, t (msec)	Radius, R (Meters)	$1 - \frac{d \ln m}{d \ln t}$	Overpressure, P (atm)	Yield, W (KT)
11.60	80.00	0.921	76.25	11.91
16.35	91.96	0.965	52.57	12.15
22.85	105.6	1.018	35.65	11.96
32.10	121.8	1.035	24.02	11.66
45.60	141.4	1.026	16.29	11.87
64.10	164.0	1.026	11.14	11.61
90.60	191.2	1.088	7.46	11.79
126.6	222.3	1.132	5.08	11.68
180.6	262.3	1.172	3.41	11.96
Average				11.84

At this pressure level the solution finally becomes inadequate, and slightly after it is expected to do so by a comparison of wave forms.

256.6	310.9	1.222	2.31	12.77
360.6	369.5	1.259	1.593	14.11
520.5	450.3	1.374	1.074	13.57
720.5	542.7	1.488	0.753	15.99
1040.5	680.0	1.532	0.504	21.93
1440.5	842.1	1.601	0.355	29.45

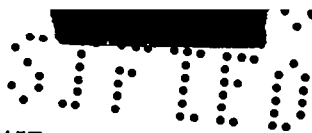
As a result of this study it seems clear enough that the IBM Run evaluates in the order of 11.8 ± 0.1 KT. The solution evidently breaks down from 1% accuracy around the 30 psi level. Even at the low value of 10 psi overpressure the apparent energy is off only by 35%, and because of the cube root dependence this means little more than 10% in pressures or distances at low pressures.

It is especially satisfying to see the solution fail near the 3 atmosphere level, precisely where the strong shock assumptions fail. As part of this study, the pressure wave forms, the IBM run, and the analytic solution were continuously compared. During the earliest part of the run, when the IBM wave form is strongly influenced by the starting conditions used, the analytic solution gives slightly higher pressures on the interior than the listings; this disagreement is expected and appears as the high value of yield 11.91 (fortuitously close) and 12.15 KT at the first two entries. Thereafter, the hydrodynamics of the machine run control the wave form, and it is interesting that this changes the IBM wave form to better agreement with the analytic solution. This consistency in wave form is associated with the consistent analytic solution yields down to the 3.4 atmosphere level. Thereafter the analytic solution wave form gives pressures which are higher than those of the IBM Run, and this discrepancy is directly associated with the high apparent yields at 2.31 atmospheres overpressure and below.



UNCLASSIFIED

UNCLASSIFIED



2.4 DERIVED CURVES FOR FREE AIR

2.4.1 Variables at the Shock Front

Once the energy of the IBM problem is determined, tables and graphs can be constructed for convenience in applying the results. For facility in yield transformations, distances and times have been scaled to 1 KT using the original run as 11.5 KT. In all graphs and charts that follow throughout this paper, ambient conditions are

$$P_0 = 1 \text{ bar, or } 10^6 \text{ dynes/cm}^2$$

$$\text{Density } \rho_0 = 1.1613 \times 10^{-3} \text{ gm/cm}^3$$

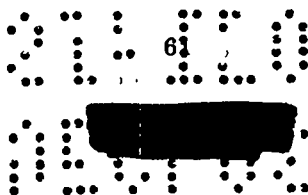
$$\text{Sound velocity } c_0 = 1138 \text{ ft/sec, or } 347 \text{ meters/sec.}$$

Transformations to other atmospheres or yields are made as described in Section 2.2.5.

Appendix A contains the listings of the radius and time, as well as the hydrodynamic variables of interest at the shock front. The pressures listed as absolute pressures in bars will also be the absolute pressure ratio in terms of whatever ambient atmosphere is chosen. The density ratio listed as η_s will be the compression ratio at the shock front. Shock velocity is listed as the dimensionless quantity U/c_0 and for other atmospheres may be converted to velocities in ft/sec or meters/sec by multiplying by the appropriate ambient velocity. Material velocities u/c_0 are listed in a fashion similar to the shock velocity.

Figure 2.4.1-1 is a plot of the peak overpressure vs distance. For convenience, the curve is also plotted with a reflection factor of 2, and, as such, is convenient for obtaining directly the peak pressures over an ideal surface from shots at or near the ground surface.

The relationship between a kiloton of TNT and the hydrodynamic kiloton is not, nor is it expected to be, a fixed quantity at all pressure levels. For most pressure levels of interest, a nuclear explosion of yield W will give the same overpressure as approximately 40% W of TNT, in the usual comparison with short tons of TNT. In comparing small charges with TNT the appropriate scaling factors may be read directly from the graph, because the horizontal displacement between the free air curve and the TNT curve and the TNT curve is, of course, the cube root of the yield. The relative efficiency is also plotted in Fig. 2.4.1-2. Because the TNT curve and the curve with a reflection factor of 2 roughly superimpose, it follows that a rough rule of thumb, valid to a few percent in distance, is that the scaling factor of approximately 100 applies between 1 lb of TNT and a 1 KT nuclear explosion.



UNCLASSIFIED

UNCLASSIFIED

From these curves and graphs many useful relationships can be derived at will. For example, if the peak pressure is plotted against the time, it will be found that the relationship $P_f \times t^{1.1} \cong$ constant is satisfied. This is expected because at high pressures P is nearly proportional to $1/R^3$, and $R \sim t^{0.4}$, $R^3 \sim t^{1.2}$; hence, $P_f \times t^{1.2}$ is approximately constant. At long distances, the pressures are usually said to approach $1/R$. At this pressure level the distance is proportional to the time, ($U \cong c_0$), so $Pt =$ constant. When variable γ is introduced, the variations in γ and the departures from the strong shock conditions result in $P \sim 1/R^{0.275}$ at a time when $R \sim t^{0.4}$, whence $Pt^{1.1} \cong$ constant. At pressures around 1 psi the shock is not yet sonic and corresponding variations in these powers also result in a proportionality of the form: $Pt^{1.1} \cong$ constant. This suggests a convenient form for a simple, approximate integration for conditions at the shock front for forming analytic expressions over a wide range of pressures. Since the shock velocity is related to the overpressure by

$$U/c_0 = \sqrt{(6/7)(P_f/P_0) + 1}$$

and

$$P_f/P_0 = A/t^{1.1}$$

it follows that

$$U/c_0 = \sqrt{(6/7)(A/t^{1.1}) + 1}$$

and further

$$dR = \int \sqrt{(6/7)(A/t^{1.1}) + 1} dt$$

This form of expression ought to give a considerably better approximation than the terminated series, sometimes used, of the form

$$R = \sum A_n t^n$$

The result that $Pt^n =$ constant, with $n \cong 1.1$ is a simple statement which applies from strong shocks with variable gamma down to regions where Fuchs' term of the $P \sim 1/R \sqrt{\log R}$ applies. Through the Rankine-Hugoniot conditions, it then completely defines all the shock conditions, and with this as a boundary condition, it defines the wave forms on the interior. So, the whole history of a shock wave could be described from this result. With this discovery one asks if there is any inherent property of shocks which makes it so, or is it only a fortuitous compromise between $n =$

62

UNCLASSIFIED

UNCLASSIFIED

1.2 and $n = 1.0$. If there were a good physical reason, it would provide a completely new basis for solving the propagation of a blast wave.

2.4.2 Hydrodynamic Variables on the Interior of a Wave

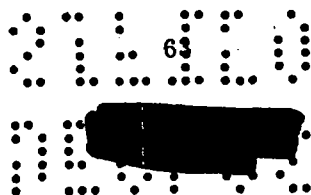
The curves in this section are a novel presentation intended to permit a rapid determination of the wave forms for static pressure, dynamic pressure, density, material velocity, or mass coordinates for any yield or atmosphere. The wave form may be obtained at constant distance as a function of time, at constant time as a function of distance, or along any arbitrary path desired in the $r-t$ plane.

On each curve the line marked "shock front" is the time of arrival curve. On the interior of the wave the positive or negative durations (where applicable) may be read from the difference in time at the shock front to the time when the variable in question passes through ambient conditions. Similarly, the positive wave length may be read from the difference in distances at the shock front at the time in question to the corresponding distance at which the variable in question passes through ambient conditions. It should be noted that the positive duration and positive wave length are different for each variable.

The method for obtaining the wave forms is similar in all figures, Figs. 2.4.2-1 through 2.4.2-5, which we will illustrate with the case of the pressure level at 1000 ft. To obtain the pressure vs time wave at this time for 1 KT, place a straight-edge along the line "1000 feet." The pressures and corresponding times are read directly at the intersection between the straight-edge and the isobars. It is even more convenient to use the bottom edge of a piece of log paper (semi-log or log-log)* as the straight-edge, if the functional modulus of the paper is the same as the graphs here. The pressure wave may then be plotted directly by extending a vertical line upward from the intersection of the paper and isobar and posting the pressure on any convenient ordinate. If desired, the wave form may then be transformed into any other set of coordinates.

For convenience, a scaling line has been drawn which illustrates the method of transforming the results to other yields. This scaling almost demands the use of these graphs on standard size paper. Tick marks are provided for 1, 2, 5, 10, 20, 50, 100, 200 and 500 KT, and 1 MT. First use or draw up a transparent 1×1 cycle logarithmic paper of the same functional modulus both in radius and time as the original, but with the coordinates labeled to suit the yield in question. Now,

* These were originally drawn on Keuffel & Esser Co. No. 359-100L logarithmic 1×1 cycle. Master ozalid copies (the original on this standard paper) are available through J-10 at LASL, and considerably facilitate the procedure.



UNCLASSIFIED

UNCLASSIFIED

slide the 1000 ft and 1 sec intersection of the transparent paper up or down 45° along the scaling line until that intersection falls on the appropriate yield. This procedure automatically scales both space and time to the yield in question and the wave forms at the proper distances and times may be read directly as illustrated in the previous paragraph for 1 KT. If the ambient atmosphere is different from $P_0 = 1$ bar the procedure is modified by using $(W/P_0)^{1/3}$ as the energy invariant instead of simply $W^{1/3}$. If the ambient sound velocity is different from 1138 ft/sec, an additional shift of the transparent sheet is required: to the right if $c_0 > 1138$ ft/sec, to the left if $c_0 < 1138$ ft/sec.

For the region in question, the density variation may be determined from the pressure curve nearly as well by using the adiabatic law as by using the density curve presented here. If it is desired to provide independently for the variations from the adiabatic law due to the different entropy, the following procedure may be used. Locate the point in question on the interior of the wave on the mass motion graph. Follow this mass motion line backward in time and until it intersects the shock front at this radius and time; the peak shock pressure and density may then be read from the table in Appendix A. The adiabatic law may safely be applied using $\gamma = 1.4$, when the pressures involved are less than 10 atmospheres. At higher pressures, a similar procedure would be followed by reading the shock values directly from the figures in Section 2.2.2 and following the corresponding adiabat down to the pressure at the time in question.

The hydrodynamic transport velocity is often of interest. The local sound velocity on the interior of the wave form may be calculated from the pressure using the adiabatic law or, if desired, by reading pressure and density both, and using the equation $c = \sqrt{\gamma P/\rho}$. In this connection, a point is often confused in the current literature. It is often assumed that the end of the positive pressure phase moves with ambient sound velocity as if positive durations were the same for all three variables, pressure, material velocity, and sound velocity. Examination of these figures or hydrodynamic considerations show that this cannot be the case. At the end of the positive pressure phase, the material velocity still has a forward component, and will not become zero until deep in the negative pressure phase. Because of the initial entropy change across the shock front, the sound velocity is also above ambient at the end of the positive pressure phase. A correct statement is that the end of the positive pressure phase always moves with a velocity greater than c_0 . Similarly, at the depth of the negative phase, sound velocity will be less than c_0 and the material velocity will usually be in a negative direction at this time. Hence, a correct statement here is that the negative phase always travels slower than ambient sound velocity. At the end of the negative pressure phase the sound velocity is again above ambient because of entropy changes, and the

UNCLASSIFIED

01:10

UNCLASSIFIED

UNCLASSIFIED

material velocity may again be more positive than at the depth of the pressure negative phase. Thus, there is a point near the end of the negative phase which travels faster than the depth of the negative phase preceding it. This "catch up" velocity is important because it enhances the production of secondary shocks on the interior of the wave near the end and depth of the negative phase.

It is sometimes incorrectly assumed that all sound signals on the interior of a shock wave eventually catch the shock front. The existence of the point at the depth of the negative phase, which travels more slowly than c_0 , which, in turn, is slower than U , constitutes a barrier preventing small signals from ever catching the front. It is, of course, possible for a finite shock of sufficient strength to be supersonic in the local medium and pass over the negative phase. However, in most cases the accumulated signals on the interior will not be this strong and the two shocks may run behind one another forever. In much the same way, other pressure signals are trapped in a series of oscillations behind the first positive and negative phases.

2.5 THERMAL RADIATION

2.5.1 Total Thermal Energy of the Bomb

In Section 2.1.4 it was shown that the entropy change associated with strong shocks resulted in pronounced residual heating on the interior of the fireball. This gives rise to the principal difference between a nuclear and a small-charge explosion, namely, the fireball and the thermal radiation from it. The basic phenomena have been described in Chapter VI of Effects of Atomic Weapons. The time dependence of the radiation rate for a nominal bomb has been estimated in Fig. 6.20 in that publication and it will be made the basis for the discussions concerning thermal radiation in this and succeeding chapters.

The main features of the thermal radiation from the bomb are briefly reviewed as follows. Following the initial detonation, the radiation rate from the bomb rapidly rises to a maximum in a fraction of a millisecond and thereafter begins to fall sharply. A minimum in the radiation rate occurs around 15 msec for a nominal bomb and thereafter the radiation rate rises to a second maximum around 0.2 to 0.4 sec. For convenience, the figure in Effects of Atomic Weapons was plotted as the log of the radiation rate vs the log of the time. This distorts the impression one would obtain from a linear plot. Only a very small fraction of the total radiation is emitted prior to the light minimum, at which time the radiation rate falls effectively to zero. The effective fraction of thermal radiation occurs relatively late compared to most phenomena, other than blast, in a

65

UNCLASSIFIED

UNCLASSIFIED

nuclear explosion. The bulk of the radiation comes during the period from 0.2 to 1 sec at rates which are several hundred times greater than at the minimum, or at times like several seconds.

Figure 2.5.1 is a linear plot of Fig. 6.20 in Effects of Atomic Weapons. Since the thermal radiation rate was given, this graph can be readily integrated to obtain the total thermal energy of the bomb by performing the integration

$$Q_T = \int_0^{\infty} (dQ/dt) dt$$

where dQ/dt is the height of the curve and the figure suitably normalized at any distance desired. It is thus found that the total thermal energy of the bomb is 8.4×10^{12} cal, or about 42% of the specified nominal yield of 20 KT.

In a later part of the section we will postulate that the "total thermal energy" of the bomb is more like 100% of the yield and meanwhile it is instructive to consider roughly the decay rate of the thermal radiation tail. A rigorous consideration of this problem presents enormous difficulties in the detailed physics of the radiative transport interacting with shock hydrodynamics. However, since radiation rates, temperatures, and emissivities are often expressed in power laws, it seems reasonable to make estimates for the power dependence in the late history of

$$dQ/dt \sim 1/t^n$$

We question whether the sharp cut-off in Fig. 6.20 near 3 sec is real or will persist, and wonder why an abrupt change should occur so late after that maximum. A temporary drop could be real and the reason is the very low opacity (and hence emissivity) of cold air, but this merely delays the emission of radiation, and would thus sustain the rate at still later times. At late times most of the heated air is returned to ambient pressure, and at a corresponding temperature, which is higher than ambient. Assume all elements of the air radiate with the temperature dependence like

$$dQ/dt \sim \epsilon(T) F(T) \sim T^b$$

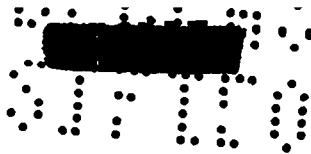
where we include the dependence of emissivity on temperature as part of the power b . In a radiating mass of gas, the temperature will fall according to the heat remaining from an original Q_0 , after $Q(t)$ has radiated away. If the specific heat is independent of the temperature

$$T \sim (Q_0 - Q)$$

After substituting for T , we have

66

UNCLASSIFIED



UNCLASSIFIED

$$\frac{dQ}{(Q_0 - Q)^b} \sim dt$$

After integrating this expression, we have

$$\frac{1}{(Q_0 - Q)^{b-1}} \sim t$$

or

$$t \sim (Q_0 - Q)^{1-b}$$

With

$$T \sim (Q_0 - Q) \sim t^{1/1-b}$$

it follows that

$$dQ/dt \sim T^b \sim t^{b/1-b} \sim 1/t^{b/b-1}$$

or

$$n = b/b - 1$$

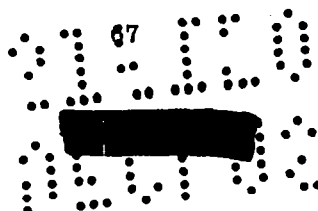
A median value of b might be 4 from the Stefan-Boltzmann law and a black body model, whence $n = 1.333$; some higher power is applicable if emissivity falls with temperature, whence, for $b = 5$, $n = 1.25$; or some lower power, whence, for $b = 3$, $n = 1.50$. These would seem to be high estimates of n , for if the radiation rate fell because part of the radiation was absorbed in some special process, the captured radiation would later re-radiate and sustain the tail fraction, thus lowering the value of n . If the emissivity falls, it will similarly sustain the rate at later times. From this we cannot definitely conclude that the sharp break at 2 sec in Fig. 6.20 is wrong, but if it is real there is little reason to expect a sharp break in slope at this time to continue for all time.

Conservation of energy also places restrictions on the decay rate. Specify τ as the time when the tail begins to behave like

$$dQ/dt = A/t^n$$

Then the radiation in the tail to infinite times would be

$$\Delta Q(\tau < t < \infty) = A \int_{\tau}^{\infty} dt/t^n = \frac{A}{(n-1) \tau^{n-1}}$$



UNCLASSIFIED

UNCLASSIFIED

It is clearly required that $n > 1$ in the tail, or the integral would diverge to infinite total thermal energy. Even for $n > 1$, there is a substantial contribution in the tail for small $n - 1$.

Because the radiation rate is quite low at times like 2 or 3 sec for a nominal bomb, there is a strong temptation to regard the radiation up to these times as the total thermal radiation. But a comparison of the thermal radiation integrated to infinite time for $1 < n < 1.5$ with the integrated thermal radiation to time τ , shows that such a tail fraction is so large that it is entirely ambiguous to speak of "total thermal radiation" at times like several seconds. One might speak of $Q(\tau)$ as the "effective radiation," but this depends in turn on an arbitrary convention for selecting τ .

This comparison between $Q(\tau)$ and the tail fraction can be done carefully on a specific pulse shape curve but the relative magnitude of the tail fraction can be illustrated as follows. From Fig. 2.5.1-1 the radiation rate over the entire sphere at 2 sec is $0.94 \times 10^7 \frac{\text{cal R meters}^2}{\text{cm}^2 \text{ sec}}$ which gives for the entire fireball

$$A = 4\pi \times 0.94 \times 10^{11} \text{ cal/sec}$$

The entire area under the curve to 3 sec integrates to 42% of the nominal bomb; by 2 sec, 93% of that has been radiated, which is 39% of the energy of the bomb or 7.8×10^{12} cal. The decay rate is then limited by the total energy so that no more than 12.2×10^{12} cal could be radiated later than 2 sec.

$$12.2 \times 10^{12} \text{ cal} \cong \frac{A}{(n-1) \tau^{n-1}}$$

or

$$(n-1) 2^{n-1} \cong \frac{4\pi \times 0.94 \times 10^{11}}{12.2 \times 10^{12}} \cong 1.0$$

This is solved with $n \cong 1.65$. A repeat of this calculation at $\tau = 1$ sec gives $n \cong 1.23$. It also means that the total thermal energy is 100% if n has values between 1.25 and 1.50. Between 1 and 2 sec, Fig. 6.20 actually shows a slope of -1.43 .

The suspicion that the decay slope should not change abruptly at 2 sec, and the low value of n for $1 < t < 2$ in Fig. 6.20 makes one suspect further that a large fraction of thermal energy may be involved in the long tail after 2 sec, and we should try to estimate the total for reasonable limiting values of n , without reference to the shape of the curve in Fig. 6.20. Writing the total thermal radiation as Q_T and the radiation up to time τ as Q_τ

UNCLASSIFIED

UNCLASSIFIED

$$\begin{aligned}
 Q_T &= \int_0^{\tau} (dQ/dt) dt + \int_{\tau}^{\infty} (dQ/dt) dt \\
 &= Q_{\tau} \left[1 + \frac{A}{Q_{\tau}^{(n-1)} \tau^{n-1}} \right]
 \end{aligned}$$

The term in the brackets involving A is the relative thermal yield in the tail fraction. Now some manipulation of the function Q(t) will show that a reasonable approximation during times from the maximum to 1 sec is

$$Q(t) = Q_{\tau} (t/\tau)^{1/2}$$

whence

$$(dQ/dt)_{\tau} = Q_{\tau}/2\tau = A/\tau^n$$

so

$$A \cong \frac{Q_{\tau} \tau^{n-1}}{2}$$

Using this approximation, we obtain

$$Q_T = Q_{\tau} \left[1 + \frac{1}{2(n-1)} \right]$$

From this we conclude that for $n = 1.5$, the tail fraction is equal to the so-called "total thermal radiation" Q_{τ} , and for $n = 1.25$, the tail fraction is twice the "total thermal radiation."

To summarize the findings in this section, we can say:

- (a) The sharp logarithmic decay in radiation rate in Fig. 6.20 is probably not real forever, and the final rate should be more like $n = 1.50$,
- (b) If the final rate is from $n = 1.25$ to $n = 1.50$ the tail fraction is such that the total thermal radiation will approach the entire energy of the bomb.

The decay rate for $n = 1.50$ is shown as a dotted line in Fig. 2.5.1-1. The differences from the original curve are hardly detectable in the interval 1 to 2 sec. It will be shown in a later section that these differences are unimportant in view of hydrodynamic perturbations to the radiation rate which could be observed at these and later times.

The discussion in Effects of Atomic Weapons leads to the general impression that the "total thermal radiation" from the bomb should be a constant fraction of the total yield, more or less independent of the yield. In the remainder of the present section we will question the simplicity of basic theoretical arguments presented here. In a later chapter we will require a more detailed

69

UNCLASSIFIED

UNCLASSIFIED

description of the thermal radiation rate and its implications, and will show that neither the "total thermal radiation" nor the "total" cal/cm² at a given point determines the effect of radiation; from this a new figure of merit for thermal radiation on thick slabs will be suggested. In the remainder of this section a different presentation of the thermal theory will be undertaken, but it is instructive to first retrace the steps which lead to the constant fraction concept.

2.5.2 Black Body Model for Thermal Radiation

The description in Effects of Atomic Weapons for thermal radiation involved several assumptions which lead directly to the result that the thermal radiation is a constant fraction of the total yield. The first is that the surface of the fireball radiates as a black body following the Stefan-Boltzmann law, namely, the radiation rate per unit area is

$$dQ/dt \sim \sigma T^4$$

where

$$\sigma = \text{a universal constant of nature, } 5.67 \times 10^{-5} \text{ ergs/cm}^2, \text{ sec deg}^4$$

T = absolute temperature of the body

Another assumption involves the sharp cut-off in transmission of air for wavelengths less than approximately 2000 Å.

With these assumptions the constant energy fraction is readily deduced. One writes that at a given time, t, the fireball surface is specified by temperature T, and the total radiation from the bomb at that time has the rate given by

$$dQ/dt = 4\pi R^2 \sigma T^4$$

The fraction of the total radiation emitted which can penetrate a significant distance in air is said to be a function of temperature only. However, since the fireball itself is a hydrodynamic phenomenon and is expected to follow hydrodynamic scaling laws, it follows that, in scaling to a larger bomb, the same temperature will occur when the fireball radius is increased by a factor of $W^{1/3}$.

This implies that the radiation rate scales like

$$dQ/dt = 4\pi W^{2/3} R^2 \sigma T^4$$

To obtain the total energy from the bomb integrate the radiation rate over the time as

$$Q_T = 4\pi\sigma \int_0^\infty R^2(t) T^4(t) dt$$

But if the fireball scales hydrodynamically, the time variation also scales like $W^{1/3}$, so

70
UNCLASSIFIED

UNCLASSIFIED

UNCLASSIFIED

$$Q_T = 4\pi \int_0^\infty (W^{1/3} R)^2 T^4(t) (W^{1/3} dt)$$

This combination of $W^{2/3}$ from distance scaling and $W^{1/3}$ from time scaling results in the thermal radiation being directly proportional to the yield, as

$$Q_T = 4\pi W \int_0^\infty R^2 T^4 dt$$

The model also implies that the details of the thermal radiation, such as the minimum and the second maximum, should also occur at times which scale like $W^{1/3}$.

In the sections which follow the assumptions used in deriving the constant fraction will be examined in more detail. One of the questions asked is whether the surface area and temperature of the fireball alone determine the thermal radiation rate. If the radiating sphere is semi-opaque, so that there is a contribution in depth, there is probably a corresponding change in the scaling laws for thermal radiation. It is recognized that a rigorous solution is almost hopelessly complex, but by asking these questions, it could be hoped that the resulting description will be a step closer toward reality.

2.5.3 Radiation in Depth

It appears inadequate to treat a material like air as if it were completely opaque at one temperature and completely transparent at another. The opacity is not a qualitative difference, but represents a quantitative difference in the diffusion rate of photons outwards in a random walk from regions of high temperatures in the interior of a fireball to the low temperatures near an observing instrument several miles distant from it. The various cross sections for scattering and absorption are complex functions of the wavelength, direction, and physical state of the medium traversed.

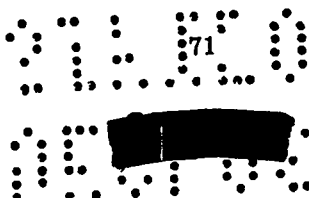
Considering absorption only, a different fraction of each wavelength from an interior particle is absorbed. The absorption might be described by the differential equation

$$dI/dx = -\lambda I$$

where λ may also depend on the temperature, density, physical state, and chemical composition of the absorber in dx . Assuming for simplicity that λ is independent of x , and, defining λ to be some average value over all wavelengths, the exponential absorption law follows

$$I/I_0 = e^{-\lambda x}$$

where x is the distance traversed. This elementary law states two factors which require a revision



UNCLASSIFIED

UNCLASSIFIED

of the simpler concept of thermal radiation: the degree of absorption through λ and the path lengths for absorption through x .

It is well known that a similar law is required to describe the radiation received at long distances, but it is usually assumed that when there are proper transmission characteristics, one could correct back to the source. Here we are doing something different by applying the absorption concept to the source itself.

These considerations suggest that the radiation rate of the bomb, especially as observed beyond the shock front, should not be as in the original equation, but should be replaced by a more complex expression, perhaps like

$$dQ/dt = 4\pi \int_0^R \int_0^\infty r^2 \epsilon(r) \sigma T^n(r) f[R-r, \theta, \lambda(\nu, r)] dr d\nu$$

where f itself is some complex function which describes the complex behavior of the absorption in the path length between the radiating particles at r and the shock front at R . This integral is intended to state that the radiation we see beyond the shock R is the sum of contributions in depth from shells of radius r and thickness dr . Each shell is characterized by its own temperature, T , a function of the radius r , and near the front of a strong shock this temperature falls rapidly with increased radius because of the different entropy changes. Associated with each temperature may be a different absorption coefficient for each wavelength from farther in the interior. The radiation which eventually escapes the shock is also a function of the kind and quantity of material lying between the interior and the exterior of the shock, which is indicated by the function f . Now, it is the introduction of the path length in f which should result in the failure of thermal radiation to scale like W . The form of the equation is not unlike the original. To the extent that radiative transport is relatively slow near the shock front, the state variables affecting absorption and re-emission are controlled primarily by the blast hydrodynamics, and these should scale. The angular dependence also scales. So, by this simple argument, one states that fraction f will be smaller for larger bombs because the path lengths $R-r$ near the shock front will be proportional to $W^{1/3}$ over some range of yield. The argument is not universal because, for a small enough bomb, the absorptive zone could be small compared with any mean free paths, and absorption arguments are not applicable; for large enough bombs (like the sun) the mean free path is negligibly short in comparison with other lengths, and true black body concepts apply. However, in the range of interest where we assume that semi-opaque conditions apply, it is noted that

$$dQ/dt \approx \text{constant} (W^{1/3} R)^2 \sim W^{2/3}$$

UNCLASSIFIED

UNCLASSIFIED

but the term f will be such that at hydrodynamically scaled times and distances, f is a decreasing function with yield, so

$$dQ/dt \sim W^{2/3} f \sim W^n$$

where $n < 2/3$.

If the assumptions leading to an elementary exponential absorption law were applicable, the factor f would be an exponential like $e^{-\lambda \rho W^{1/3}(R-r)}$, the yield dependence might be conceived of as taking place over a limited range of yields, something like

$$dQ/dt \sim W^{2/3} R^2 e^{-W^{1/3} \rho \lambda r}$$

In diffusion processes, where the mean free path is short, the dependence on a path length x might be like e^{-x^2} instead of simply e^{-x} . Since the argument is only qualitative, assume a simple exponential form for illustrative purposes only and the effect of the $W^{1/3}$ in the negative exponent is of interest. When the yield is small, or effectively zero, the value of the exponential is close to 1, and there is no spatial effect on thermal scaling because of longer path lengths for absorption. Hence, $Y \sim W$ where Y is the thermal yield. Nothing is said here nor implied for what values of W this occurs. As the value of $W^{1/3}$ increases there is a range over which the failure of scaling could be approximated through

$$e^{-x} \cong (1 - x) \quad \text{for } x \ll 1$$

This means that over a higher range of yields the thermal yield will not quite scale with the total yield. For example, over a certain range we could arbitrarily choose a certain variation like $W^{0.92}$ which implies that over this range the thermal radiation would be less than expected from straight scaling, falling slowly at higher yields. For larger values of W this approximation fails in turn, and one would require a rigorous expression for the exponential. In a high range of yields the thermal radiation rate from the bomb would be almost limited by the exponential absorption. When the value of x is small, then a fivefold change in yield increases the exponent from $x = 0.01$ to $x = 0.05$, and reduces the thermal radiation (from a constant fraction) to 0.99 in one case, and to 0.95 in the second case—a difference which may be too small to detect within the scatter of experimental observation. When x is originally large, say, a number like 2, a fivefold change in yield would then reduce the thermal radiation from a factor of $e^{-2} \cong 0.14$, down to $e^{-5} \cong 0.00675$, for a total of 20 times from a constant fraction.

73
UNCLASSIFIED

UNCLASSIFIED

UNCLASSIFIED

For a range of still larger explosions, it is probably true that the black body concept would again apply everywhere in the history, and, here again, the constant fraction concept might be applicable but, of course, a much smaller fraction than in the range of low yields.

The above arguments are intended to be merely qualitative, but are sufficient to show that the radiation rate (and by implication the total effective thermal radiation) is not a constant fraction of the total yield, but might generally be described as a concave downward curve on logarithmic coordinates, falling to a lower fraction at high yields, as indicated in Fig. 2.5.3-1. The figure is also intended to be only qualitative.

The absorption coefficient λ is dependent on a large number of factors: the temperature of the absorbing air, its density, physical state, and chemical composition and the wavelength of the radiation itself. In *Effects of Atomic Weapons* the assumption is made that a certain critical wavelength exists, around 2000 Å, below which cold air is completely opaque, and above which the air is completely transparent. This is an idealization; the absorption coefficients for cold air are shown in Fig. 2.5.3-2. While it emphasizes the essential physics, the cut-off concept is not adequate for temperatures with spectra containing a great deal of energy in the range between 1400 and perhaps 3000 Å. By the Planck distribution these wavelengths are the maxima corresponding to 25,000 and 10,000°—roughly the temperature of the shock during early fireball growth before breakaway. During earlier stages of growth, nearly the entire fraction of radiation from the interior will be absorbed in the zone of high density near the shock front or the cold air just ahead of it. When the temperatures fall considerably below these values, the spectrum is distributed over longer wavelengths, to which the air is more transparent. In this general region, the absorptive path lengths play a significant role in affecting the scaling, for here the fraction of energy which is captured near the shock front will be a function of the thickness of the absorptive zone behind the shock front, in a complex way. In summary, the f_0 referred to in Equation 6.11 of *Effects of Atomic Weapons* is dependent on yield, and decreases with yield.

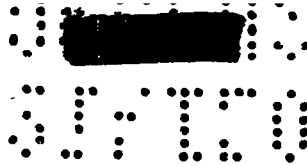
It is only during this period that the concept of "partition of energy" has any real meaning in the sense that it separates the fraction of bomb energy which appears as blast from a fraction which appears as thermal radiation. During the very earliest stages of bomb growth nearly the entire energy of the bomb is present as radiant energy in which the energy density is given by

$$E \sim \frac{4 \sigma T^4}{c}$$

where, in this case, c is the velocity of light. At high enough temperatures this quantity greatly

74

UNCLASSIFIED



exceeds

UNCLASSIFIED

$$E_i = P/(\gamma - 1) \cong \rho T/(\gamma - 1) \text{ constant}$$

which, in a stricter sense, is the hydrodynamic energy. Because of the hydrodynamics, the interior of the fireball is much hotter than the regions near the shock front and much lower in density. Within this region radiation transport of energy plays a predominant role. As we approach the shock front the temperatures cool and density increases rapidly because, in general, the mean free path behaves something like T^3/ρ . By the analytic solution, for $\eta_s = 11$, $q = 30$

$$T^3/\rho \sim P^3/\rho^4 \sim \frac{[(1-k) + k(r/R)^{32}]^3 (\xi_s - 1)^3}{(r/R)^{120} \rho_s^4}$$

Once $k(r/R)^{32} \ll 1 - k$, the mean free path for radiation would behave like $1/r^{120}$. This means that an isobaric, isothermal, isopycnic sphere is formed on the interior of the shock but, at its outer edges, the very sharp drop in mean free path results in almost complete absorption. The zone between the isothermal sphere and the shock front then constitutes an absorptive zone in which the conversion of radiant energy to hydrodynamic energy may take place for some time after the shock itself has ceased to propagate by radiative transport.

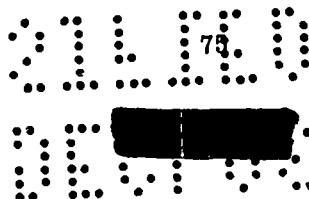
This zone is close to the shock front and provides the close connection between the interior and the shock front which makes the analytic solution possible. The degree and rate of support which it gives to the shock will vary from bomb to bomb as the thickness of the zone changes in hydrodynamic scaling, and is one of the fundamental reasons for the failure of similarity scaling for strong shocks.

We will investigate in a later section what fraction of the total thermal radiation of the bomb is likely to be involved in this partition of energy before breakaway.

The same concept of exponential absorption applies after breakaway, because most of the radiation on the interior is still at too short wavelengths to move any appreciable distance. To the extent that the absorption coefficients depend on the temperature and density of air, the paths for hydrodynamic invariance scale like $W^{1/3}$ and, on a scale basis, the absorption-heating process is held down, almost as if the absorption coefficient increased by $W^{1/3}$.

2.5.4 Absorption External to Sphere of Effective Radiation

The usual equation which expresses the total incident number of calories at a point (R, θ) from the bomb is given by:



UNCLASSIFIED

$$Q_T = \frac{Y \cos \theta e^{-\text{const } R}}{4\pi R^2}$$

: : [REDACTED] : :
 : : [REDACTED] : :
 : : [REDACTED] : :
 : : [REDACTED] : :

UNCLASSIFIED

In general, the constant is considered as part of an over-all measurable "absorption per mile," related to visibility, and tables are so given in *Effects of Atomic Weapons*. By implication and usage, the constant is regarded as a function only of the local atmosphere, independent of a nuclear explosion and independent of time. In this section we investigate what is required to describe this absorption in more detail for practical considerations. The distinction between absorption within the sphere of effective radiation (in the previous section) as opposed to absorption external to it (in this section) is somewhat arbitrary, but has been made principally because the absorption external to the sphere of effective radiation is the only type which has been generally considered.

A large number of hydrodynamic phenomena influence the absorption constant both in space and time. The purpose of this section is to point these out, partly because they show the ambiguity in quoting "transmission" and, in turn, a thermal yield. They indicate a requirement for a criterion for thermal radiation which is less sensitive to these effects. So far as the effectiveness of total radiation at a distance is concerned, many of these have the same quantitative effect as shown in the previous section, because they introduce factors in the exponent for absorption which is of the form

$$e^{-\rho W^{1/3}}$$

Shock Dust

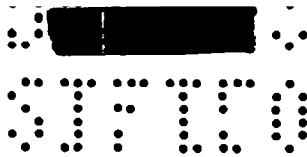
It is a major consideration of Chapter 4 (and of interest here because it affects the total thermal radiation) that dust raised by the shock at the ground surface shields the surface itself from further thermal radiation. At most distances of practical interest, the shock arrives shortly after the second maximum, and can readily reduce the "total cal/cm²" by a factor of 2. The effect depends on the local surface and is yield dependent through the length of the positive and negative phases for material velocity, which scale like $W^{1/3}$.

Dust and Smoke Raised by Thermal Radiation

This is a major consideration of Chapter 5 and is again of interest here for any object exposed to the radiation, not necessarily at the ground surface. The effect is most likely to occur during the rapid rise in radiation rate prior to the second maximum, and thus not only reduces the integrated calories markedly by a factor of 2 but, of more importance, it will reduce the maximum

76
 : : [REDACTED] : :
 : : [REDACTED] : :
 : : [REDACTED] : :

UNCLASSIFIED



CONFIDENTIAL

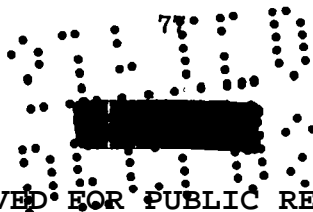
rate of thermal radiation which definitely influences the peak surface temperatures achieved. The fraction absorbed tends to be yield dependent for the thickness of the thermal layer, follows $Q(t)$ closely, and therefore scales like a hydrodynamic length. On the other hand, the effect tends to be self-compensating because the less radiation reaching the surface through absorption, the less dust and smoke will be raised.

Wavelength and Angular Dependence

The effectiveness of thermal radiation is a strong function of the wavelength and the angular dependence of the incident radiation, which are intimately connected with the spectral distribution. Both are effectively yield dependent because they depend on actual distances from the bomb, which are usually larger by $W^{1/3}$ at points of the same hydrodynamic interest, like peak pressure. They also depend, in good part, on other effects, such as the cloud chamber effect. They illustrate very well the ambiguity associated with total thermal radiation with respect to either effective thermal radiation or thermal effects. By conservation of energy we demand that the total thermal radiation approach 100% of the bomb, and whatever the absorption processes for thermal radiation, the entire amount should eventually reappear after successive conversions to hydrodynamic energy and entropy changes. So, the absorption process we speak of in transmissions less than 100% is, in the last analysis, only temporary, and in the long run does not affect the total thermal radiation. Absorption results in a smoothing out of the thermal pulse shape, which markedly reduces the effectiveness of thermal radiation, not only by reducing the radiation rate near its maximum, but also by converting it to longer (infrared) wavelengths where subsequent delays by H_2O and CO_2 absorption are much more acute. The analysis in a later section will show that about one-half the thermal radiation from the bomb would be at wavelengths below 2200 \AA and above $10,000 \text{ \AA}$ which are not transmitted directly in air over any reasonable length, and therefore in any reasonable time.

Normal Cloud Cover

This is a yield dependent effect in the crude sense that the expected integrated thickness of cloud covers increases as $W^{1/3}$ just as the distances of hydrodynamic interest increase as $W^{1/3}$. This is simply the observation that cloud cover would never be a matter of consideration on small-charge explosions. This effect by itself almost precludes the possibility of accurate predictions for thermal radiation.



CONFIDENTIAL

UNCLASSIFIED

Local Density and Temperature

The density changes the apparent thermal yield in a very fundamental way. According to previous discussions, the absorptive path lengths increase basically as $W^{1/3}$, absorbing larger fractions of energy on large bombs and probably changing the spectral distribution by absorbing some wavelengths differently from others in a nonlinear fashion. Primarily, it is the mass of absorbing material which counts and in the perturbations to the basic scaling ρ_0 behaves like $W^{1/3}$ in increasing the mass in this path length. If, in any way, the fraction of effective thermal yield or the radiation rate is believed to vary with yield, it follows that similar changes would result from a change in density corresponding to a change in $W^{1/3}$. Since the point about path lengths was originally argued from a perturbation, which goes like $W^{1/3}$, it means that we can equally regard the dependence as $\rho_0 W^{1/3}$.

The dependence on density could be argued in a different way. A reasonable model at late times is one in which the fireball is regarded as a hot motionless sphere after the hydrodynamic effects have passed. Regard the radiation as diffusing outward through the cold regions near the edge. ρ characteristically appears in the diffusion equation in such a way that one expects similarity variables to exist which depend on the square root of the density, but it is probably an understatement to call this argument oversimplified. There is a further effect of density through time dependence. In subsequent chapters it will be argued that, from the standpoint of effect, the longer time duration on large bombs decreases the effectiveness of the thermal radiation by the square root of times, or as $W^{1/4}$ since times scale like $W^{1/2}$. This is a perturbation from a simple dependence like $W^{1/3}$ scaling because of path lengths. If ρ_0 behaves like $W^{1/3}$ then we also expect that the effectiveness of thermal yield will be decreased through the time dependence.

Without a detailed consideration, it is not clear how ambient temperatures will affect these results. For those wavelengths which appear by direct transmission, the hydrodynamic temperature will be roughly proportional to the ambient temperature, and the radiation rates strongly decreased as the ambient temperature decreases. However, much of the radiation appears only after diffusion and degradation to visible wavelengths at the outside of the fireball or, that is, when certain absolute temperatures are reached near the fireball surface. In this case, much of the radiation which initially was at too short a wavelength to leak out through the fireball is shifted. In a colder atmosphere, this early spectrum is shifted closer to wavelengths in which air is transparent, and by these arguments the same amount of thermal energy could be delivered in a shorter time.

UNCLASSIFIED

UNCLASSIFIED

The above arguments on density and temperature are particularly applicable since they apply to the main radiation pulse. While they apply in the same measure to the thermal pulse before the minimum, this fraction has always been known to be small, and was originally estimated by Hirschfelder and Magee as something like 1% of the thermal energy. Even this fraction may be high and could be more like 0.3% so that, even if the effective fraction at this time is increased by a factor of 10, through decrease in density, there is no material change in the effectiveness of this portion of the radiation in producing effects. On the other hand, a very serious change in effectiveness of thermal radiation is associated with the suggestion that the main radiation pulse can be similarly affected by variations in local densities.

Cloud Chamber Effect

The cloud chamber is typical of these effects because it interposes a blanket of fog, literally and figuratively, between the fireball and an observer. With perfect spherical symmetry, the effect is very small because the process is principally one of scattering light, and the direct absorption is small. The thickness of the layer depends upon the local humidity and upon the yield of the bomb through the hydrodynamic length of that region in the negative phase which is below the dew point. The discrete water particles scatter light enormously, and the total absorption could be high after successive scattering into ground surfaces, even though only a small chance of absorption occurred after each scattering collision. Figure 2.5.4.-1 is a result of a study using the temperatures in the negative phase, as deduced from Figs. 2.4.2-1 to 2.4.2-4, and applied to the radiation rate of Fig. 2.5.1-1. It suggests that something like 25% of the total radiation could be screened by the cloud chamber if the tail fraction of Fig. 6.20, Effects of Atomic Weapons, is assumed correct. If, as we expect, there is a long tail fraction of radiation, which is not shown in Fig. 6.20, Effects of Atomic Weapons, then as much as 75% of the total thermal radiation could be affected except that, when the shock becomes weak enough and the air not saturated, the cloud chamber effect will lift as well as move outward.

With perfect spherical symmetry, all scattering, and zero absorption, the cloud chamber effect would be negligible, but the practical import arises from the lack of spherical symmetry. When ambient humidity is higher near the ground, and low at altitude, the cloud chamber should form roughly as a toroidal ring surrounding the burst or, in any case, with a cloud below the bomb and relatively clear air above. Then the inner surface of the cloud preferentially scatters light to altitude and away from the ground. The spherical symmetry is further destroyed by the presence of the ground surface, where the pure absorption probability is high for each photon scattered into

UNCLASSIFIED

UNCLASSIFIED

it. The cloud chamber effect suggests that the capture of thermal radiation near the ground in the negative phase can locally enhance the hydrodynamic energy there, increasing the positive phase length, but it is probably too deep within the wave, too late in time, and confined to a region too close to the ground to influence markedly the pressures at the shock front. The change in apparent thermal energy, as well as any hydrodynamic reinforcement, is of course expected to be more serious on large bombs than on small bombs and more serious for dense and humid atmospheres than for rarified and dry atmospheres.

Change in Air Density by the Shock

The variation in air density caused by the shock could conceivably change the effective transmission by changing the average density so that

$$\int_0^R \rho \, dr \neq \rho_0 R$$

For very small bombs or bombs fired in rare atmospheres, where the bulk of the thermal radiation comes out early, this effect would be part of the absorptive zone discussion in the previous section. For bombs of nominal yields, and in ordinary atmospheres, the effect is probably small also because the mean free path for air is very long for the radiation of interest. The effect is also small because of compensating effects. By conservation of mass for spherical waves, the average density from burst center to the shock is such that

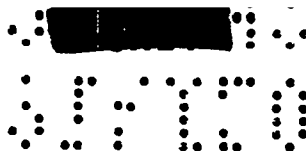
$$\int_0^R \rho \, dr < \rho_0 R$$

However, this occurs because most of the path is through the rarefied air of the isothermal sphere, the surface of which is regarded as the radiating surface. The average density from the end of the density positive phase at distance x to the shock front at R is certainly above normal

$$\int_x^R \rho \, dr > \rho_0 (R - x)$$

When and how much the transmission is increased or decreased depends on the detailed hydrodynamics in every case, with a realistic consideration of where radiative transport actually puts the isothermal sphere. Without recourse to a detailed discussion, the effect can be estimated as increasing the path of air by a length comparable to the positive phase length of the shock wave, and will not be serious until the positive phase length of the blast is comparable to the mean free path for light absorption.

UNCLASSIFIED



UNCLASSIFIED

Rise of Fireball

This could conceivably change the effective transmission by changing the distances to the bomb and carrying the fireball in or out of local strata of clouds, if present. It would be yield dependent because gravity does not scale. It can be shown, as a hydrodynamic exercise, that a weightless sphere (like the vacuous fireball) will rise with an acceleration of 2 g in any fluid. On large bombs, the whole time scale is increased and the fireball is not necessarily raised to a corresponding scaled height in

$$S = 1/2 at^2 = gt^2$$

However, even if the time of interest extended to 3 sec for thermal radiation of a nominal bomb, it would lead to a rise of 200 ft, which is only 2/3 the fireball radius. The fireball rise could be of academic interest in causing a change in the apparent radiation rate in the long tail; at 10 sec $S = gt^2$ gives a rise of 3200 ft.

Function I(t) as a Figure of Merit for Thermal Radiation

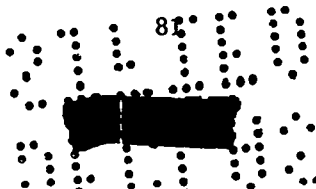
The ambiguity surrounding the total thermal yield in integrated flux need not be as distressing as it may appear at first. The fact is that neither the total thermal yield nor a critical cal/cm² usually determines the effect of thermal radiation. In the work on theory of surface effects in Chapter 5, we will derive a general solution to the conduction equation for an arbitrary flux rate, and an integral result which is useful and which can be integrated graphically.

The surface temperature of a thick slab exposed to thermal radiation at time t is related to the flux rate through

$$T_s(t) = \frac{a}{\sqrt{\pi h \rho \sigma}} \int_0^t \left(\frac{dQ/d\tau}{\sqrt{t-\tau}} \right) d\tau$$

where τ is a dummy variable for time. The constants in front of the integral are all characteristics of the material exposed to the radiation. They play the same role in this calculation as the ordinary concept of the critical cal/cm², except that such critical energy is yield dependent and has little meaning. We define the integral as I(t) and it is readily integrated graphically from the thermal pulse dQ/dt. Since this integral enters so directly into the calculation of surface temperatures, it is suggested that it be used to replace the concept of total cal/cm², which is ordinarily used to describe the same thing but which is, in fact, ambiguous.

In the succeeding section, (2.5.5), it is presumed that the total thermal radiation from the bomb is known, namely close to 100%. There is no need to express this quantity in view of all the



UNCLASSIFIED

UNCLASSIFIED

pitfalls which will be introduced through the transmission at late times. On the other hand, the function $I(t)$ represents the effective fraction of total thermal radiation.

In particular, one is not interested in the complete history of $I(t)$ but only in its maximum value, which is reached shortly after the second maximum. From this flux rate, the function $I(t)$ can be calculated until it reaches a maximum value. In principle, this is not much more difficult than integrating the area under a flux vs time curve, although there are some tricks which are useful in performing this integration. A point here, however, is that if the thermal flux shape is known up to the time t_{\max} , the maximum temperature is not affected by the shape of the flux curve afterwards or, in other words, by the "total thermal radiation." It is expected that the function $I_{\max}(t)$ will be yield dependent, but it further turns out that, to a reasonable approximation, $I_{\max}(t)$ scales in such a way that the surface temperatures actually behave like hydrodynamic variables. The most important aspect is that $I_{\max}(t)$ has a practical meaning on effects, whereas total thermal yield does not.

There are other practical advantages to the use of this function to replace the concept of total thermal yield because of the effects on transmission discussed in this section. The maximum in $I(t)$ appears shortly after the second thermal maximum and may be located approximately in time in the region in which the flux is decaying like $t^{1/2}$. With regard to the hydrodynamic effects discussed previously, the following comments are pertinent. Shock wave obscuration almost always occurs after $I_{\max}(t)$ is reached. Thermal dust obscuration will begin before $I_{\max}(t)$ but it seems likely that $I_{\max}(t)$ is probably less sensitive to thermal dust than is total thermal yield. The band width and angular dependence is of less serious importance because the long wavelengths are emitted at a slow rate and do not contribute materially to the maximum surface temperature or the effective total thermal radiation. Normal cloud obscuration will affect $I(t)$ just as it does the effective thermal yield, but one worries less about the rise of the fireball changing the cloud obscuration. The maximum in $I(t)$ occurs before the cloud chamber effect sets in and the figure of merit is thereby not affected by it. The density compression in the shock front would affect it, but could be taken as part of the over-all yield dependence. Since $I_{\max}(t)$ occurs relatively early there is little worry about the fireball changing the path length or moving it into local cloud cover. The local density and time dependent details of the radiation affect $I(t)$ but are much more meaningful when the results are interpreted in terms of surface temperatures.

82

UNCLASSIFIED

UNCLASSIFIED

2.5.5 Effective Thermal Radiation from Space and Time Dependence

If we accept Fig. 6.20 of Effects of Atomic Weapons as approximately representing the thermal radiation rate of the bomb during most of the main pulse, then it is readily shown that the strength of the shock front is not strongly connected with the thermal radiation emitted. By the time the thermal radiation from a nominal bomb has reached its maximum rate, near 0.2 sec, the shock pressure is near 100 psi, the shock radius near 800 ft; but the fireball radius is only 400 ft, and its pressure has returned close to its ambient value. For pressures of practical interest, well below 100 psi, the shock front is even more separated from the fireball. A homely example is this: If it is possible for an observer to feel the shock front pass at a time when the bomb is still radiating, it is clear that some sort of an inner core is the principal source of the radiation and is well detached from the shock front. In this paper, we divorce ourselves completely from the temperatures of the shock front in describing thermal radiation and choose instead the criterion that the radiation is principally controlled by the residual temperatures left in the air, after the air has returned to ambient pressures and the shock wave history is essentially complete for the material in question.

In Section 2.1.4 it was shown that

$$\eta_f = \frac{\mu \xi_s + 1}{\xi_s + \mu_0} (1/\xi_s)^{1/\gamma}$$

If we accept the ideal gas law as a rough approximation, it follows that the residual absolute temperature will be inversely proportional to this final density. Consider a gram of air, originally shocked to a pressure ξ_s . Its excess temperature will be given by $T/T_0 - 1$, and the residual absolute temperature of this air is given by

$$T_f/T_0 \cong \frac{\xi_s^{1/\gamma} (\xi_s + \mu_0)}{\mu \xi_s + 1} = (1 + P_f)^{5/7} \cdot \frac{(P_f + 7)}{6 P_f + 7}$$

where P_f is now the overpressure in atmospheres and γ is assumed to be 1.4. We will require the behavior of this function at low values of pressure. To obtain this dependence we will split the right-hand term into two parts. The first part expands as an infinite series by the binomial theorem

$$(1 + P_f)^{5/7} = 1 + 5/7 P_f - (1/2 \cdot 5/7 \cdot 2/7) P_f^2 + (1/6 \cdot 5/7 \cdot 2/7 \cdot 9/7) P_f^3 - \dots$$

The second part is a quotient which expands as

UNCLASSIFIED

UNCLASSIFIED

$$\frac{7 + P_f}{7 + 6P_f} = 1 - 5/7 P_f + 30/49 P_f^2 - 180/343 P_f^3 + \dots$$

These series may then be multiplied together and the interesting result is that the first three terms of the product drop out. This is the third order difference mentioned in Section 2.1.4. After dropping out higher terms, we have remaining a heat Q_f , which is capable of radiating by virtue of its elevated temperature.

$$Q_f \sim T/T_0 - 1 \sim 10/343 P^3$$

Now assume that at low pressures the overpressure follows a law given by

$$P \sim 1/R^n$$

It is often assumed that the exponent n is exactly 1 at long distances. However, if we now integrate the energy potentially capable of radiation by residual heat, it will be the sum of contributions from shells of radius R , and thickness dR , and the heat per unit volume within each shell will be proportional to $1/R^{3n}$. The total residual heat then becomes $\sim 4\pi \int R^2 dr/R^{3n}$. This integral will diverge for all values of $n \leq 1$. Hence, it follows that the pressure wave must decay by some value of $n > 1$, otherwise we would imply an infinite amount of heat left behind the shock. On the other hand, the shock wave itself does exhibit powerful tendencies to behave like $P \sim 1/R$, because of the sonic approximation at long distances. This competition itself leads to a reasonable compromise: That all the energy of the bomb finally appears as residual heat left behind the shock, and this is the eventual death of the shock wave which controls the pressure decay at long distance.

Figure 2.5.5-1 is a plot of this residual heat as a function of the radius R , which was roughly estimated from the free air curve of Appendix A.

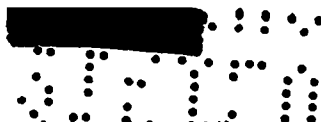
Having plotted $R^2 \Delta T$, the area under this curve represents the total energy of the bomb. The temperatures are also proportional to Q_f . A striking result from this figure is the large amount of heat contained in the immense volumes at low residual temperatures.

The radiation rate strongly affects the effective thermal radiation. The radiation rate is roughly proportional to T^4 according to the Stefan-Boltzmann law. This function $dQ/dt \sim T^4$ is also plotted on a relative scale on the figure as a dashed line. From this it is clear that a sharp cut-off occurs from air initially at 300 ft for a 1 KT bomb. So, one can say, as a result of this combination of a large entropy difference, and the T^4 dependence in turn, that residual heat from material initially beyond 300 ft from the burst center will never contribute materially to the thermal radiation rate which may appear to an external observer.

84

UNCLASSIFIED

UNCLASSIFIED



The effective thermal radiation may be deduced from these simple concepts from Fig. 2.5.5-1. First, one may say that no radius inside of 50 ft will contribute strongly to the early thermal radiation; most of this radiation will have been absorbed near the shock prior to the light minimum. This fraction of radiation, so trapped, eventually appears principally as blast energy. On the other hand, the radiation rate from material beyond 300 ft is too slow in comparison with radiation from material inside of 300 ft to be recorded on an instrument or to affect surface temperatures of irradiated objects. By comparing the area between 300 and 50 ft with the total area under the curve, one finds that the ratio is approximately 50%. If it were possible to build a device which could measure extremely low radiation rates and if it were possible to confine the atmosphere surrounding the explosion, one might very well find 100% of the bomb's energy present, over all wavelengths and in infinite time. There is a further reason, however, why even this 50% is an overestimate. The bulk of the radiation in the tail exists at low temperatures, and for wavelengths above 10,000 Å the air is quite opaque because of absorption bands due to both CO₂ and water vapor. Hence, it follows that the contribution from material at these low temperatures is almost bound to be absorbed successively, again well behind the shock front or, in any case, within a reasonable distance from the bomb.

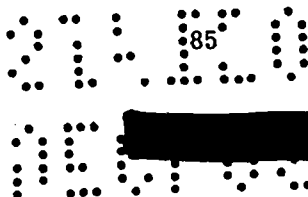
It is reasonable to question how absorbing lengths can be involved which scale like $W^{1/3}$, as in Section 2.5.3 when, at the same time, most of the radiation comes from material deep within the shock, which is assumed to have returned to ambient pressure. The answer is in part the absorption external to the sphere of effective radiation, which is controlled by shock parameters, such as the cloud chamber effect, and $\int \rho dr$. But, in addition, the absorption coefficients are sensitive to density and temperature and the radiation must diffuse through air which is left at certain residual temperatures and densities, with path lengths varying as $W^{1/3}$ in scaling.

The time dependence of the radiation rate from the bomb falls naturally into three categories: before the light minimum, during the minimum, and during the second maximum.

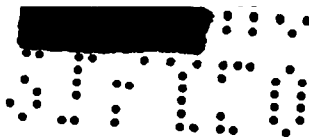
As has been previously discussed, the period before the light minimum constitutes a period during which absorption is nearly complete. With the absorption model assumed in the previous section, we may now describe the meaning of the light minimum. Prior to the light minimum pressures are approximately proportional to $1/R^3$ and temperatures follow a similar law

$$T \sim 1/R^3$$

Then, according to the Stefan-Boltzmann law, the radiation rate per unit fireball area goes as



UNCLASSIFIED



UNCLASSIFIED

$$dQ/dt \sim T^4 \sim 1/R^{12}$$

But during this period of strong shock, the radius of the shock is roughly given by

$$R \sim t^{0.4}$$

from which it follows that

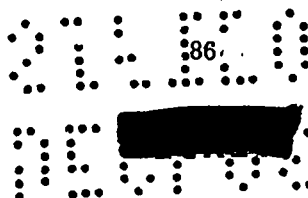
$$dQ/dt \text{ (total)} \sim 4\pi R^2 T^4 \sim 1/R^{10} \sim 1/t^4$$

This is the same time dependence as shown in Fig. 6.20, Effects of Atomic Weapons, between 0.2 ms and 10 ms. At this time, however, the shock front and the interior have cooled to more transparent wavelengths, and a greater fraction of the interior radiation is seen by an external observer. The increase in the transmitted fraction partially offsets the decrease in radiation rate due to the cooling-expansion of the fireball, and the radiation rate curve becomes concave upwards on a logarithmic plot. Eventually, as the fireball temperatures pass into more and more transparent wavelengths, the compensation in rates is complete. We could, therefore, define the minimum as the time at which the rate of decrease in dQ/dt , due to cooling, is exactly equal to the rate of increase of dQ/dt by the change of transmission for the wavelengths involved. In other words, the minimum does not occur because of some sort of a minimizing process, but quite the opposite, because of the presence of increasing transmission.

As pointed out in Effects of Atomic Weapons, the formation of oxides of nitrogen in the air probably contributes strongly to the low surface temperatures near breakaway. Such compounds probably deepen the minimum and delay it in time. However, the presence of such compounds is part of the argument for the role of absorptive path lengths, and does not negate the qualitative arguments presented previously.

As the fireball cools further a greater fraction of energy is present in wavelengths to which air is transparent and absorptive compounds will disappear so dQ/dt will continue to rise. Because of the energy so radiated, this reservoir on the interior will eventually be depleted. Sooner or later the rate of decrease caused by cooling and depleting will just offset the increase due to transmission. In a way similar to that for the light minimum, we can define the second maximum as that time at which these rates all cancel.

With these definitions of the minimum and second maximum, there are marked changes in the concept of how these details of the thermal radiation rate ought to scale in time. Without entering into the enormous complexity of the details involved, one can say something about the time dependence of thermal radiation.



UNCLASSIFIED

UNCLASSIFIED

Conservation of energy will place gross restrictions on the time dependence. We require that in the long run, all the energy is degraded to thermal and there must exist some $Q_T \cong W$ such that

$$Q = \int_0^{\infty} dQ/dt dt \sim W$$

By the conventional model, $dQ/dt \sim R^2$, and with the fireball scaling hydrodynamically in size, this alone would demand that time scale like $W^{1/3}$. However, by an absorption model during early stages, dQ/dt is less than proportional to $W^{2/3}$, and this demands that times scale with a correspondingly larger dependence than $W^{1/3}$. In reality, the situation is much more complex than can be described in a simple manner because the "highness" or "lowness" will be different for changes in yield at different times. Nonetheless, if it were possible to draw normalized radiation rates for bombs over a limited range of yields with $dQ/dt \sim W^n$ then the time scale must also be restrained to behave like W^{1-n} . In particular, $n < 2/3$, so time must scale by a power greater than $1/3$; the next obvious gross choice is a whole number fraction like $1/2$.

The scaling law is expected to be different for each wavelength, depending on the degree to which it is initially absorbed. For some wavelengths and path lengths $W^{1/3}$ scaling could well apply. For other path lengths the phenomenon could be considered a diffusion process. In nearly any diffusion and conduction process in which the parameter is constant, and the mean free path short, the differential equations are such that similarity variables can be formed, involving linear distances and the square root of the time as x/\sqrt{t} . During the late fireball stage, it might be regarded as a hot sphere of gas, at ambient pressure, with little or no material motion; some fraction of the radiation could be described by such a similarity variable.

Now, the main features of the fireball are controlled by the hydrodynamics in which the distance and time scale like $W^{1/3}$. If, by virtue of diffusion, a perturbation is imposed which delays time and goes like the square root power, the net effect of the perturbation is $\sqrt{W^{1/3} t} = W^{1/6} t$. Multiplying a function which ought to scale like $W^{1/3}$ by a perturbation which goes like $W^{1/6}$ results in an over-all time dependence, which goes like $W^{1/3} \times W^{1/6} = W^{1/2}$. In this very crude way one suspects that the times at which the minimum and second maximum will occur scale more like $W^{1/2}$ than $W^{1/3}$.

These definitions of the maxima and minima apply to scaling, which is illustrated qualitatively in Fig. 2.5.5-2. If we go to a smaller bomb or a rare atmosphere, the absorptive zone of air between the isothermal sphere and the shock front will decrease in thickness; relative to a larger bomb, the transmitted fraction of radiation will always be higher. Hence, one will not have to wait relatively as long for the rate of increase of transparency to just offset the cooling of the fireball.

01110
87
01110

UNCLASSIFIED

UNCLASSIFIED

This means that on the basis of hydrodynamic time $W^{1/3}$, the time of the minimum will occur earlier, just as we deduced the $W^{1/2}$ dependence. At the same time the radiation rates at the minimum will be higher, which means, in turn, that greater amounts of energy will be depleted from the bomb at relatively earlier times. The second maximum, which involves the depletion, should then also occur at a time earlier than indicated by $W^{1/3}$ and again about as we have deduced from the $W^{1/2}$ law. Because the integrated radiation lost prior to the maximum has been larger, one will not have to wait as long for the second maximum to set in, and it would seem that the radiation rate at the second maximum will fall in the case of this smaller bomb.

As we go to still smaller bombs, the radiation rate at the minimum will shift higher and earlier in time, and the second maximum will shift to a lower rate and also earlier in time. For a small enough bomb and a rare enough atmosphere, sooner or later so much radiation will have escaped that the light minimum and the second maximum will coalesce into an inflection point.

In the limit as $W \rightarrow 0$ or as $\rho \rightarrow 0$ even the inflection will disappear because the shock front will now be too thin in thickness or too rare in density to absorb any radiation from the inner core. In the ultimate limit and for a weightless bomb, the entire energy of the bomb should escape in a single pulse. Hydrodynamic scaling in itself might show that the blast pressures approach zero in this limit, but radiative transport effects an equally strenuous reduction; no blast appears because radiant energy was never converted to hydrodynamic energy in the first place.

For a bomb burst in a very rare atmosphere, the major effect from an atomic bomb would no longer be blast. The effective thermal radiation would be enhanced, not only because of the greater transmission exterior to the radiating sphere at these altitudes, but by large factors through the fraction which escapes the radiating sphere. There is even more. In a succeeding chapter it will be shown that the surface temperature of irradiated objects is also dependent on the radiation rate, as well as the total radiation received and this greatly increases surface temperatures when the bomb can rapidly divest itself of its energy through thermal radiation at early times.

2.5.6 Scaling Laws for Thermal Radiation

We will require a description of thermal radiation in relation to its effect on the shock wave. It is convenient to describe the scaling of thermal radiation relative to blast scaling by giving a comparison of the relative thermal effect at a certain pressure level as the yield of a bomb is changed.

The total radiation received at a hydrodynamic point depends on the model used. In the black body model, in which $Y \sim W$, the total thermal radiation incident at a point will be given by:

UNCLASSIFIED
88
UNCLASSIFIED

UNCLASSIFIED

$$Q_T = \frac{Y \cos \theta e^{-\text{const } R}}{4\pi R^2} \sim \frac{W \cos \theta e^{-\text{const } R}}{4\pi R^2}$$

In hydrodynamic scaling, angles are preserved so $\cos \theta$ is invariant. Distances scale like $W^{1/3}$ and, neglecting the atmospheric absorption in $e^{-\text{const } R}$,

$$Q_T = \frac{a W \cos \theta}{4\pi (W^{1/3} R)^2} \sim W^{1/3}$$

According to this model then, the incident thermal radiation will increase according to $W^{1/3}$ at a given pressure level.

In the absorption model, thermal radiation will be somewhat less than $Y \sim W$, so that the total number of calories at a given hydrodynamic point may increase or decrease depending on whether $n > 0.67$ or $n < 0.67$ in the relationship $Y = a W^n$

$$Q_T \sim Y/R^2 \sim W^{n-0.67}$$

A primary interest in thermal radiation is the surface temperatures produced by it. This introduces another dependence, for the longer the time duration during which a given amount of thermal radiation falls, the lower will be the surface temperatures produced by it. A pertinent example here is normal sunlight which delivers 2 cal/min/cm² at the earth's surface; this is 10 cal in 5 min, and according to the critical tables in Effects of Atomic Weapons, the same radiation from a nominal bomb will char wood. In general, this dependence is inversely proportional to the square root of the times involved. In a previous section it was shown that the time of the radiation scales like $W^{1/2}$. Combining these dependencies, we have

$$T_s \sim Q_T/t^{1/2} \sim \frac{Y \cos \theta}{R^2 t^{1/2}} \sim \frac{W^n}{W^{2/3}(W^{1/2})^{1/2}} \sim W^{n-0.67-0.25} = W^{n-0.92}$$

If, in particular, n has the value 0.92 over a range of points of interest in yield, then the surface temperature is independent of the yield at a point of hydrodynamic invariance, i.e., at the same pressure level.

It is these dependencies which will lend insensitivity to the effect of thermal radiation on blast. Q_T behaves like hydrodynamic length $W^{1/3}$ for $n \cong 0.92 \cong 1$ which is as required for some of its effects, whereas the surface temperatures behave like a hydrodynamic variable.

For a very large change either in ambient conditions or in yield, this insensitivity disappears. As assumed in Section 2.5.3 for nominal bombs, nearly all the thermal radiation at early times is absorbed in the zone behind the shock front. Within reasonable changes of yield, the blast at the

UNCLASSIFIED

UNCLASSIFIED

shock front is effectively 100% of the total energy of the bomb, and the total thermal radiation also approaches 100% of the bomb. But for a very small bomb or one detonated in a very rare atmosphere, these assumptions are no longer valid. A much larger fraction of the bomb's energy will then appear as thermal radiation during strong shock phases and a corresponding smaller fraction will appear as blast. In this case, not only will the effective radiation increase in comparison with what might be expected from a nominal bomb fired at sea level but the surface temperatures will increase further because of the shorter time duration of thermal pulse. The increased fraction of radiation rate occurs prior to the light minimum. The fraction after the minimum decreases if the total is considered 100%, but this fraction may be shortened in duration, or literally shifted from the "tail" to the main pulse, and thereby increase surface temperatures markedly.

2.6 EFFICIENCY OF A NUCLEAR EXPLOSION

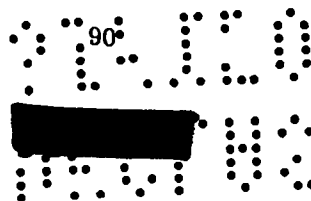
2.6.1 Waste Heat Concept

It is usually taken as common knowledge that the "efficiency" of a nuclear explosion is considerably less than that from TNT. Fuchs introduced the concept of "waste heat" from entropy changes, which accounts for this reduction. The argument is often extended to represent it as a loss in energy, solely because the temperatures left behind (by entropy changes) in a nuclear explosion are, of course, enormously greater than those left behind by a small-charge explosion.

We investigate this concept more closely. In the first place, the analytic solution or a direct integration as it was applied to the IBM Problem M in Section 2.3.2 evaluates the hydrodynamic energy as it is actually present within the wave. If the energy is so evaluated and radiation energy density is small, there is no meaning to the "efficiency" because the energy present is counted once and for all as hydrodynamic energy.

Next, one could argue with equal plausibility that the heating due to the entropy change actually enhances pressures at the shock front because the high temperatures also imply that the specific volumes are larger for the material on the interior of the shock. If the material on the inside occupies a greater volume than it would if it cooled to ambient temperature, it follows that the air in the layer between the fireball and the shock radius would have to exist at somewhat higher average density and, therefore, higher average pressures. This means, of course, that the shock front pressures would be higher, not lower, because of the $\int P dV$ work done by this inner core.

Another way to state the problem is by using variable gamma theory. By the time radiation rates are near or beyond the maximum, the pressures on the interior will be effectively at ambient



UNCLASSIFIED

UNCLASSIFIED

pressure P_0 . The excess internal energy per unit volume near the fireball is then

$$P_0/(\gamma - 1) - P_0/(\gamma_0 - 1)$$

It follows that there is no waste of energy directly through the temperature because the internal energy per unit volume can differ only through the pressure, if the ideal gas law held and γ were identical for all material within the shock front. In thinking of the energy over the blast wave at late times there is this natural disposition to assume that $\gamma = \gamma_0 = 1.4$ when only low pressures are involved. The result from the curves in Section 2.2.2 is the failure of the ideal gas law at normal pressure but at very high temperatures. Here the value of γ falls to values below 1.2. If the ideal gas law fails in such a way that $\gamma < \gamma_0$, a substantial fraction of the bomb's energy is tied up in energy at the center of the bomb even though the pressures are returned to ambient. It follows that the energy available at the shock front will be reduced, but, the hydrodynamic energy, if evaluated over the entire sphere, will not be smaller than it would be had the ideal gas law held.

It is obvious, however, that if this hot material radiates and a substantial fraction of energy is observed as thermal radiation beyond the shock front, then there must be a corresponding decrease in hydrodynamic energy within the shock. The point is that the IBM run did not allow the material to radiate, and energy was conserved within the shock by the adiabatic law; the direct integration counted all the energy. Even if it did radiate, the analytic solution was applied at times when the depletion of energy due to radiative cooling-contraction would not be manifest at the shock front. Whether radiative cooling ever affects the shock front pressures will be considered in detail in subsequent sections.

In summary, heat is not wasted directly because of the entropy change, but may be wasted because of a failure of the ideal gas law.

2.6.2 Efficiency with Respect to TNT

It is well known that the peak pressure vs distance curve from a nuclear explosion falls below what would have been expected from direct scaling small-charge high explosives. While this has generally been attributed to the waste heat concept, it is probably worthwhile to investigate this comparison more closely.

In the first place, it is not clear, at least to the author, what is meant by a kiloton of TNT. In practice it refers to short tons of TNT; in Section 2.2.1 it was noted that metric tons was meant. The true efficiency of a nuclear explosion with respect to small charges has little quantitative meaning unless the total energy behind the TNT shock wave and behind a nuclear shock wave are both known.

91

UNCLASSIFIED

UNCLASSIFIED

In the previous section it was shown that higher total energy is required for a point source explosion to produce a given pressure at the shock front because of the failure of the ideal gas law on the interior of the wave. In the energy integration of the IBM Run in Section 2.3.2 this point was tested directly and it was found that, under the assumption $\gamma = 1.4$ throughout the wave at low pressures, the apparent energy of the same bomb was only 5.5 KT instead of 11.5 KT, as obtained from using more realistic values of γ . Now, TNT explosions never reach the enormous shock pressure reached by nuclear explosions and the residual temperatures in the interior are correspondingly lower. It is to be expected then that even with the same pressure wave form for both types of explosives the departures from the ideal gas law are much milder in the case of a TNT explosion, and that the total energy implied in the pressure wave is, therefore, smaller than for the same wave on a nuclear explosion. To compound this difficulty, however, the center of a TNT explosion is hardly air, but over surprisingly large volumes will be an atmosphere composed largely of decomposition products from the TNT explosion, mostly oxides of nitrogen and carbon. In evaluating the energy behind a shock for such an explosion, the equation of state for that material would have to be known. It would be surprising if it turned out that $\gamma = 1.4$, but even more surprising if it agreed with pure air at these temperatures.

The description of a high explosive wave has been given by Kirkwood and Brinkley. The author understands that this work was done with $\gamma = 1.4$ and further, that an arbitrary fit was made of this theory to empirical data for TNT charges. It is suggested that whatever agreement occurred was because of the chance that the average γ for the decomposition products of TNT was close to 1.4. Whatever fitting was required is evidence that the γ was not 1.4.

It is clear from the analytic solution and the discussions of partition of energy that nuclear explosions can hardly be expected to scale with TNT. These variations depend on a large number of factors and should be resolved by detailed tests on both types of explosions. It is not to be expected that the failure of scaling will be the same at all pressure levels.

A priori then, the assumption of a constant efficiency of a nuclear explosion in comparison with TNT is not justified. Fortunately, through the IBM Run and the analytic solution, comparisons with TNT are unnecessary.

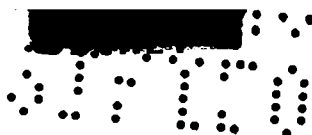
2.6.3 Partition of Energy

Because of the presence of types of energy other than blast on nuclear explosions there is a natural disposition to assume that a natural partition of energy occurs which somehow divides the energy of the bomb into a number of mutually exclusive fractions. Thus

92

UNCLASSIFIED

UNCLASSIFIED



Blast + Thermal + Nuclear = Total

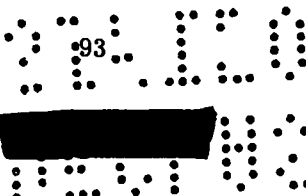
50% + 35% + 15% = 100%

We wish to consider the concept of partition more closely.

As is well known, not all of the energy from fission is released promptly; about 11% appears after the first second in delayed fission products. But this is not a bona fide loss to the shock wave because it occurs much too late, and by the convention stated on page 14, Effects of Atomic Weapons, it is not included in the energy value of the radiochemical kiloton of 10^{12} cal. By the same convention, it was not included in the evaluation of energy in the analytic solution nor in the direct integration of energy behind the wave. Some energy from gamma rays or neutrons could be behind the shock front, and to this extent the stopping process would contribute to local heating which, in turn, would raise the local temperature, expand the air and, to a limited extent, reappear as hydrodynamic energy. If this absorption occurred deep within the wave, it might never make itself apparent at the shock front. However, the density distribution behind the shock front contributes strongly to the probability that this absorbed energy will be manifest at the shock front, because the shock is a dense layer of air in which the probability of capture is high, and the hydrodynamic transport of energy is fast. The interior of the blast wave is low in density, so the probability of capture there is very small. Like the absorption of radiation near the shock front, this reinforcement of the blast wave depends, of course, on yield. For small bombs, the neutrons and gamma rays will escape the shock completely and a considerable portion of the energy can be manifested at long distances from the bomb. For large bombs, all scaled dimensions increase and, because of the exponential nature of the absorption process, the trapping of energy behind the bomb may be fairly complete. These differences correspond to a failure of hydrodynamic scaling in comparison with a total yield.

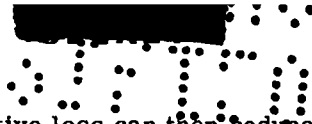
Thermal radiation from the bomb reinforces the wave from arguments similar to those applied above for gamma rays and neutrons. There is a further important difference, however, because of the substantially larger fraction of the total energy which appears as thermal radiation and the time at which it occurs. As was discussed previously, only a small fraction of the thermal energy appears prior to the light minimum. Most of the thermal radiation appears long after breakaway when the shock is a considerable distance ahead of the fireball. There is no question that the radiation from the fireball represents a bona fide loss in hydrodynamic energy to the shock wave during the time it is observed well in advance of the shock front itself.

93



UNCLASSIFIED

UNCLASSIFIED



The question is whether this radiative loss can then reduce the pressures at the shock front. This question can be resolved by an analysis of the figures given in Section 2.4.2. Energy signals are propagated behind a shock front with the velocity $u + c$ forward, and $u - c$ backward. The radiative loss to the blast wave, which appears as thermal radiation will result in contractive cooling, a rarefaction which can propagate forward with the velocity $u + c$. From Fig. 2.4.2-4 one may calculate the local velocity $u + c$ and determine the paths by which signals from the interior can reach the shock front. It will then be found that, at high pressures, signals within the shock front will always catch the shock front. Around the time the shock falls to something like 40 to 50 psi, a negative phase begins to develop in the shock front. This means that there is always some point within the shock in which the velocity $u + c$ is less than U . A signal behind this point will never reach the shock front. In the present report this difference has been made the basis for the distinction between strong shocks and weak shocks.

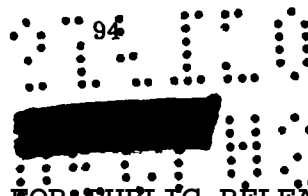
The method of characteristics supplies a similar and more powerful argument why signals well within a weak shock can never catch the shock. Once the negative phase develops, it means that two values of the Riemann invariant, approximately $u + 5c$ for a weak shock in spherical waves, can be found behind the shock front. This value is invariant along the path $u + c$, which is usually called the characteristic. It is a property of this method that characteristics cannot cross and a definite value of the Riemann invariant is associated with each part of the shock. It follows then that wherever multiple values of characteristics occur within the wave, signals from both points cannot reach the shock front. This point will be investigated in greater detail in Section 3.7* but, for the time being, merely note that this double value of the Riemann invariant within the wave occurs around 40 psi. This is about the time when thermal radiation is rising to its maximum rate. This means that the rarefaction associated with the emission of most of the thermal radiation will be restricted behind the negative phase, where it has no chance of attenuating the shock front, but could deepen the negative phase.

2.7 THE SHOCK FRONT IN FREE AIR

2.7.1 Proofs for the Existence of a Sharp Shock

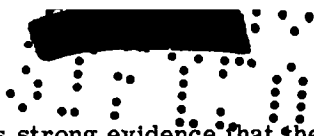
As a prerequisite for discussions in later chapters it is useful to examine whether the shock front for free air is actually sharp, or whether it could be a slow rise.

* Part II, LA-1665.



UNCLASSIFIED


UNCLASSIFIED



The existence of the fireball itself is strong evidence that the shock front at early stages is sharp. As shown in an early section of this chapter, the presence of a perfectly sharp shock front is not, in fact, a necessary condition for the validity of the Rankine-Hugoniot equations. These equations are merely a conservation of mass, momentum, and energy across an undefined boundary, which could be quite broad. It is only required that this boundary be quasi-stable in the sense that there is no source or sink of mass, momentum, or energy within it; if this is so, the Rankine-Hugoniot equations hold across the boundary regardless of the variations within it. It follows that the entropy change will result precisely as predicted by the Rankine-Hugoniot equations. If the shock were sufficiently broad so that the Rankine-Hugoniot equations were no longer valid, one would require an approach to the adiabatic law as a substitute for the Rankine-Hugoniot energy equation. From this it would follow that no entropy change occurred across the shock front, and since subsequent changes are adiabatic, it would be tantamount to the statement that the fireball does not exist. On this argument, one judges that the shock front is effectively sharp.

More direct evidence is afforded by the direct observation of refraction "hooks" caused by the shock wave itself. Such refraction can be observed in a number of photographs released of nuclear explosions. The rocket trail technique for photographing this refraction was suggested by, and done at the request of, Los Alamos Scientific Laboratory a number of years ago, and has since been developed and used extensively by Naval Ordnance Laboratory.

A third and less direct argument for sharp shock is based on the reflection process. The reflected pressure at normal incidence from a shock is, of course, a strong function of the incident pressure. As will be shown in detail in Chapter 3, LA-1665, the pressure multiplication, meaning the ratio of reflected pressure to incident pressure, varies from a factor of 2 at low pressures to factors like 12 or 13 for very high pressures. This finite result is obtained with the assumption of a sharp shock. While the details are too lengthy to warrant their inclusion here, the pressure multiplication can be derived in a similar fashion by using an adiabatic rise across the shock front instead of the Rankine-Hugoniot energy equations. It is then found that the pressure multiplication at high pressures increases without limit, rather than being limited to a finite value. This would mean that the pressures on the ground below tower shots of nuclear explosions would rise to many millions of atmospheres. Without disclosing security information, it seems clear from craters like Trinity, that no such enormous pressures occurred. The pressures may have been many thousands of atmospheres, but could hardly have been millions of atmospheres.



95

UNCLASSIFIED

UNCLASSIFIED

2.7.2 Possible Perturbation to Sharp Shocks

There are a number of other mechanisms by which the shock front could be a slow rise at high pressures. We wish to consider briefly these possible effects on the validity of the Rankine-Hugoniot equations.

First, as is well known, a nuclear explosion is accompanied by a considerable release of energy in the form of gamma rays and neutrons. These are stopped in air; eventually their energy will appear as degraded thermal energy from the production of secondary electrons. It might be supposed that the increase in temperature from this decay would raise the local temperature and, hence, the local sound velocity in the vicinity of a nuclear explosion. To some extent, this increase in ambient sound velocity ahead of the shock will increase the shock velocity and hence the apparent hydrodynamic energy. It can be easily shown, however, that the temperature rise due to this heating, is only a matter of a few degrees even close to the bomb itself, and is, therefore, insignificant in affecting the propagation of the shock.

The thermal radiation from the bomb is a mechanism similar to gamma rays. Here, however, the shock front itself is the source of the thermal radiation. While it is entirely possible to heat the air in the form of a precursor tail in front of the shock front, it follows that the shock front itself will be reduced in pressure strength because of this radiative loss. If this boundary is small enough, as indeed it appears to be, then the Rankine-Hugoniot equations are still valid across it. Physically this means that the shock velocity may be increased by virtue of raising the ambient sound velocity just ahead of it, but, by the same token, the shock pressure will be reduced just enough to compensate for the increase in sound velocity. It is of further interest to investigate the validity of the Rankine-Hugoniot energy equations, even under the assumption that such radiative losses are occurring. The relationship between the shock velocity and the pressure is given by

$$U = \sqrt{\frac{(P - P_0)}{(V_0 - V)}} V_0 = \frac{1}{V_0} \sqrt{\frac{(P - P_0)}{(1 - V/V_0)}}$$

In any case, the denominator in this expression is a number like 5/6 for $\gamma = 1.4$, and with variable gamma more nearly like 11/12 at the very high pressures where such radiative loss could be expected. Now, if the radiative loss at the shock front were complete enough to limit the shock temperature to a fixed value, then $V/V_0 \rightarrow 0$, and in this case, the denominator would be a number more like 1. It follows that, even if the pressure-density relationship followed an isotherm instead of the Rankine-Hugoniot "adiabat," the relationship between shock velocity and shock pressure

96
UNCLASSIFIED

UNCLASSIFIED

[REDACTED]
97

UNCLASSIFIED

would be affected only as the square root of $11/12$ differs from the square root of 1. Further, one expects that the Rankine-Hugoniot equations would apply up to pressures of the magnitude of 1000 atm. The departure from the Rankine-Hugoniot energy relationship, small as it is, would not occur until the shock pressures themselves were very much larger than 1000 atm.

In summarizing the present chapter, we recall that the free air wave from an atomic bomb has been derived solely from the principles of conservation of mass, momentum, and energy. This has been done for a nuclear explosion on its own merit through IBM Problem M, independent either of tests on small charges or of tests on nuclear explosions themselves. The thermal radiation from the bomb has been shown not to affect seriously the apparent blast energy at the shock front. Finally, we have no reason to suspect strong departures from these equations because of the nature of the shock process on nuclear explosion.

97
[REDACTED]

UNCLASSIFIED

[REDACTED]
S: T: O

UNCLASSIFIED

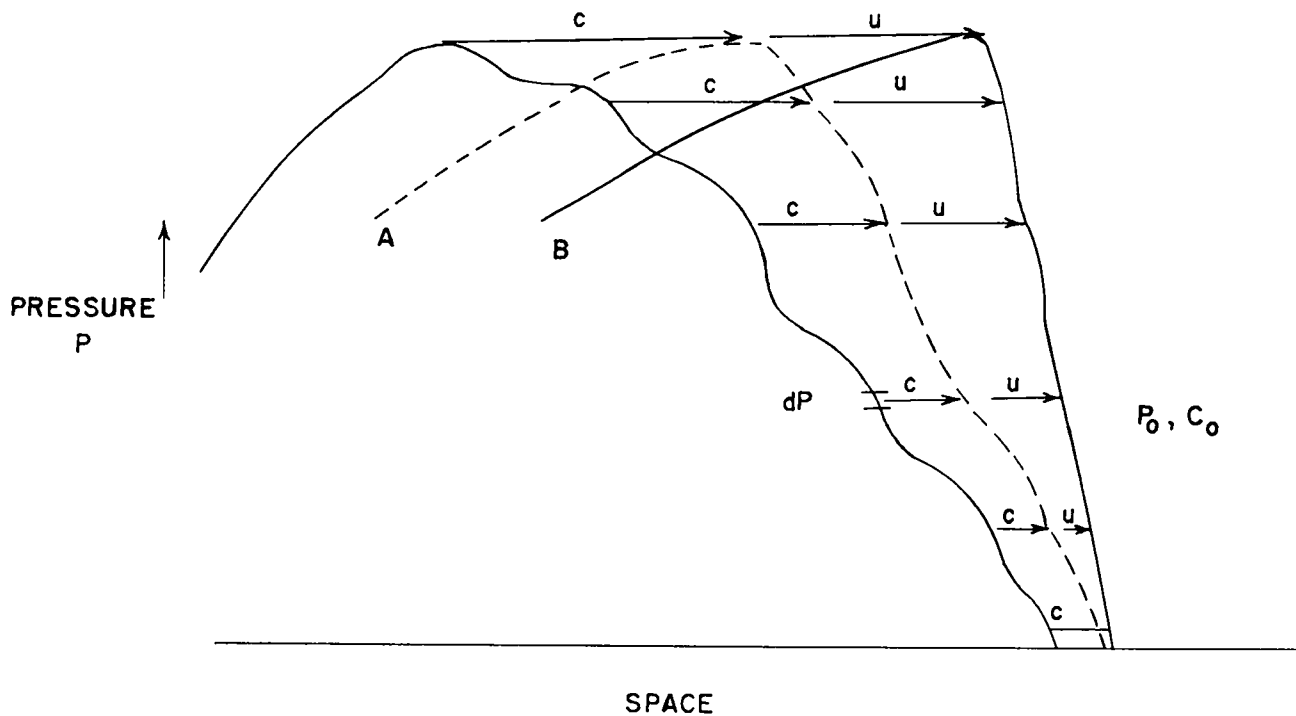


Fig. 2.1.2a The process of "shocking up."

98
S: T: O

UNCLASSIFIED

UNCLASSIFIED

UNCLASSIFIED

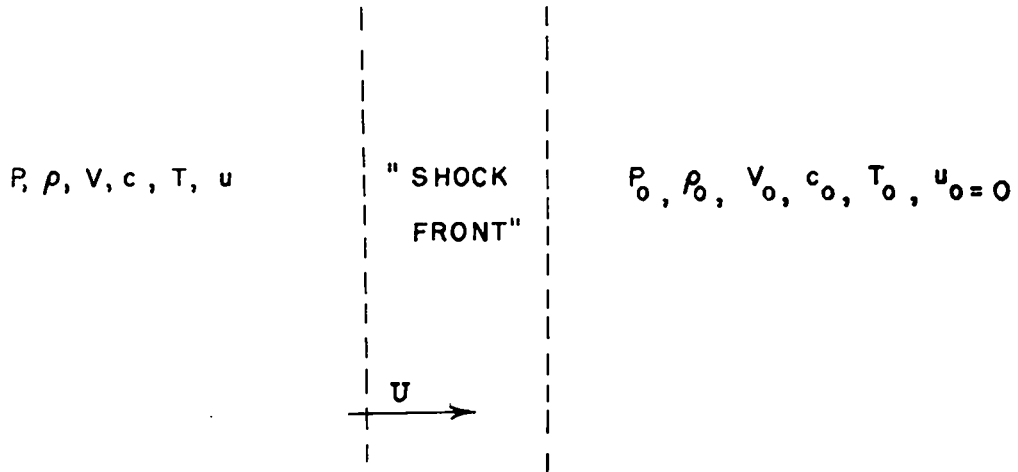
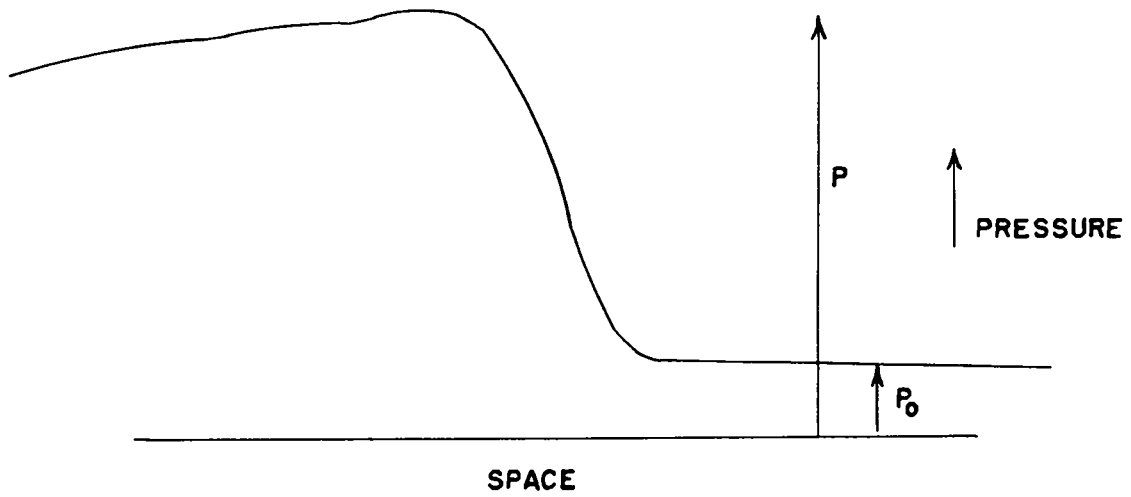


Fig. 2.1.2b Definitions for deriving the Rankine-Hugoniot equations.

UNCLASSIFIED

UNCLASSIFIED

SECRET

UNCLASSIFIED

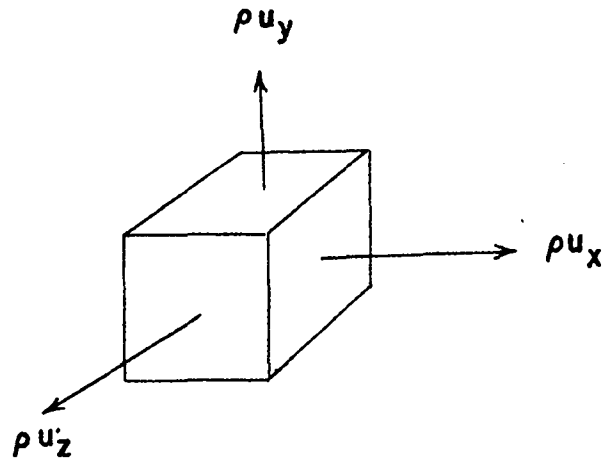


Fig. 2.1.3-1 The unit volume for differential conservation of mass.

100

UNCLASSIFIED

[REDACTED]
3:10

UNCLASSIFIED

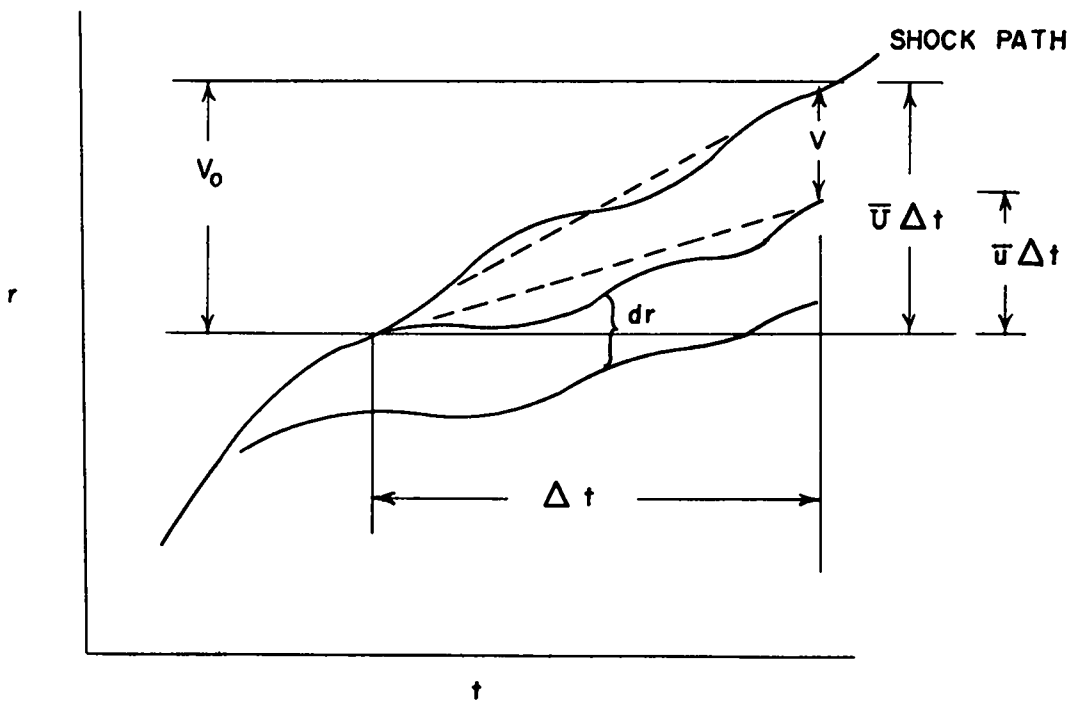


Fig. 2.1.3-2 The r-t plot for a shock.

10
[REDACTED]

UNCLASSIFIED

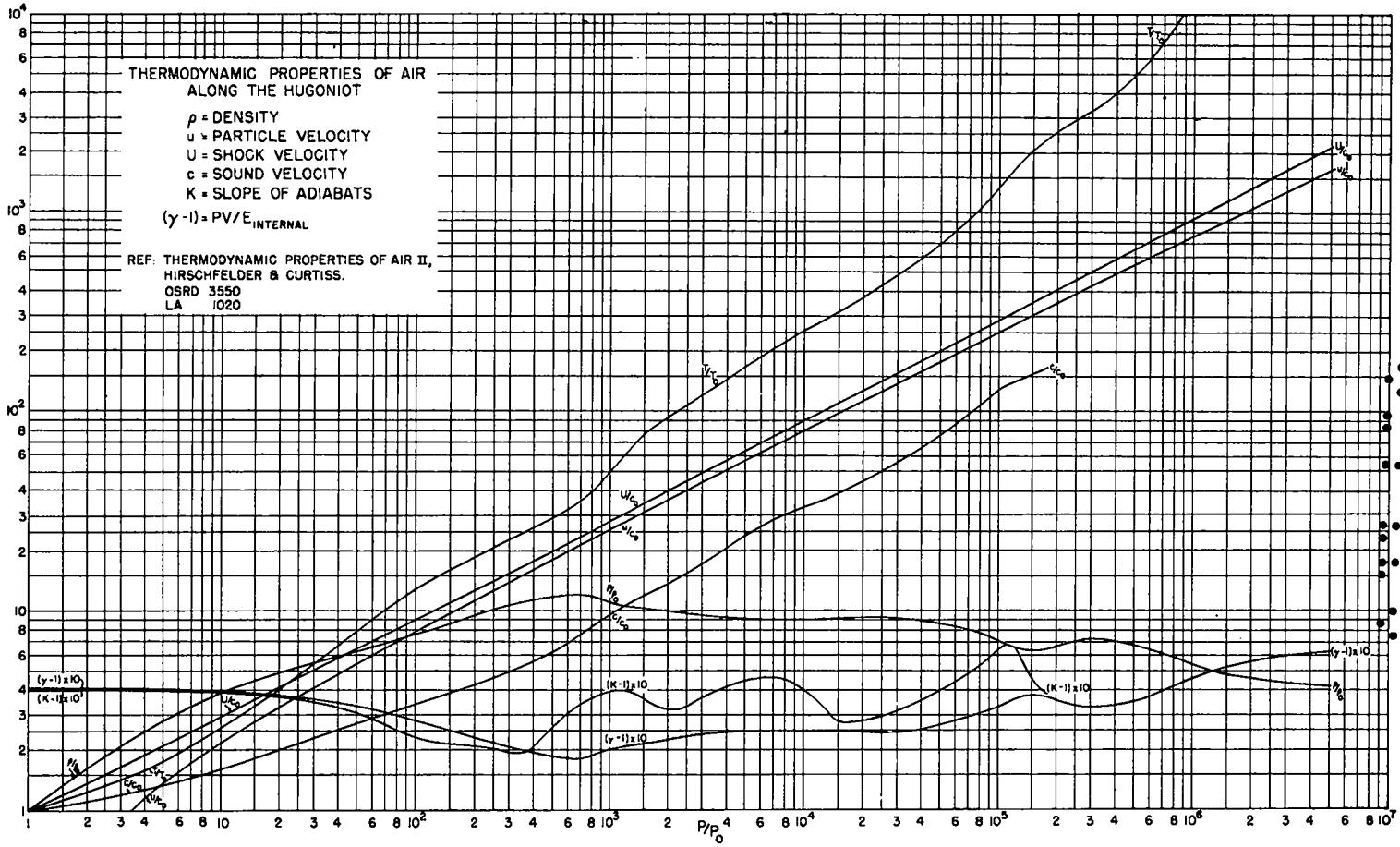


Fig. 2.2.2-1

UNCLASSIFIED

UNCLASSIFIED

[REDACTED]

UNCLASSIFIED

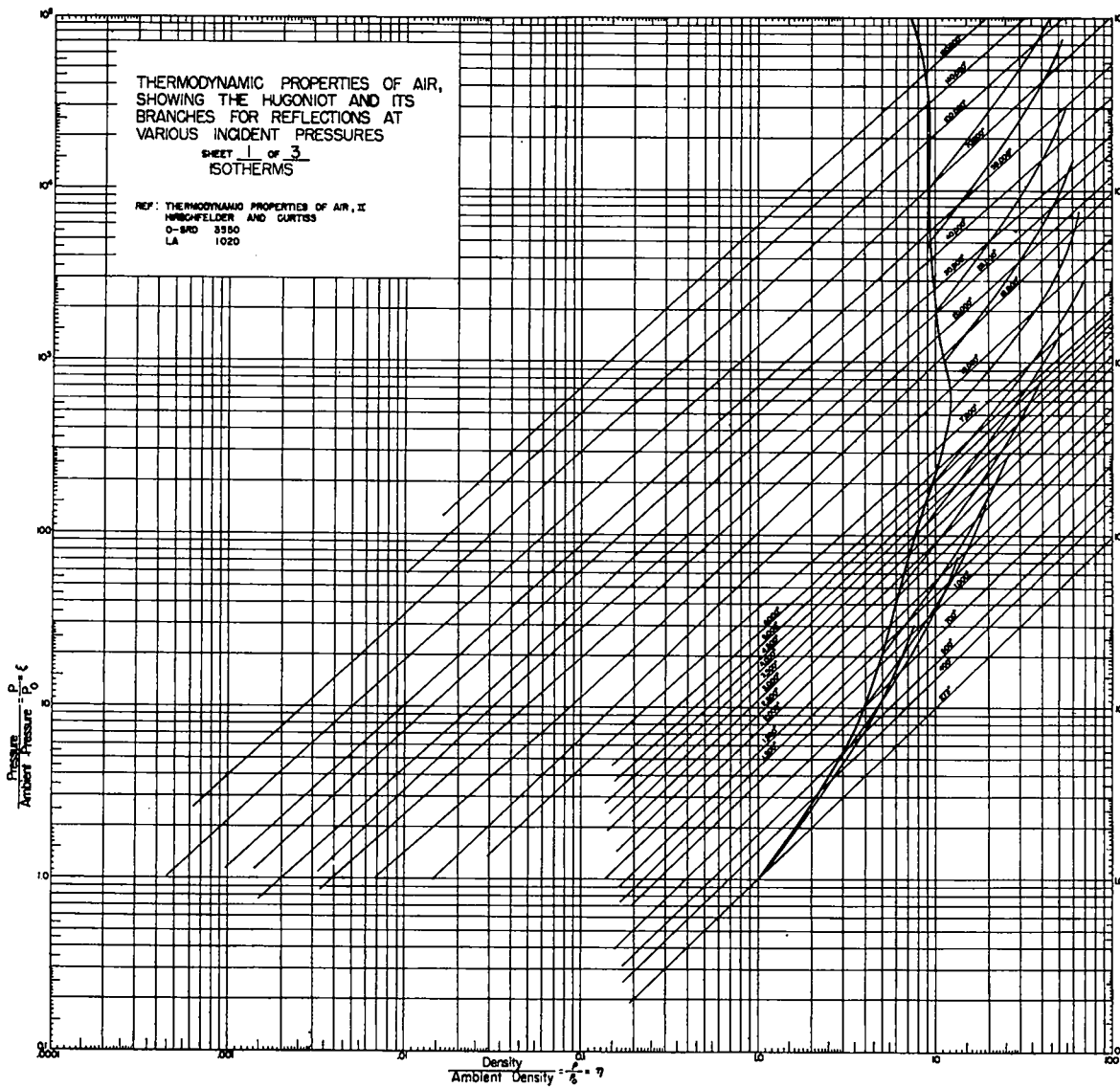


Fig. 2.2,2-2

[REDACTED]

UNCLASSIFIED

UNCLASSIFIED

UNCLASSIFIED

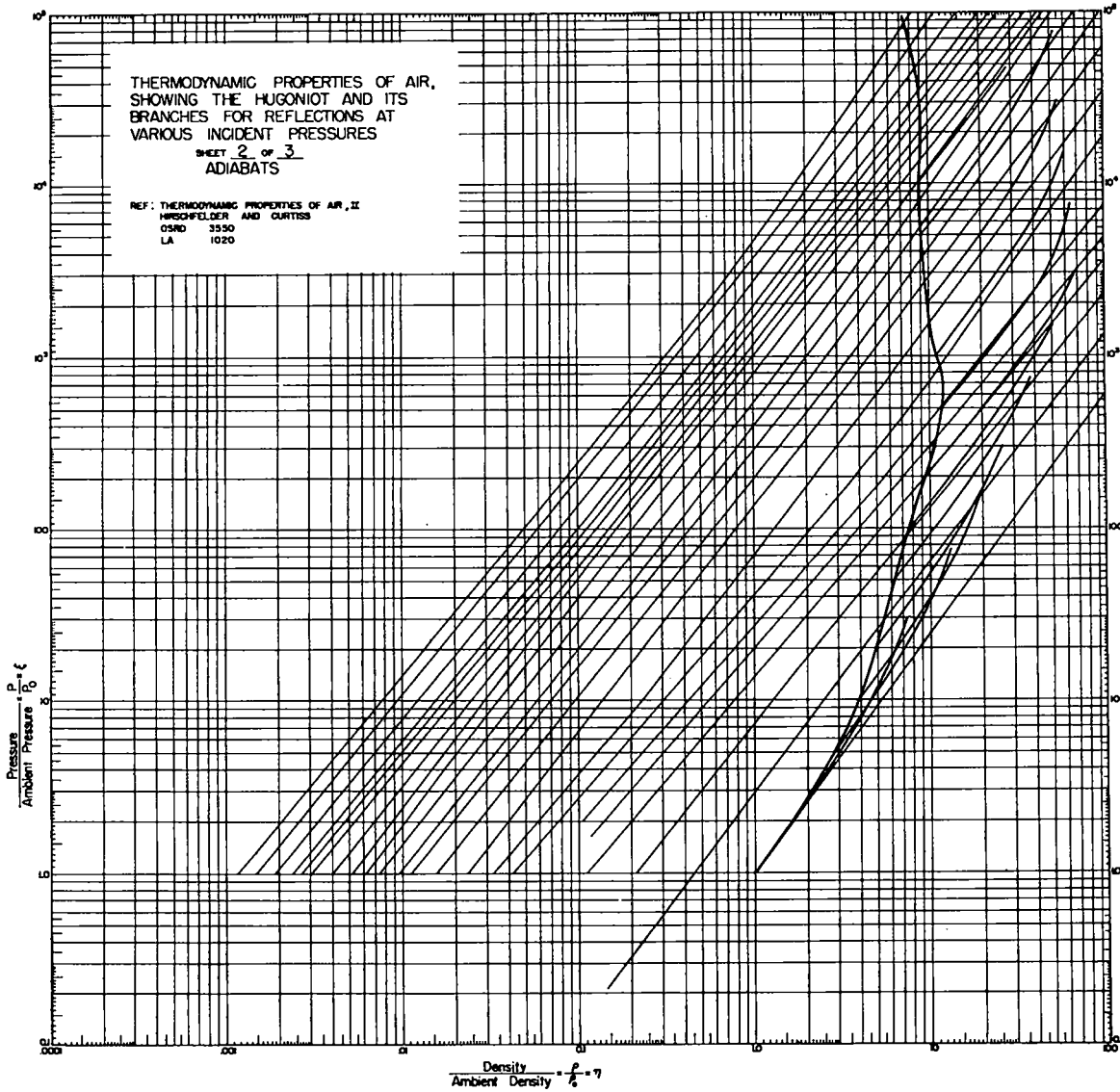


Fig. 2.2.2-3

UNCLASSIFIED

UNCLASSIFIED

[REDACTED]

UNCLASSIFIED

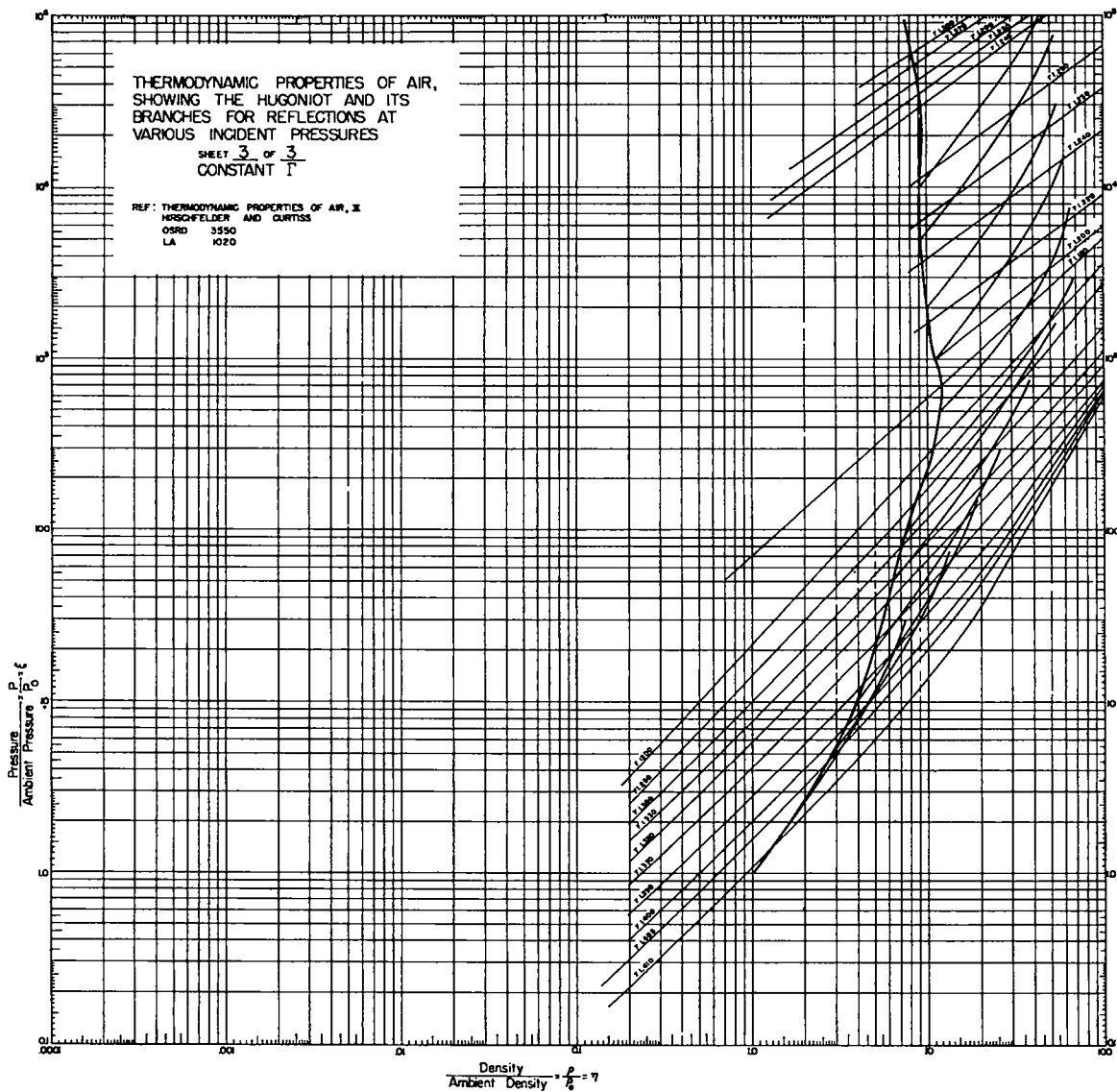


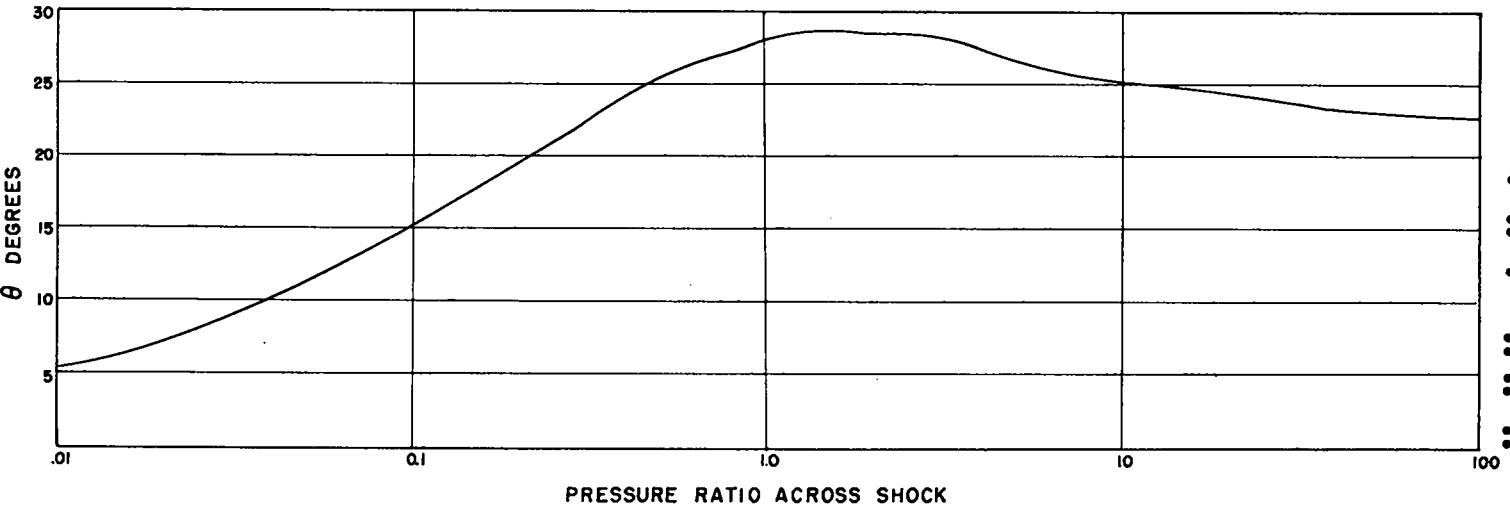
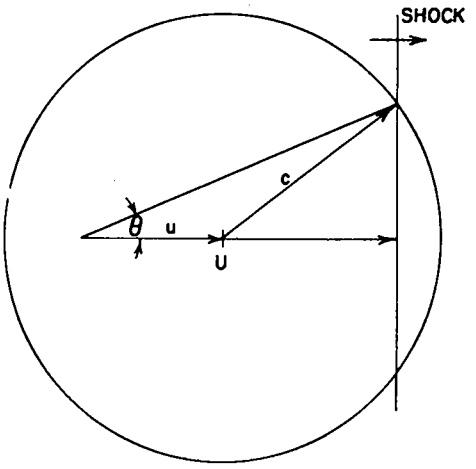
Fig. 2.2.2-4

[REDACTED] 105 [REDACTED]

UNCLASSIFIED

SECRET

UNCLASSIFIED



LATERAL FEEDING OF ENERGY NEAR SHOCK FRONT
FIGURE 2.2.5.-2

Fig. 2.2.5-2 Lateral feeding of energy near shock front.

SECRET

UNCLASSIFIED

[REDACTED] 011700
011700

UNCLASSIFIED

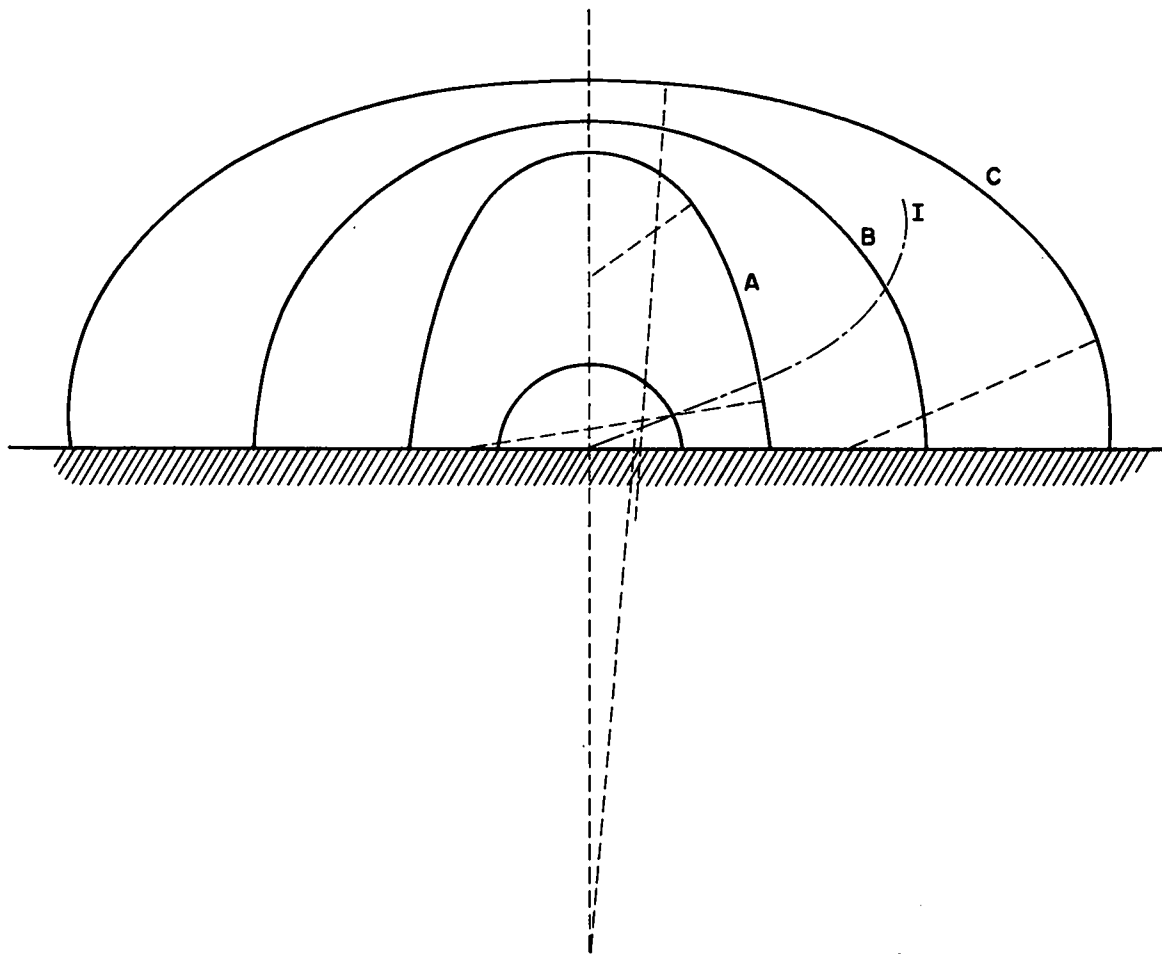


Fig. 2.2.5-3 Growth of a shock front in an inhomogeneous medium.

011700 108

[REDACTED]

UNCLASSIFIED

SECRET

UNCLASSIFIED

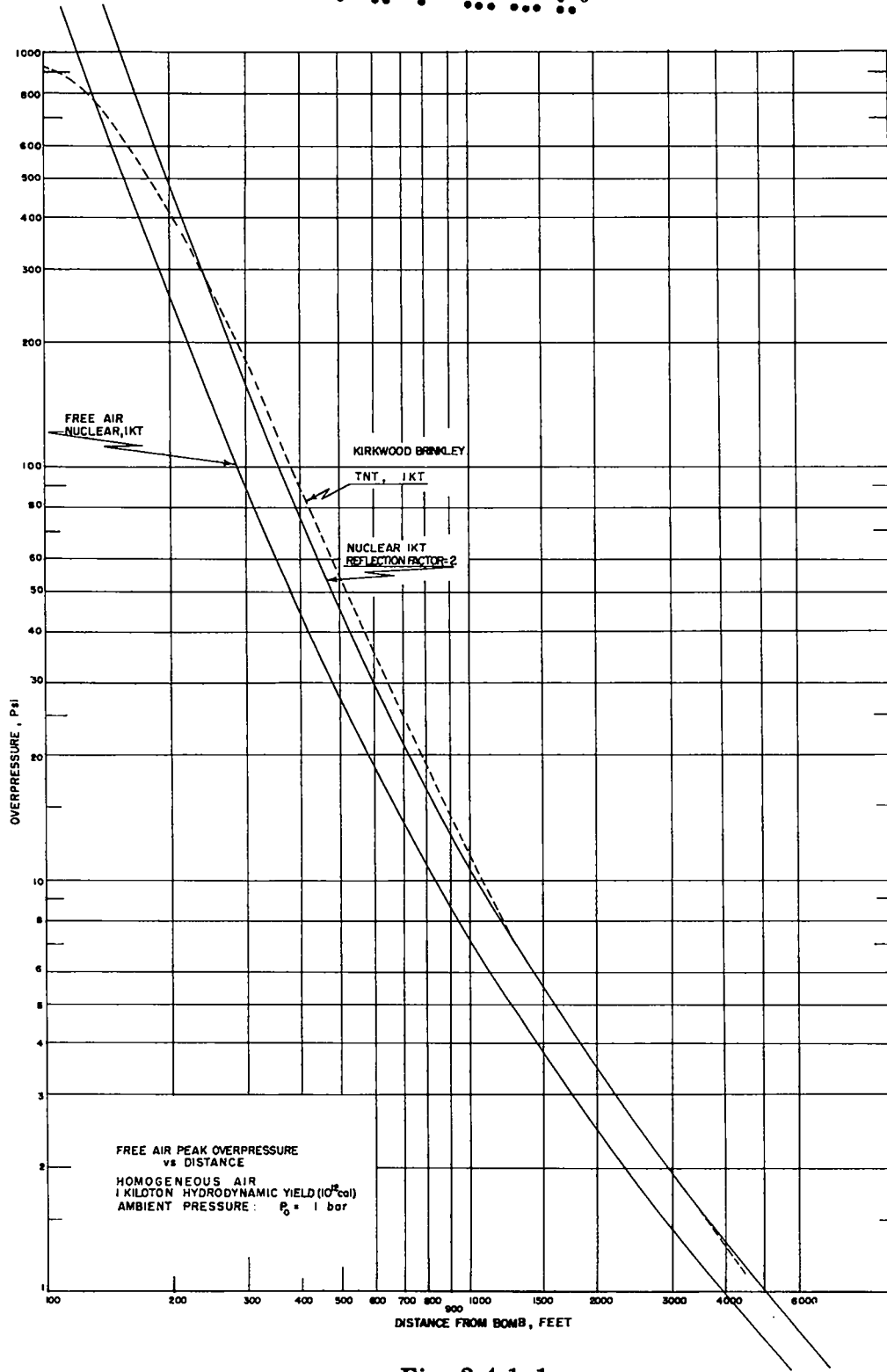


Fig. 2.4.1-1

SECRET

UNCLASSIFIED

SECRET

UNCLASSIFIED

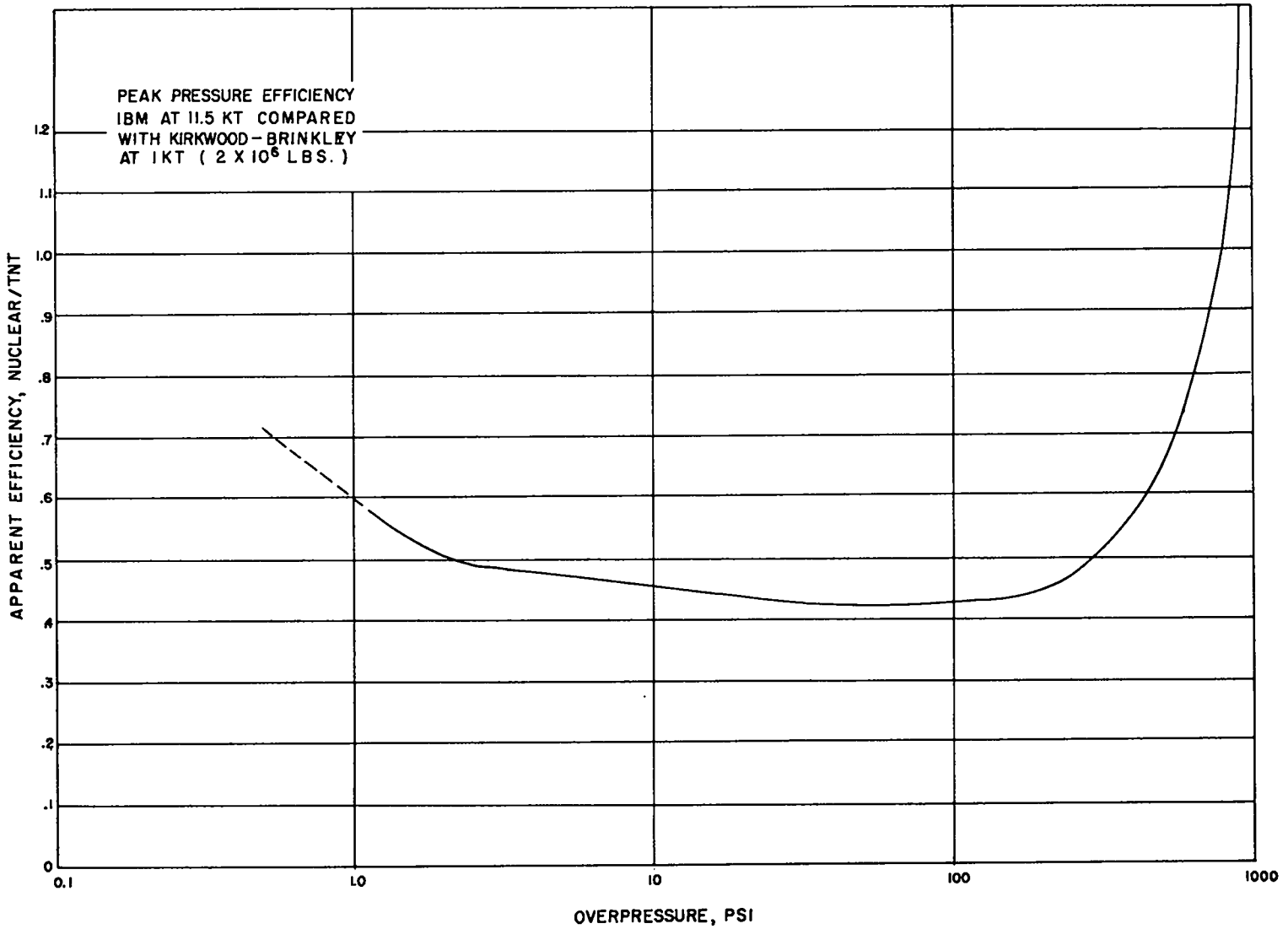


Fig. 2.4.1-2

SECRET

UNCLASSIFIED

SECRET

UNCLASSIFIED

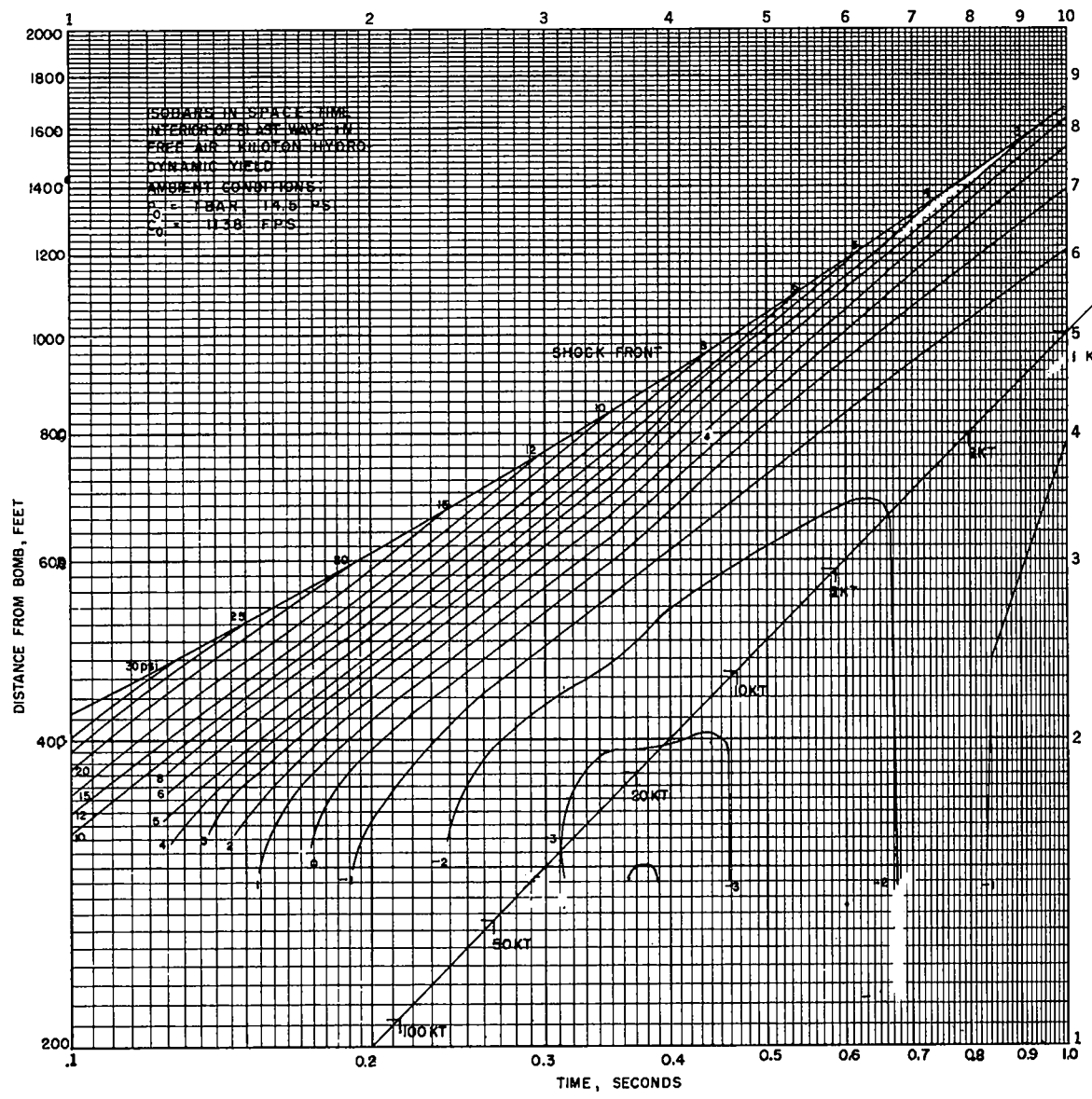


Fig. 2.4.2-1 Isobars in space-time.

SECRET

UNCLASSIFIED

SECRET

UNCLASSIFIED

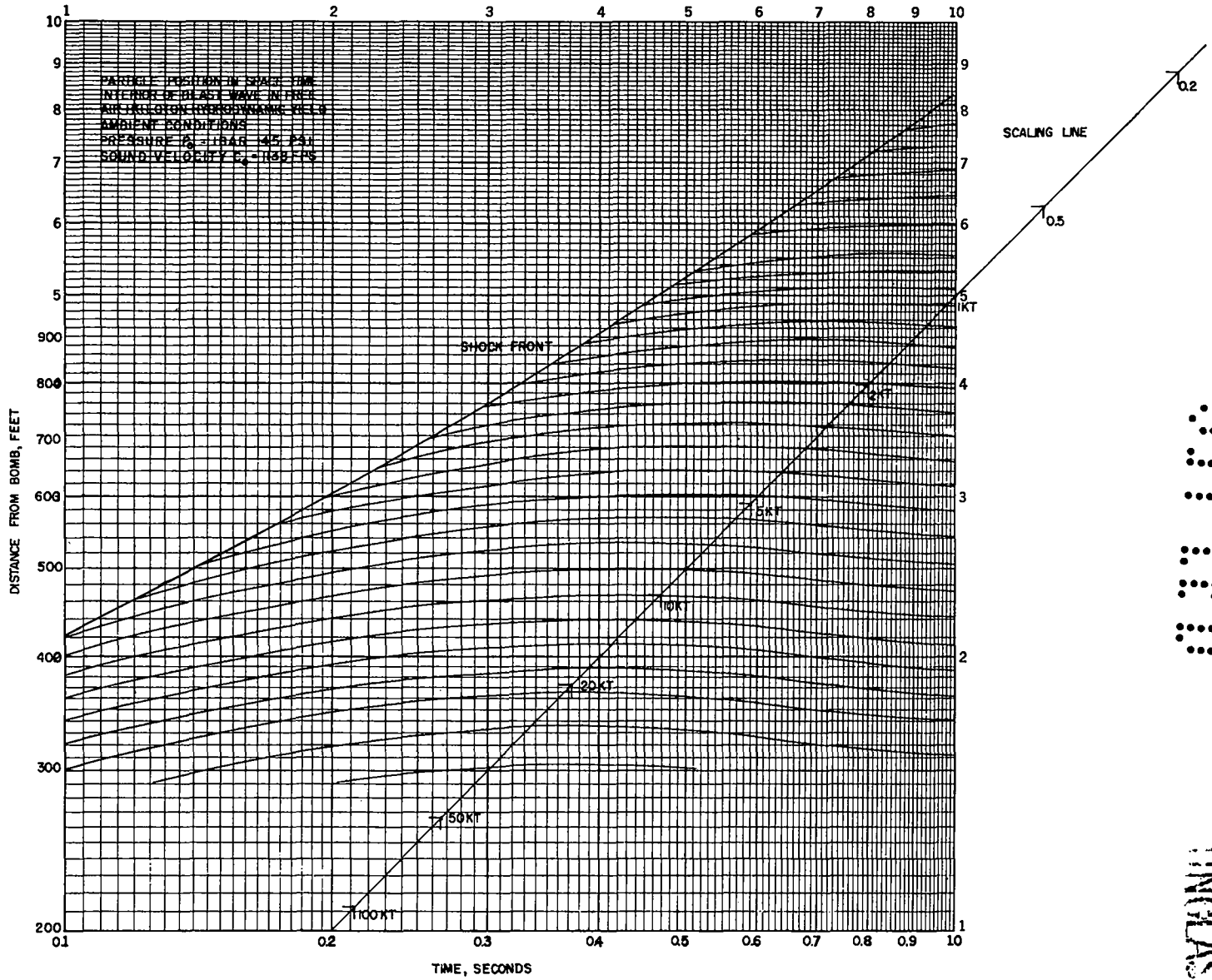


Fig. 2.4.2-2 Particle position in space-time.

SECRET

UNCLASSIFIED

APPROVED FOR PUBLIC RELEASE

UNCLASSIFIED

SECRET

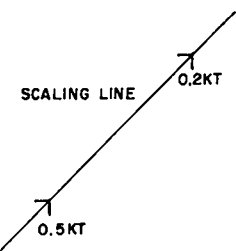
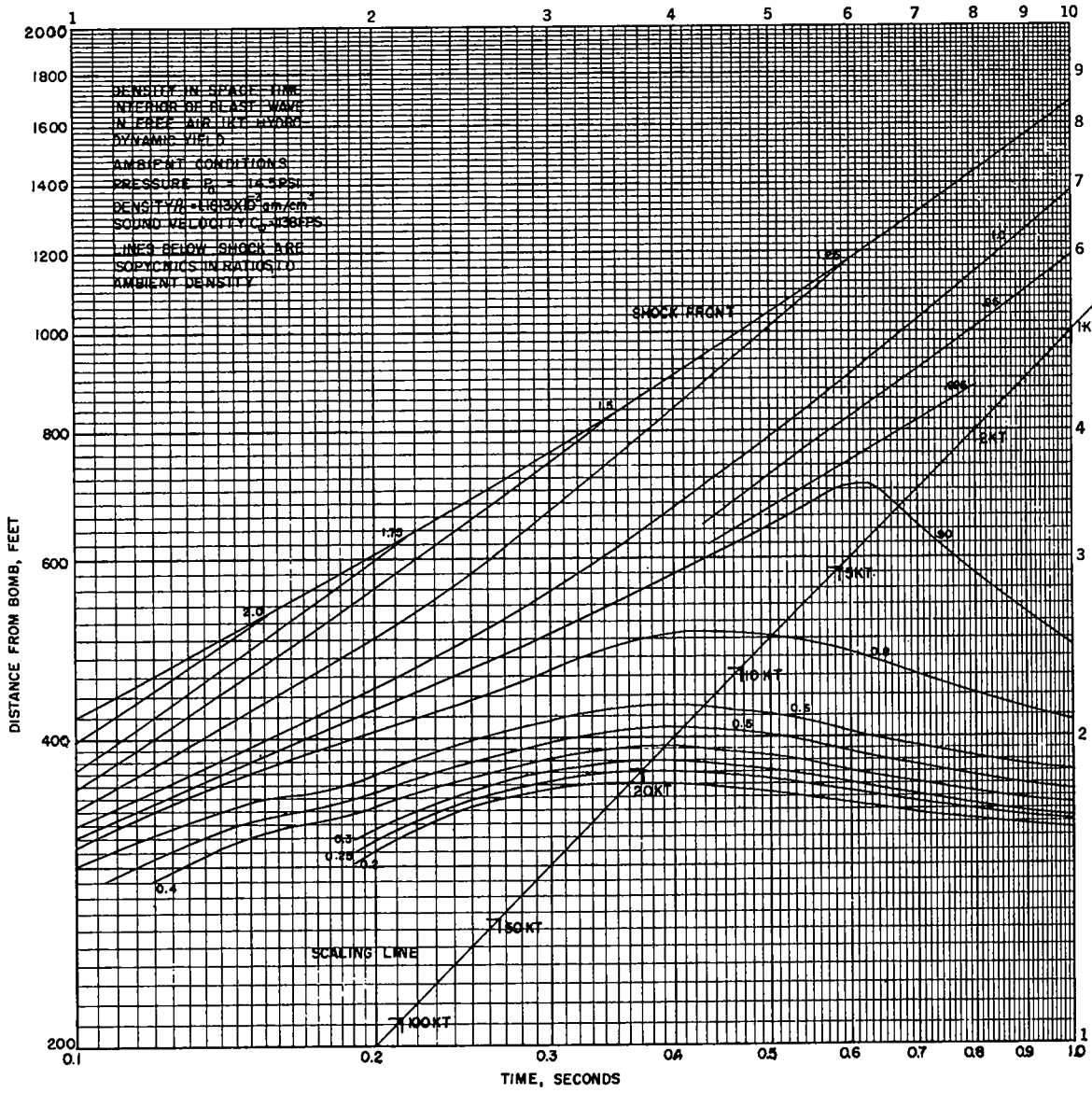


Fig. 2.4.2-3 Density in space-time.

UNCLASSIFIED

SECRET

APPROVED FOR PUBLIC RELEASE

APPROVED FOR PUBLIC RELEASE

SECRET

UNCLASSIFIED

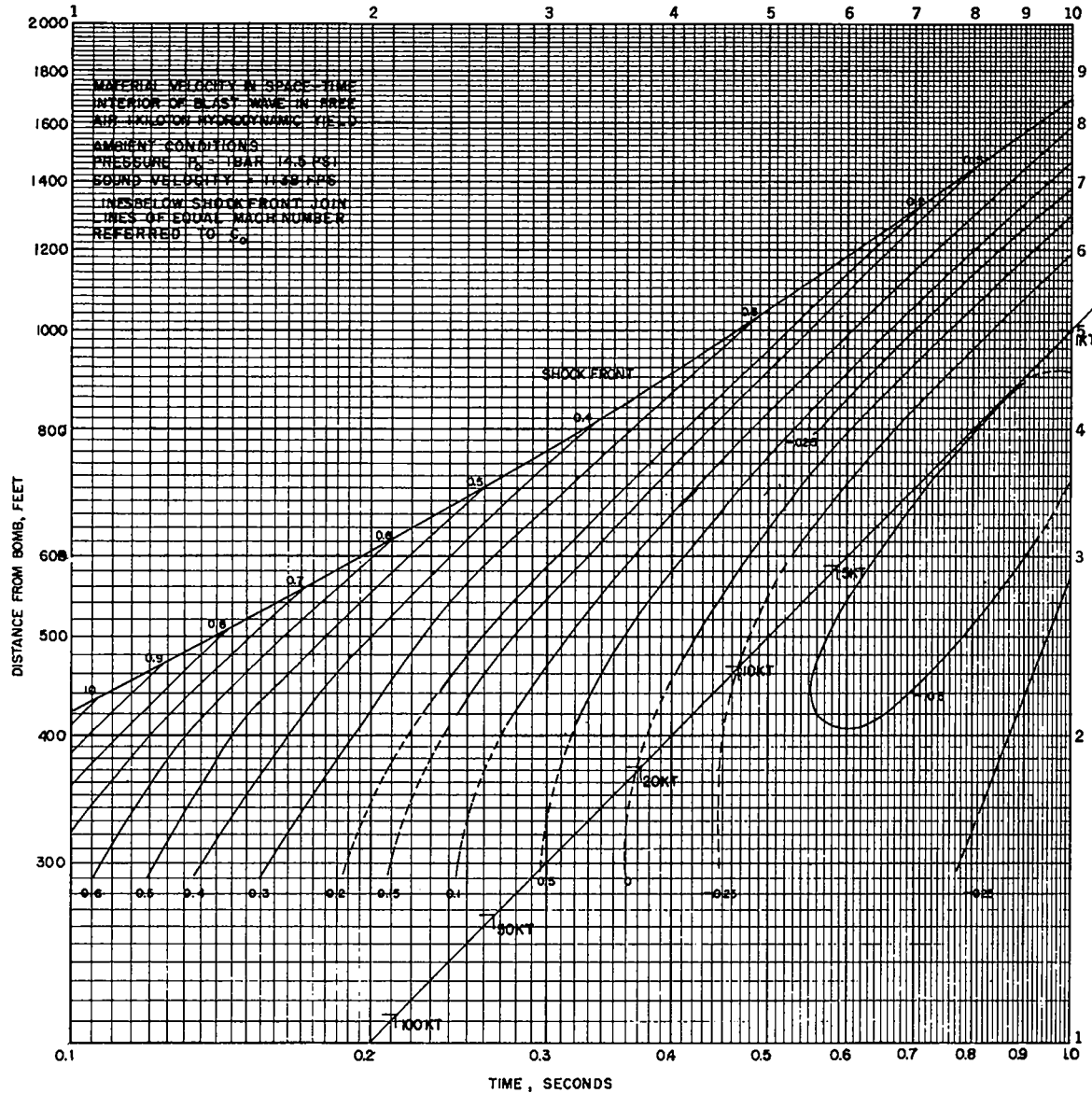


Fig. 2.4.2-4 Material velocity in space-time.

SECRET

UNCLASSIFIED

APPROVED FOR PUBLIC RELEASE

SECRET

UNCLASSIFIED

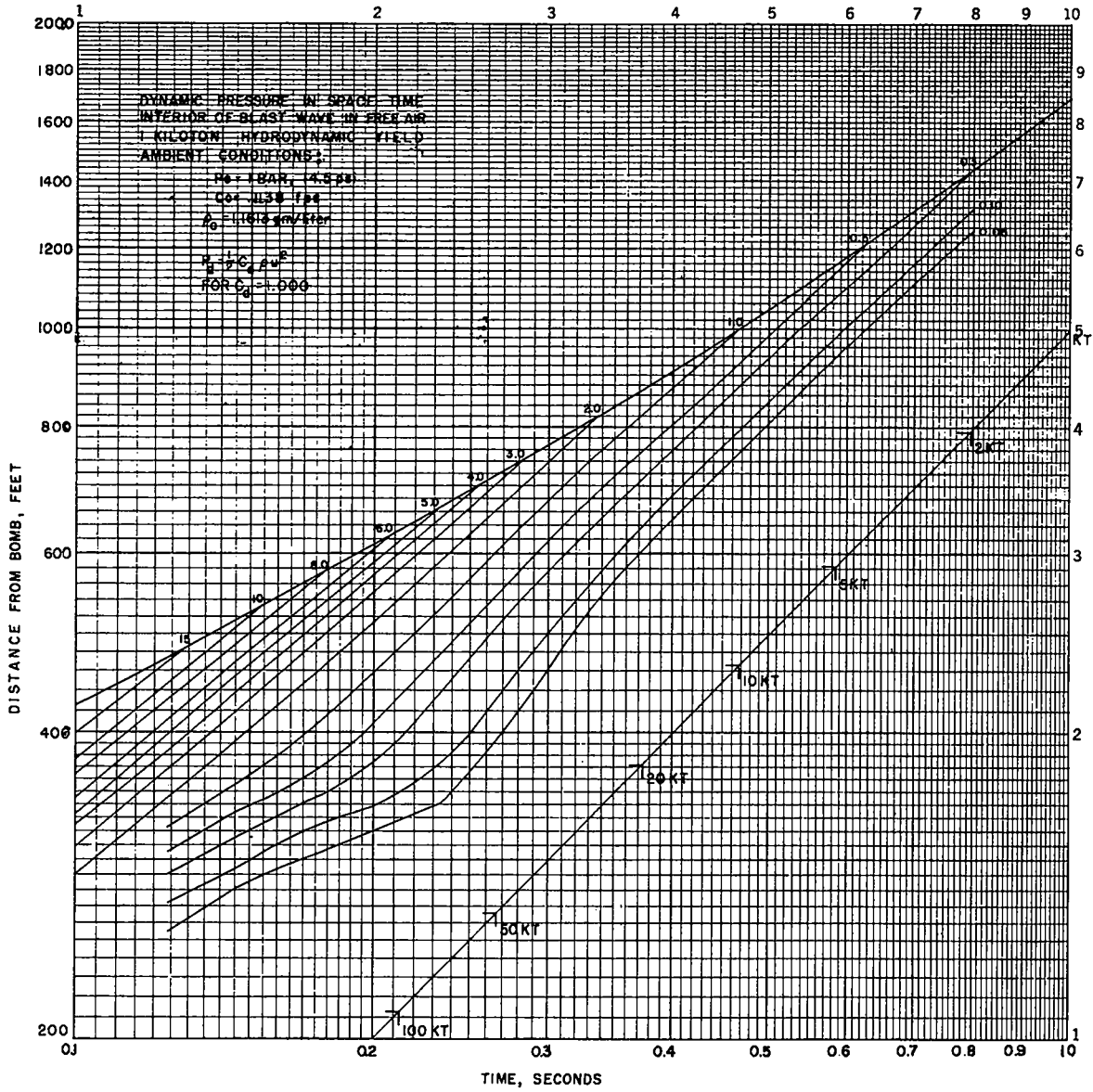
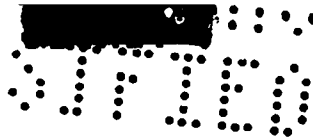


Fig. 2.4.2-5 Dynamic pressure in space-time.

SECRET

UNCLASSIFIED



UNCLASSIFIED

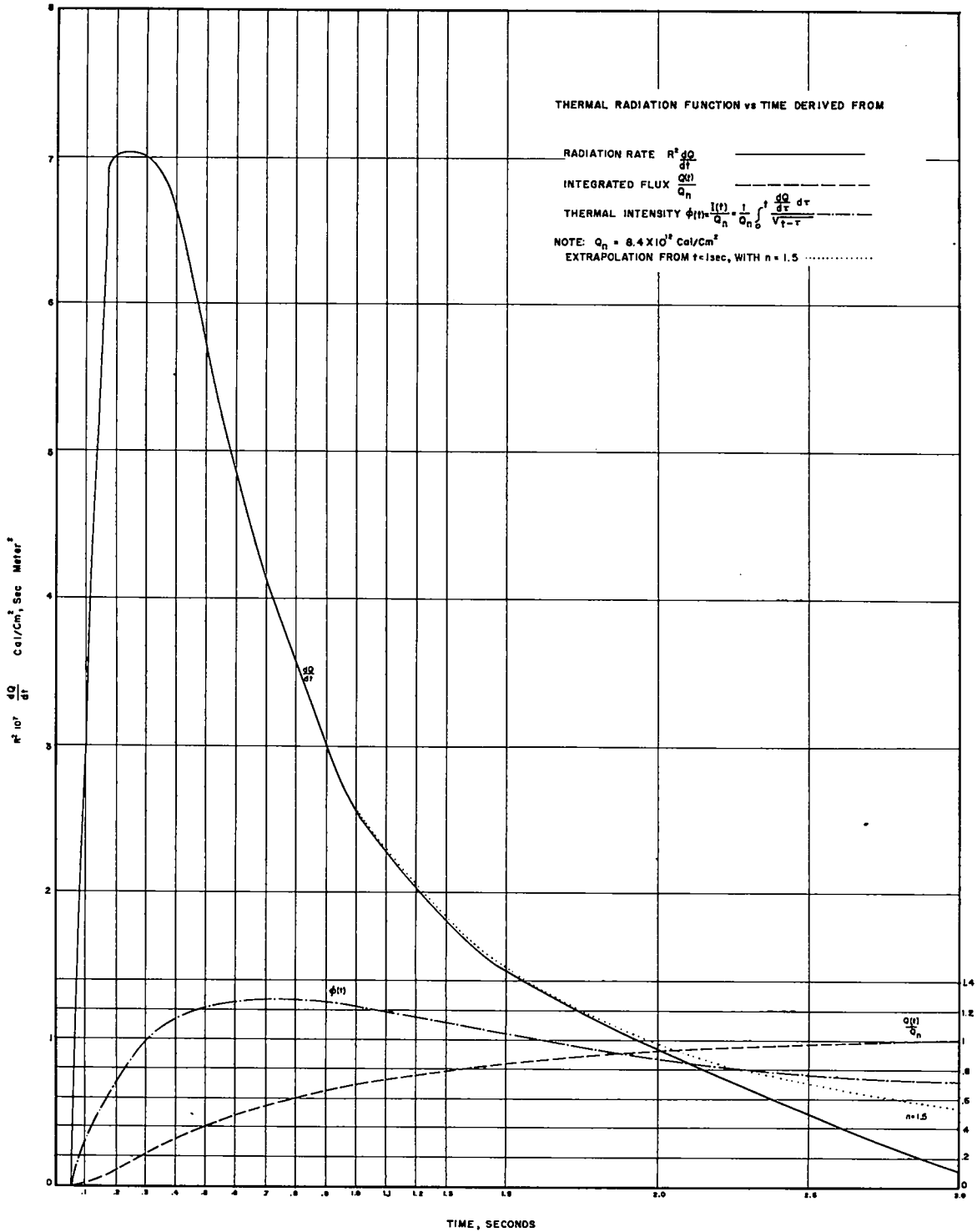
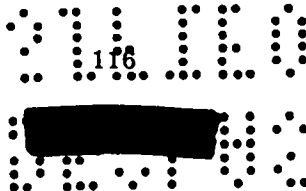


Fig. 2.5.1-1 Thermal radiation function vs time.



UNCLASSIFIED

SECRET

UNCLASSIFIED

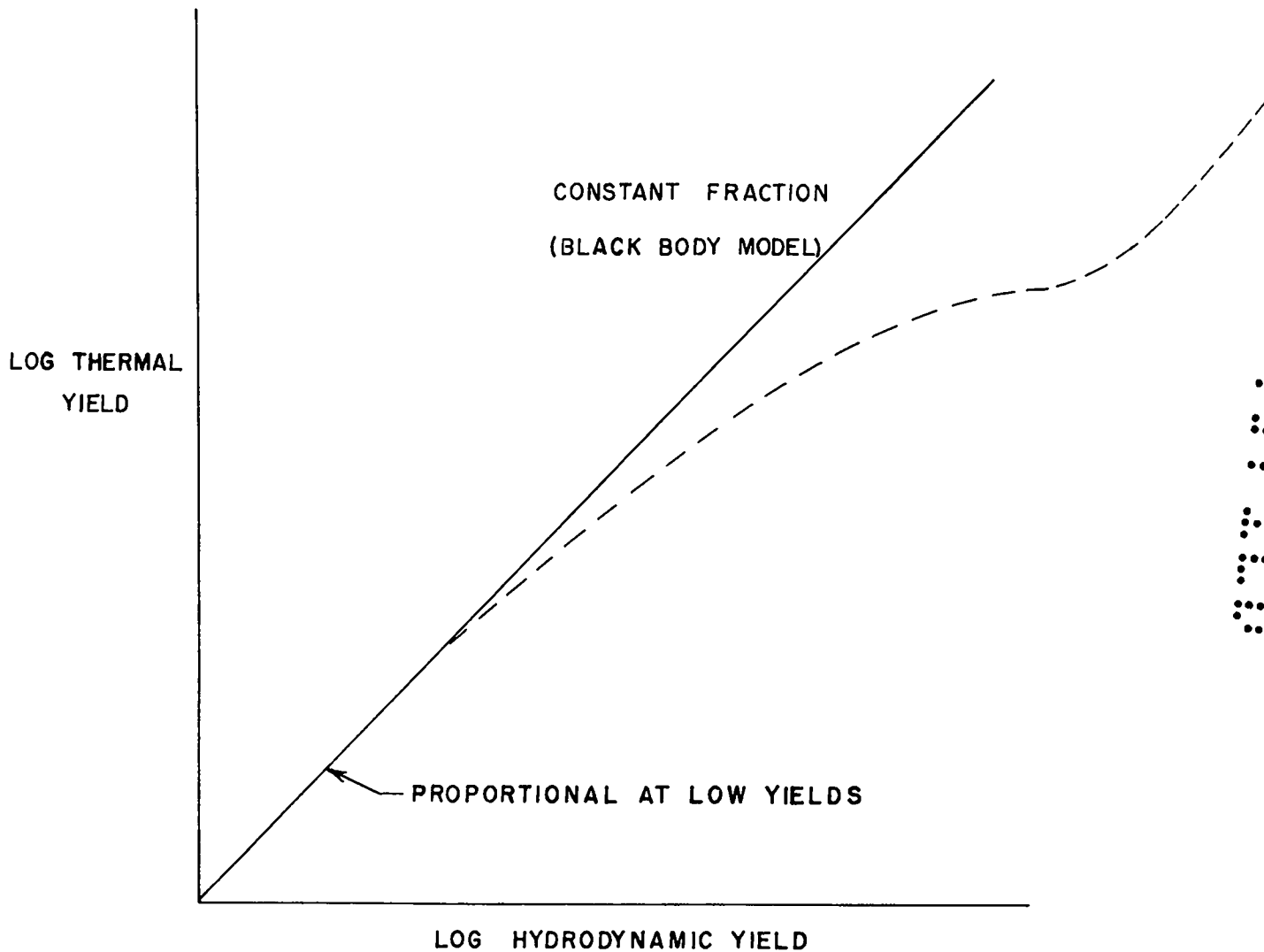


Fig. 2.5.3-1 Qualitative presentation of thermal yield vs total yield. This is of the form $T \sim W^n$ with $n = 1$ at low yields, $n < 1$ at higher yields, and $n = 1$ again at very high yields.

SECRET

UNCLASSIFIED

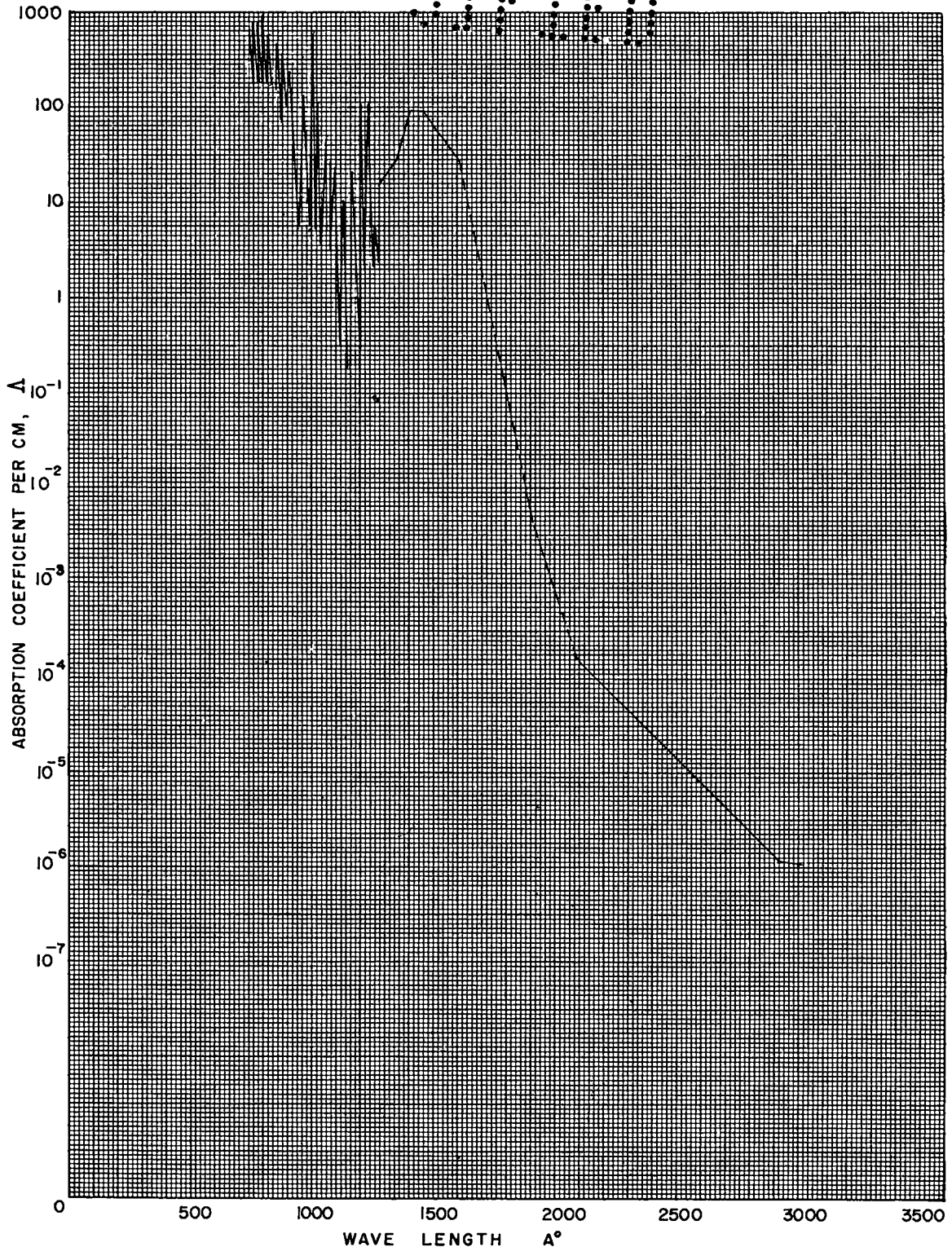


Fig. 2.5.3-2 Absorption coefficient of air vs wave length

148

UNCLASSIFIED



UNCLASSIFIED

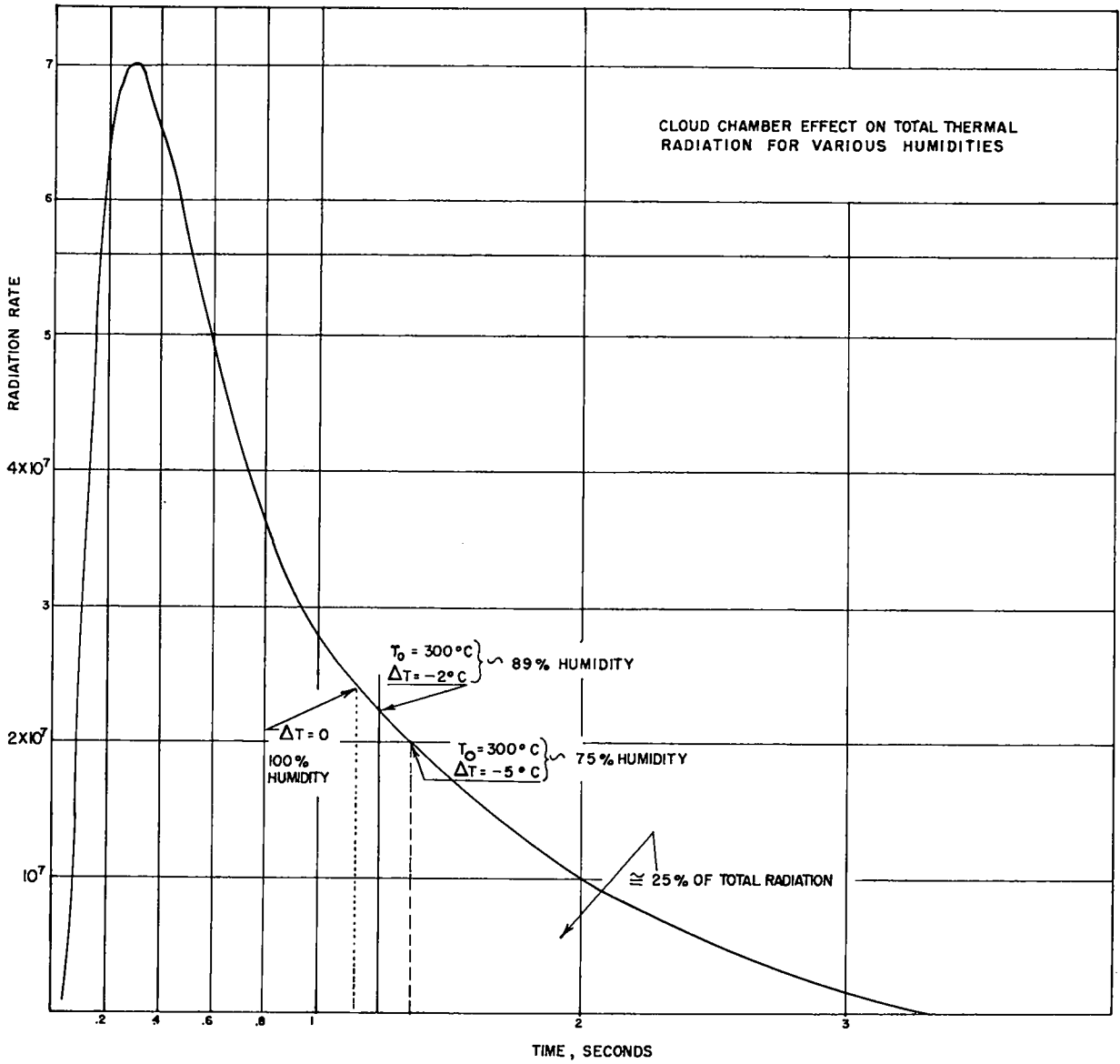
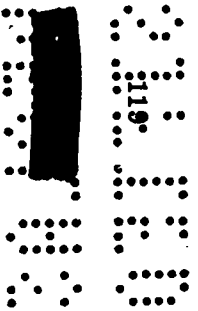
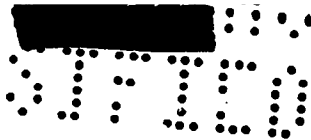


Fig. 2.5.4-1



UNCLASSIFIED



UNCLASSIFIED

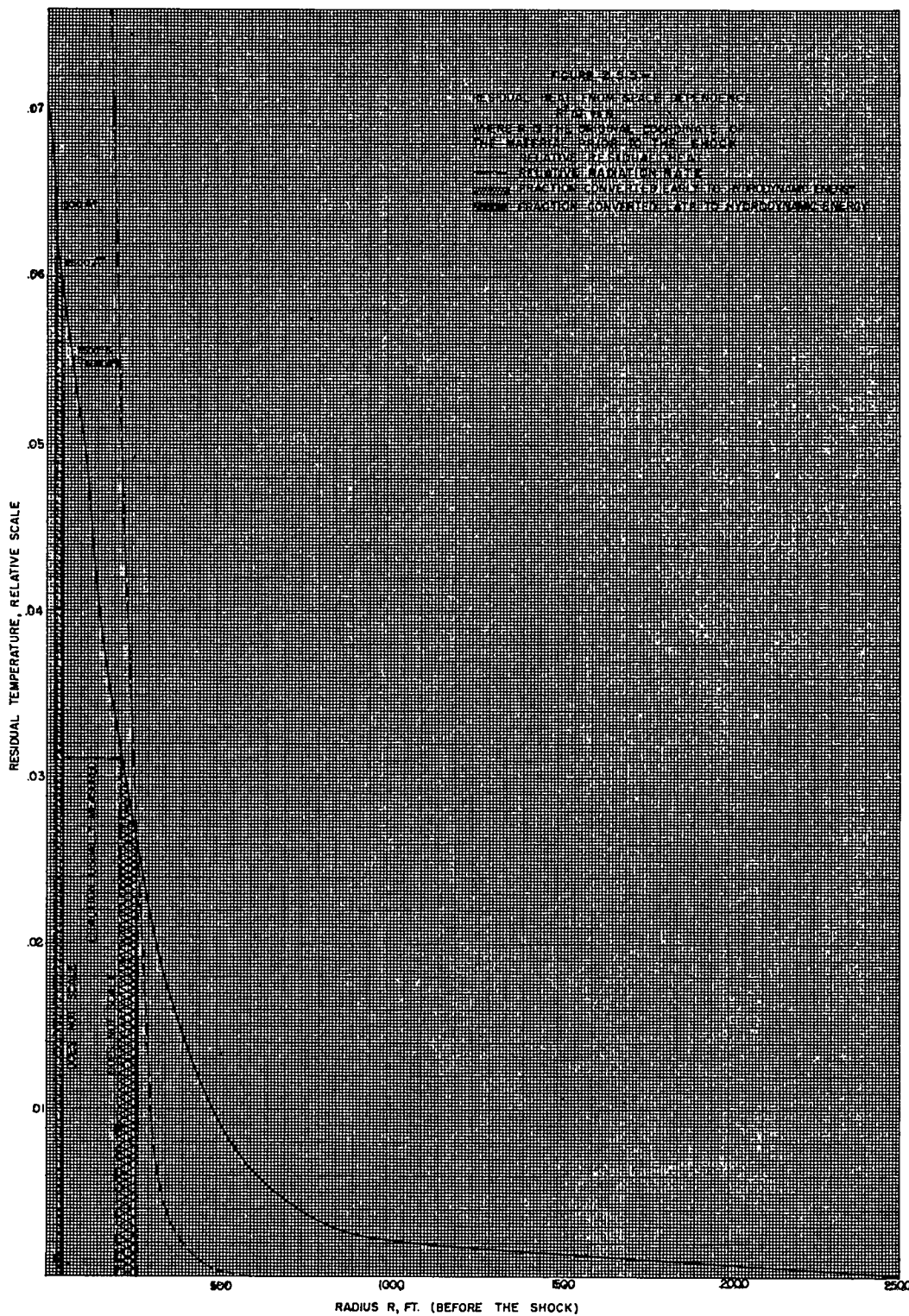
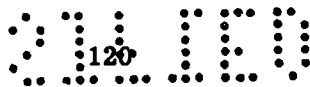


Fig. 2.5.5-1 Residual heat from space dependence $R^2 \Delta T$ vs R.



UNCLASSIFIED

[REDACTED]

UNCLASSIFIED

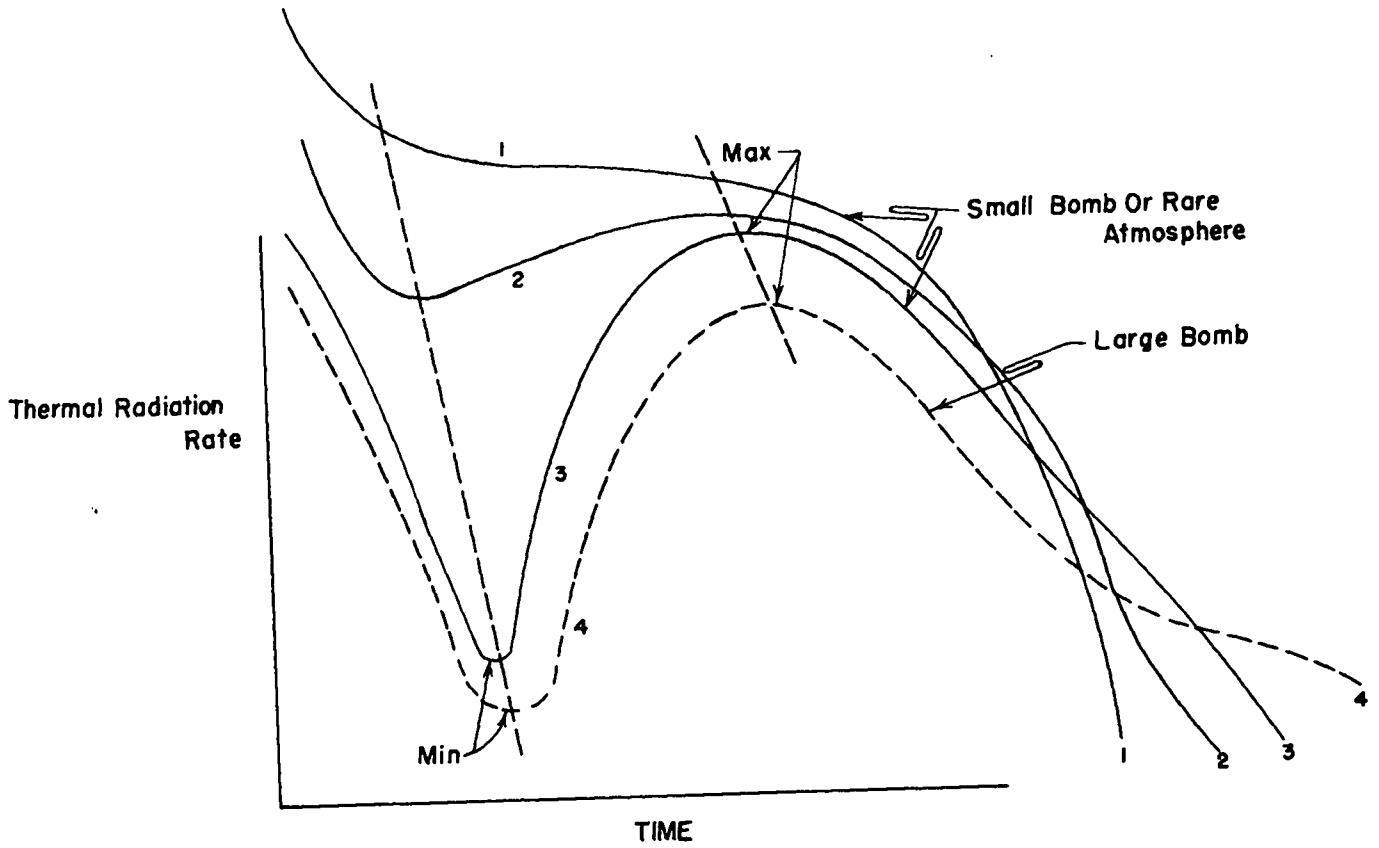


Fig. 2.5.5-2 Dependence of the thermal pulse shape on yield.

121
[REDACTED]

UNCLASSIFIED

[REDACTED]
SECRET

UNCLASSIFIED

Appendix A

SHOCK CONDITIONS FOR 1 KT IN FREE AIR

Ambient Conditions:

$$P_0 = 14.505 \text{ psi}$$

$$c_0 = 1138.45 \text{ ft/sec}$$

$$\rho_0 = 1.1613 \times 10^{-3} \text{ gm/cm}^3$$

Taken from IBM Problem M, the Energy of which was Deduced in Two Ways:

1. Direct evaluation of energy from the wave forms, using the equation of state in LADC-1133 (11.5 KT).

2. From evaluation with the analytic solution from the radius-time data (11.8 KT).

The value used to scale to 1 KT was 11.5 KT.

SECRET
122

UNCLASSIFIED

UNCLASSIFIED

UNCLASSIFIED

Time 30M	Time milliseconds	Radius feet	Pressure atmosphere	area Pressure PSI	Density gm/liter	$\eta = \rho/c_0$	Adiabatic Velocity ft/sec	V/c_0	Material Velocity ft/sec	u/c_0	Rayleigh pressure psi
0	5.139 148	116.1062	72.2481	1105.89	8.21156	7.24323	9055.0	7.9538	7804.9	6.8557	3456.3
1	5.249 906	117.1056	75.9495	1087.05	8.36913	7.20649	8981.2	7.8890	7235.0	6.7943	3377.6
2	5.360 463	118.0948	74.4525	1065.34	8.31937	7.16384	8895.2	7.8134	7653.7	6.7229	3287.3
3	5.471 420	119.0747	72.8955	1042.76	8.27019	7.12149	8804.8	7.7340	7568.4	6.6480	3195.5
4	5.582 178	120.0457	71.5100	1022.66	8.22392	7.08165	8723.4	7.6625	7491.7	6.5806	3113.5
5	5.692 936	121.0076	70.1664	1003.18	8.17990	7.04374	8643.8	7.5926	7416.7	6.5147	3035.1
6	5.803 693	121.9609	67.8463	969.525	8.10284	6.97739	8504.4	7.4702	7285.4	6.3994	2901.0
7	5.914 450	122.8885	65.4386	934.405	8.02003	6.90608	8357.0	7.3407	7146.9	6.2777	2763.2
8	6.025 208	123.8113	64.1941	916.555	7.97870	6.87049	8279.8	7.2729	7074.4	6.2141	2693.5
9	6.135 966	124.7271	63.5420	907.111	7.95465	6.84978	8238.9	7.2369	7036.0	6.1803	2656.3
10	6.246 723	125.6379	62.9695	898.793	7.93238	6.83060	8202.9	7.2053	7002.2	6.1506	2623.5
11	6.357 480	126.5436	62.1170	886.429	7.90431	6.80643	8189.2	7.1579	6951.6	6.1062	2576.6
12	6.468 238	127.4428	61.1160	871.910	7.86896	6.77599	8085.0	7.1018	6891.8	6.0537	2521.1
13	6.578 996	128.3342	59.0820	842.410	7.79605	6.71321	7953.4	6.9862	6768.8	5.9456	2409.4
14	6.689 753	129.2009	56.8060	809.399	7.71320	6.64187	7803.4	6.8544	6628.6	5.8225	2286.1
15	6.800 510	130.0616	55.5960	791.849	7.66839	6.60328	7722.3	6.7832	6552.9	5.7840	2221.2
16	6.911 268	130.9153	54.9590	782.611	7.64516	6.58328	7679.3	6.7454	6512.8	5.7208	2187.4
17	7.022 026	131.7681	54.5460	776.620	7.63059	6.57023	7651.2	6.7207	6486.6	5.6977	2165.7
18	7.132 783	132.6145	54.2026	771.640	7.61459	6.55635	7627.8	6.7002	6464.8	5.6786	2146.7
19	7.243 540	133.4568	53.5690	762.450	7.59317	6.53851	7584.4	6.6620	6424.4	5.6431	2113.9
20	7.354 298	134.2913	52.2210	742.899	7.54285	6.49519	7491.2	6.5820	6337.6	5.5669	2043.6
21	7.465 056	135.1110	50.7090	720.969	7.48115	6.44205	7385.1	6.4870	6238.8	5.4801	1964.2
22	7.575 813	135.9252	49.7190	706.611	7.44272	6.40902	7314.8	6.4252	6173.3	5.4225	1913.2
23	7.686 570	136.7336	49.2088	699.182	7.41802	6.38855	7278.1	6.3930	6139.2	5.3926	1886.2
24	7.797 328	137.5330	48.7025	691.955	7.40153	6.37349	7242.3	6.3615	6105.9	5.3633	1861.3
25	7.908 086	138.3391	48.3286	686.445	7.38459	6.35890	7214.7	6.3373	6080.3	5.3409	1841.6
26	8.018 843	139.1362	47.7809	678.501	7.36445	6.34156	7174.9	6.3023	6043.4	5.3084	1814.3
27	8.129 600	139.9286	46.8960	665.666	7.32866	6.31074	7110.1	6.2452	5983.1	5.2555	1769.7
28	8.240 358	140.7100	45.9231	651.556	7.28545	6.27353	7038.0	6.1821	5916.2	5.1967	1720.1
29	8.351 116	141.4864	45.1117	639.787	7.25360	6.24610	6977.3	6.1288	5859.9	5.1473	1680.1
30	8.461 873	142.2574	44.6430	632.989	7.22830	6.22432	6942.1	6.0979	5827.2	5.1185	1655.6
31	8.572 630	143.0237	44.0240	624.011	7.20633	6.20540	6895.1	6.0566	5783.6	5.0802	1626.0
32	8.683 388	143.7859	43.6190	618.137	7.18537	6.18735	6864.2	6.0294	5754.9	5.0550	1605.2
33	8.794 146	144.5438	43.0775	610.284	7.16321	6.16827	6822.6	5.9929	5716.4	5.0212	1578.9
34	8.904 903	145.2973	42.4290	600.878	7.13066	6.14024	6772.5	5.9489	5668.9	4.9800	1550.0
35	9.015 660	146.0424	41.5370	587.941	7.09364	6.10836	6702.9	5.8877	5605.5	4.9238	1503.5
36	9.126 418	146.7826	40.9665	579.666	7.06559	6.08021	6658.1	5.8484	5563.9	4.8873	1475.4
37	9.237 176	147.5179	40.4502	572.178	7.04313	6.06502	6617.1	5.8124	5525.9	4.8539	1450.8
38	9.347 933	148.2493	40.0269	566.038	7.02431	6.04851	6582.0	5.7815	5493.5	4.8254	1429.9
39	9.458 690	148.9767	39.6689	560.846	7.00548	6.03245	6554.7	5.7526	5468.0	4.8030	1412.9
40	9.569 448	149.7007	39.2716	555.084	6.98610	6.01576	6522.6	5.7294	5438.4	4.7770	1393.7
41	9.680 206	150.4211	38.8279	548.648	6.96557	5.99808	6486.7	5.6978	5405.1	4.7478	1372.7
42	9.790 963	151.1378	38.2809	540.715	6.93562	5.97229	6442.3	5.6588	5363.7	4.7114	1345.9
43	9.901 720	151.8466	37.5760	530.404	6.90223	5.94354	6383.7	5.6074	5309.8	4.6641	1312.7
44	10.012 478	152.5516	37.0547	522.930	6.87688	5.92171	6340.9	5.5698	5270.3	4.6294	1288.5
45	10.123 236	153.2523	36.6465	517.010	6.85618	5.90388	6306.9	5.5399	5238.7	4.6016	1269.2
46	10.233 993	153.9493	36.2817	511.719	6.83761	5.88789	6276.2	5.5129	5210.4	4.5767	1252.1
48	10.455 51	155.3301	35.5776	501.507	6.80077	5.85617	6216.7	5.4607	5155.3	4.5283	1219.2
50	10.677 02	156.7001	34.8165	490.468	6.76158	5.82242	6151.7	5.4036	5095.1	4.4755	1184.0
52	10.898 54	158.0554	34.0420	479.235	6.72127	5.78771	6082.7	5.3467	5033.3	4.4212	1148.6

123

Time IBH	Time Machinists	Latent ft	Pressure atmos-ft	Pressure psi	Density g/liter	$\gamma \frac{D}{R}$	Speed velocity ft/min	$\frac{V}{C}$	Relative velocity ft/min	$\frac{W}{C}$	Dynamic pressure psi
54	11.120 05	159.3964	33.1930	466.920	6.675 29	5.74812	6010.4	5.2795	4964.6	4.3608	1109.8
56	11.341 57	160.7180	32.3780	455.100	6.629 56	5.70874	5938.2	5.2160	4897.9	4.3023	1072.8
58	11.563 08	162.0277	31.7510	446.006	6.592 68	5.67698	5881.9	5.1666	4845.8	4.2565	1044.2
60	11.784 60	163.3251	31.0600	435.984	6.552 14	5.64207	5819.3	5.1116	4787.9	4.2056	1013.2
62	12.006 11	164.6049	30.3483	425.662	6.510 62	5.60632	5754.0	5.0642	4727.6	4.1527	981.56
64	12.227 63	165.8745	29.8074	417.817	6.476 85	5.57224	5705.8	5.0101	4681.3	4.1120	957.43
66	12.449 14	167.1331	29.3039	410.514	6.445 58	5.55031	5656.7	4.9688	4637.7	4.0737	935.14
68	12.670 66	168.3807	28.8393	400.875	6.405 06	5.51542	5593.9	4.9136	4579.7	4.0227	906.14
70	12.892 17	169.6103	27.9742	391.228	6.364 68	5.48065	5530.3	4.8577	4521.0	3.9712	877.52
72	13.113 69	170.8320	27.5470	385.032	6.334 82	5.45494	5489.0	4.8215	4482.7	3.9375	858.64
74	13.335 20	172.0530	27.0984	378.526	6.305 59	5.42977	5445.3	4.7831	4442.4	3.9021	839.38
76	13.556 72	173.2444	26.6413	371.896	6.27492	5.40336	5400.3	4.7436	4400.8	3.8656	819.74
78	13.778 23	174.4353	26.0259	362.971	6.232 15	5.36653	5339.3	4.6900	4344.4	3.8161	793.44
80	13.999 75	175.6077	25.4120	354.067	6.189 31	5.32964	5277.6	4.6358	4287.4	3.7660	767.43
82	14.221 26	176.7734	25.0190	348.367	6.161 72	5.30588	5237.6	4.6006	4250.5	3.7336	750.92
84	14.442 78	177.9307	24.7060	343.827	6.139 57	5.28681	5205.7	4.5726	4221.0	3.7077	737.87
86	14.664 29	179.0808	24.4150	339.606	6.117 58	5.26787	5175.7	4.5463	4193.2	3.6833	725.59
88	14.885 81	179.9904	23.8790	331.832	6.078 51	5.23423	5120.0	4.4973	4141.7	3.6380	703.33
90	15.107 32	181.3469	23.3200	323.725	6.037 44	5.19886	5061.3	4.4458	4087.4	3.5903	680.38
92	15.328 84	182.4658	23.0310	319.533	6.015 23	5.17974	5030.6	4.4188	4059.1	3.5655	668.54
94	15.550 35	183.5784	22.8410	316.777	5.99876	5.16556	5010.3	4.4010	4040.4	3.5490	660.56
96	15.771 87	184.6855	22.6240	313.630	5.98023	5.14960	4987.1	4.3806	4018.9	3.5301	651.52
98	15.993 38	185.7868	22.1220	306.349	5.941 37	5.11614	4932.9	4.3330	3968.8	3.4861	631.25
100	16.214 90	186.8686	21.6070	298.880	5.89972	5.08027	4876.6	4.2835	3916.6	3.4403	610.46
102	16.436 41	187.9472	21.3552	295.228	5.87910	5.06252	4848.6	4.2589	3891.3	3.4181	600.50
104	16.657 93	189.0200	21.1910	292.846	5.86446	5.05025	4830.6	4.2431	3874.1	3.4030	593.77
106	16.879 44	190.0879	21.0030	290.120	5.84920	5.03677	4809.7	4.2248	3854.7	3.3859	586.25
108	17.100 96	191.1506	20.7650	286.668	5.83011	5.02033	4783.1	4.2044	3830.2	3.3644	576.94
110	17.322 47	192.2071	20.3230	280.257	5.78998	4.98579	4733.2	4.1576	3784.0	3.3238	559.22
112	17.543 99	193.2443	19.8050	272.744	5.74446	4.94658	4673.9	4.1055	3729.1	3.2756	538.85
114	17.765 50	194.2770	19.5380	268.871	5.72041	4.92587	4643.1	4.0784	3700.6	3.2506	528.43
116	17.987 02	195.3043	19.3760	266.522	5.70748	4.91473	4624.4	4.0620	3683.2	3.2353	522.29
118	18.208 53	196.3280	19.2930	265.318	5.69795	4.90453	4614.7	4.0535	3674.2	3.2274	518.87
120	18.430 05	197.3486	19.1730	263.578	5.68679	4.89692	4600.4	4.0409	3661.2	3.2160	514.20

124

UNCLASSIFIED

Time FOM	Time Miles/hr.	Radius feet	Pressure atmosphere	Pressure P.S.I.	Density gm/liter	$\eta = \rho/c$	Shock Velocity ft/sec	v/c_0	Material Velocity ft/sec	u/c_0	Dynamic pressure psi
122	18.65156	198.3657	18.8480	258.864	5.65688	4.87116	4562.6	4.0077	3622.0	3.1815	500.58
124	18.81308	199.3677	18.4540	253.149	5.61938	4.83887	4515.8	3.9666	3592.5	3.1468	486.48
126	19.09459	200.3653	18.2100	249.610	5.59663	4.81928	4485.1	3.9397	3554.3	3.1021	476.93
128	19.31611	201.3578	18.0640	247.493	5.58237	4.80700	4469.0	3.9255	3539.2	3.1088	471.67
130	19.53762	202.3464	17.9270	246.129	5.57058	4.79685	4457.6	3.9155	3528.6	3.0995	467.86
132	19.75914	203.3319	17.7940	244.707	5.55849	4.78783	4449.0	3.8904	3502.0	3.0761	459.00
134	19.98065	204.3077	17.6780	243.994	5.55238	4.78034	4437.7	3.8629	3473.0	3.0506	449.30
136	20.20217	205.2798	17.5720	243.296	5.550457	4.77401	44374.8	3.8428	3451.7	3.0319	442.37
138	20.42368	206.2476	17.4670	242.483	5.54902	4.77269	44359.4	3.8292	3437.4	3.0194	437.59
140	20.64520	207.2113	17.3640	242.264	5.54725	4.77146	44340.3	3.8125	3419.7	3.0038	431.90
142	20.86671	208.1706	16.8520	229.914	5.45877	4.70057	4320.2	3.7998	3401.0	2.9874	425.91
144	21.08823	209.1256	16.6160	226.491	5.43247	4.67792	4290.6	3.7688	3373.5	2.9632	417.02
146	21.30974	210.0698	16.3390	222.474	5.40290	4.65246	4255.5	3.7380	3340.9	2.9346	406.78
148	21.53126	211.0105	16.1580	217.819	5.38311	4.63542	4232.5	3.7178	3319.5	2.9158	400.11
150	21.75277	211.9464	16.0160	217.789	5.36769	4.62214	4214.3	3.7018	3302.5	2.9009	394.90
152	21.97429	212.8796	15.8790	215.802	5.35384	4.61021	4196.7	3.6863	3286.1	2.8865	389.98
154	22.19580	213.8078	15.7710	214.226	5.33980	4.59812	4187.6	3.6783	3277.0	2.8785	386.81
156	22.41732	214.7326	15.6320	212.220	5.32437	4.58484	4164.7	3.6582	3256.4	2.8604	380.85
158	22.63883	215.6536	15.4180	209.116	5.30032	4.56413	4136.8	3.6337	3230.5	2.8376	373.11
160	22.86035	216.5651	15.1860	205.751	5.27288	4.54050	4106.3	3.6069	3202.1	2.8127	364.70
162	23.08186	217.4721	15.0130	203.242	5.25237	4.52254	4083.1	3.5888	3180.7	2.7939	358.44
164	23.30338	218.3749	14.8710	201.182	5.23651	4.50918	4064.6	3.5703	3163.2	2.7785	353.33
166	23.52489	219.2738	14.7570	199.529	5.22309	4.49762	4049.3	3.5569	3149.0	2.7660	349.35
168	23.74641	220.1693	14.6440	197.890	5.20996	4.48632	4034.2	3.5436	3134.9	2.7537	345.38
170	23.96792	221.0613	14.4910	195.671	5.19086	4.46987	4013.5	3.5254	3115.5	2.7366	339.86
172	24.18944	221.9466	14.3180	193.162	5.16868	4.45077	3990.1	3.5099	3093.7	2.7175	333.70
174	24.41095	222.8284	14.1800	191.160	5.15103	4.43057	3971.3	3.4883	3076.2	2.7021	328.80
176	24.63247	223.6888	14.0490	189.260	5.13645	4.42302	3953.3	3.4705	3059.4	2.6873	324.29
178	24.85398	224.5633	13.9520	187.853	5.12309	4.41151	3937.9	3.4608	3046.9	2.6764	320.83
180	25.07550	225.4344	13.8440	186.287	5.10956	4.39986	3925.1	3.4479	3033.0	2.6641	317.04
182	25.29701	226.3023	13.7320	184.662	5.09544	4.38770	3909.5	3.4341	3018.5	2.6514	313.16
184	25.51853	227.1667	13.6680	182.864	5.07939	4.37388	3892.0	3.4187	3002.5	2.6374	308.89
186	25.74004	228.0265	13.4760	180.949	5.06212	4.35901	3873.8	3.4027	2985.1	2.6221	304.28
188	25.96156	228.8825	13.3560	179.209	5.04540	4.34461	3857.0	3.3879	2969.4	2.6083	300.09
190	26.18307	229.7247	13.2270	177.328	5.02923	4.33064	3838.7	3.3719	2952.3	2.5933	295.69
192	26.40459	230.5834	13.1090	175.627	5.01382	4.31742	3821.9	3.3571	2936.6	2.5795	291.66
194	26.62610	231.4284	13.0220	174.475	4.99871	4.30441	3806.7	3.3438	2922.3	2.5669	287.95
196	26.84762	232.2699	12.8770	172.262	4.98198	4.29000	3788.8	3.3280	2905.6	2.5522	283.70
198	27.06913	233.1070	12.7530	170.463	4.96452	4.27497	3770.9	3.3123	2888.8	2.5375	279.46
200	27.29065	233.9404	12.6370	168.781	4.94844	4.26112	3754.1	3.2976	2873.1	2.5237	275.54
202	27.51216	234.7702	12.5310	167.293	4.93352	4.24827	3738.7	3.2840	2858.7	2.5110	271.95
204	27.73368	235.5969	12.4290	165.764	4.91951	4.23621	3723.8	3.2709	2844.7	2.4987	268.53
206	27.95519	236.4204	12.3410	164.488	4.90621	4.22476	3711.0	3.2597	2832.7	2.4882	265.55
208	28.17671	237.2410	12.2480	163.139	4.89318	4.21354	3697.3	3.2477	2819.8	2.4769	262.45
210	28.39822	238.0586	12.1400	161.572	4.87737	4.19992	3681.3	3.2336	2804.9	2.4638	258.84
212	28.61974	238.8717	12.0220	159.861	4.86602	4.18498	3663.8	3.2201	2788.4	2.4493	254.89
214	28.84125	239.6818	11.9210	158.376	4.84501	4.17206	3645.8	3.2051	2774.2	2.4368	251.52
216	29.06277	240.4887	11.8330	157.120	4.83151	4.16043	3635.6	3.1935	2761.8	2.4259	248.58
218	29.28428	241.2928	11.7490	155.901	4.81887	4.14955	3623.0	3.1824	2749.9	2.4155	245.81

125

UNCLASSIFIED

Time IBM	Time milliseconds	Radius feet	Pressure atmosphere	core pressure Psi	distance inches	$\rho = \rho/\rho_0$	bl. h. velocity ft/sec	v/c_0	material velocity ft/sec	u/c_0	Dynamic pressure psi
220	29.56586	242.0939	11.6700	154.756	4.89670	4.13907	3561.1	3.1719	2738.7	2.4056	243.18
222	29.72731	242.8924	11.5860	153.537	4.79440	4.12888	3598.4	3.1608	2726.7	2.3941	240.45
224	29.74883	243.6883	11.5050	152.362	4.78177	4.11760	3586.1	3.1500	2715.2	2.3850	237.79
226	30.17034	245.0619	11.4090	150.970	4.76685	4.10475	3571.5	3.1372	2701.4	2.3729	234.65
228	30.39186	245.2706	11.3080	149.505	4.75086	4.09278	3556.0	3.1235	2686.8	2.3601	231.35
230	30.61337	246.0569	11.2200	148.229	4.73443	4.07864	3559.9	3.1270	2674.0	2.3488	228.45
232	30.83489	246.8400	11.1315	146.945	4.72323	4.06719	3528.9	3.0997	2661.2	2.3376	225.64
234	31.05640	247.6206	11.0527	145.802	4.71058	4.05630	3516.6	3.0889	2649.7	2.3275	223.09
236	31.27792	248.3982	10.9771	144.706	4.69819	4.04563	3504.9	3.0787	2638.5	2.3176	220.62
240	31.72095	249.2459	10.8980	142.253	4.67824	4.02156	3478.4	3.0554	2613.5	2.2957	215.18
244	32.16398	251.4796	10.6374	139.779	4.64260	3.99776	3451.5	3.0318	2588.1	2.2734	209.77
248	32.60701	253.0047	10.5087	137.912	4.61915	3.97757	3431.1	3.0138	2568.7	2.2563	205.58
252	33.05004	254.5199	10.3743	135.963	4.59684	3.95836	3407.7	2.9950	2548.3	2.2384	201.36
256	33.49307	256.0264	10.2204	133.731	4.57470	3.93499	3384.9	2.9733	2524.8	2.2178	196.50
260	33.93610	257.5183	10.0601	131.406	4.55236	3.91144	3358.9	2.9504	2500.1	2.1961	191.52
264	34.37913	259.0030	9.9459	129.717	4.52131	3.89332	3340.2	2.9340	2482.3	2.1804	187.92
268	34.82216	260.4782	9.8375	128.177	4.50169	3.87642	3322.5	2.9184	2465.4	2.1656	184.57
272	35.26519	261.9463	9.7028	126.224	4.47704	3.85520	3300.3	2.8989	2444.2	2.1470	180.42
276	35.70822	263.4017	9.5658	124.237	4.45114	3.83289	3277.5	2.8789	2422.5	2.1279	176.20
280	36.15125	264.8501	9.4545	122.622	4.43008	3.81476	3258.9	2.8626	2404.7	2.1123	172.81
284	36.59428	266.2902	9.3518	121.133	4.40955	3.79708	3241.6	2.8474	2388.1	2.0977	169.64
288	37.03731	267.7220	9.2171	119.199	4.38474	3.77572	3218.8	2.8274	2366.2	2.0784	165.59
292	37.48034	269.1420	9.0885	117.314	4.35907	3.75361	3196.8	2.8080	2345.2	2.0600	161.72
296	37.92337	270.5544	8.9792	115.729	4.33726	3.73483	3178.0	2.7915	2327.2	2.0442	158.45
300	38.36640	271.9587	8.8770	114.246	4.31678	3.71720	3160.4	2.7761	2310.2	2.0292	155.40
304	38.80943	273.3552	8.7618	112.576	4.29316	3.69686	3140.4	2.7585	2290.9	2.0123	151.98
308	39.25246	274.7409	8.6468	110.908	4.26902	3.67607	3120.3	2.7408	2271.5	1.9953	148.59
312	39.69549	276.1197	8.5480	109.475	4.24871	3.65858	3102.9	2.7255	2254.8	1.9806	145.71

UNCLASSIFIED

UNCLASSIFIED

Time IBM	Time milliseconds	Radius feet	Pressure atmosphere	over pressure PSI	Density gm/lt	$\gamma = \rho/\rho_0$	Shock Velocity ft/sec	v/c_0	material Velocity ft/sec	u/c_0	Dynamic Pressure psi
316	40.13852	277.4912	8.46150	108.220	4.23014	3.64259	3087.6	2.7121	2239.9	1.9675	143.16
320	40.58155	278.8557	8.35720	106.707	4.20776	3.62332	3.0690	2.6958	2.220	1.9518	140.14
324	41.02458	280.2098	8.25150	105.174	4.18441	3.60321	3.0504	2.6792	2.2036	1.9356	137.06
328	41.46761	281.5572	8.16490	103.918	4.16225	3.58757	3.0345	2.6655	2.1885	1.9223	134.59
332	41.91062	282.8991	8.09420	102.890	4.14987	3.57347	3.0217	2.6542	2.1761	1.9115	132.56
336	42.35367	284.2349	8.01820	101.791	4.13347	3.55935	3.0079	2.6421	2.1627	1.8997	130.41
340	42.79670	285.5647	7.92540	100.445	4.11226	3.54408	2.9909	2.6272	2.1462	1.8852	127.77
344	43.23973	286.8845	7.83120	99.0784	4.08937	3.52137	2.9736	2.6120	2.1293	1.8703	125.06
348	43.68276	288.1985	7.74790	97.8702	4.07060	3.50521	2.9582	2.5984	2.1143	1.8572	122.75
352	44.12579	289.5065	7.67580	96.8245	4.05369	3.49065	2.9448	2.5867	2.1012	1.8457	120.73
356	44.56882	290.8083	7.59360	95.6323	4.03459	3.47403	2.9284	2.5731	2.0862	1.8325	118.44
360	45.01185	292.1017	7.51080	94.4313	4.01403	3.45450	2.9139	2.5595	2.0711	1.8192	116.14
364	45.45488	293.3896	7.43660	93.3552	3.99649	3.44139	2.8999	2.5472	2.0573	1.8071	114.10
368	45.89791	294.6717	7.36920	92.3776	3.97605	3.42724	2.8872	2.5361	2.0448	1.7961	112.25
372	46.34094	295.9480	7.30400	91.4320	3.96389	3.41332	2.8747	2.5251	2.0326	1.7854	110.77
376	46.78397	297.2188	7.22340	90.2629	3.94480	3.39697	2.8593	2.5116	2.0173	1.7720	108.29
380	47.22700	298.4818	7.14790	89.1679	3.92490	3.37975	2.8443	2.4987	2.0031	1.7595	106.23
384	47.67003	299.7389	7.07810	88.1555	3.90760	3.36485	2.8312	2.4869	1.9898	1.7478	104.36
388	48.11306	300.9908	7.01710	87.2708	3.89214	3.35154	2.8194	2.4765	1.9782	1.7376	102.74
392	48.55609	302.2375	6.95120	86.3150	3.87513	3.33689	2.8065	2.4652	1.9654	1.7264	100.97
396	48.99912	303.4772	6.88490	85.3534	3.85737	3.32160	2.7936	2.4539	1.9525	1.7151	99.199
400	49.44215	304.7123	6.82560	84.4195	3.84206	3.30841	2.7819	2.4436	1.9410	1.7049	97.633
404	49.88518	305.9427	6.77480	83.7565	3.82838	3.29643	2.7718	2.4347	1.9311	1.6963	96.306
408	50.32821	307.1685	6.72430	83.0241	3.81554	3.28558	2.7618	2.4259	1.9212	1.6876	95.002
412	50.77124	308.3903	6.66620	82.1814	3.79945	3.27172	2.7502	2.4157	1.9086	1.6774	93.461
416	51.21427	309.6047	6.59980	81.2184	3.78199	3.25669	2.7369	2.4041	1.8964	1.6658	91.749
420	51.65730	310.8151	6.54990	80.4946	3.76788	3.24454	2.7269	2.3953	1.8865	1.6571	90.455
424	52.10033	312.0212	6.50550	79.8507	3.75557	3.23394	2.7179	2.3874	1.8785	1.6492	89.301
428	52.54336	313.2235	6.46260	79.2285	3.74383	3.22383	2.7092	2.3797	1.8689	1.6416	88.204
432	52.98639	314.4220	6.40900	78.4511	3.72892	3.21099	2.6983	2.3702	1.8580	1.6320	86.828
436	53.42942	315.6141	6.35250	77.6316	3.71319	3.19744	2.6868	2.3601	1.8465	1.6219	85.595
440	53.87245	316.7987	6.29660	76.2407	3.69608	3.17410	2.6721	2.3427	1.8268	1.6046	82.972
444	54.31548	317.9873	6.24660	74.9034	3.67892	3.15100	2.6480	2.3260	1.8077	1.5879	80.663
448	54.75851	319.1799	6.19660	73.6097	3.66327	3.12862	2.6295	2.3097	1.7881	1.5715	78.444
452	55.20154	320.3749	6.14660	72.3827	3.64821	3.10704	2.6116	2.2940	1.7712	1.5558	76.354
456	55.64457	321.5712	6.09660	71.2184	3.63376	3.08628	2.5933	2.2779	1.7528	1.5396	74.247
460	56.08760	322.7692	6.04660	69.9156	3.61908	3.06632	2.5755	2.2623	1.7348	1.5239	72.214
464	56.53063	323.9687	6.00000	68.7582	3.60511	3.04720	2.5585	2.2474	1.7175	1.5086	70.294
468	56.97366	325.1697	5.95660	67.6646	3.59094	3.02977	2.5421	2.2329	1.7010	1.4941	68.490
472	57.41669	326.3720	5.91550	66.6316	3.57676	3.01296	2.5264	2.2192	1.6850	1.4801	66.779
476	57.85972	327.5760	5.87660	65.6470	3.56316	2.99614	2.5104	2.2051	1.6686	1.4657	65.043
480	58.30275	328.7817	5.83920	64.4346	3.54965	2.97938	2.4934	2.1902	1.6544	1.4506	63.266
484	58.74578	329.9892	5.80330	63.4309	3.53639	2.96267	2.4761	2.1767	1.6397	1.4368	61.659
488	59.18881	331.1987	5.76890	62.4795	3.52331	2.94601	2.4593	2.1639	1.6268	1.4237	60.161
492	59.63184	332.4102	5.73600	61.5904	3.51044	2.92940	2.4427	2.1518	1.6067	1.4113	58.762
496	60.07487	333.6237	5.70460	60.6694	3.49768	2.91284	2.4262	2.1392	1.5920	1.3984	57.320
500	60.51790	334.8392	5.67470	59.6643	3.48507	2.89633	2.4107	2.1254	1.5758	1.3842	55.784
504	60.96093	336.0567	5.64530	58.7926	3.47261	2.87987	2.3958	2.0711	1.5617	1.3718	54.449
508	61.40396	337.2762	5.61740	57.9760	3.46030	2.86346	2.3790	2.1020	1.5483	1.3600	53.204
512	61.84699	338.4977	5.59100	57.2262	3.44814	2.84716	2.3624	2.0915	1.5366	1.3497	52.109
516	62.28992	339.7212	5.56610	56.4067	3.43613	2.83091	2.3461	2.0799	1.5224	1.3373	50.864

Time IBM	Time milliseconds	Radius feet	Pressure atmosphere	ambient PSI	Density gm/liter	$\eta = \rho/a_0$	Shock Velocity ft/sec	v/c_0	Normal Velocity ft/sec	u/c_0	Dynamic Pressure psi
772	90.64394	403.9979	3.9689	43.6603	2.90079	2.49788	2142.2	1.8817	1284.6	1.1284	32.291
780	91.53000	405.8928	3.9395	42.6339	2.88844	2.48725	2134.6	1.8750	1276.4	1.1212	31.741
788	92.41666	407.7809	3.9076	42.1712	2.87515	2.47580	2126.3	1.8677	1267.5	1.1134	31.160
796	93.30212	409.6607	3.8746	41.6926	2.86119	2.46378	2117.7	1.8602	1258.1	1.1051	30.275
804	94.18518	411.5335	3.8440	41.2488	2.84807	2.45248	2109.7	1.8531	1249.5	1.0975	29.991
812	95.07424	413.3993	3.8145	40.8209	2.83562	2.44176	2102.0	1.8464	1241.2	1.0903	29.470
820	95.96030	415.2292	3.7867	40.4177	2.82376	2.43155	2094.6	1.8399	1233.2	1.0832	28.965
828	96.84636	417.1112	3.7600	40.0305	2.81234	2.42172	2087.5	1.8336	1225.5	1.0765	28.493
836	97.72342	418.9579	3.7320	39.6244	2.80027	2.41132	2080.0	1.8270	1217.4	1.0693	27.992
844	98.61148	420.7973	3.7036	39.2125	2.78770	2.40050	2072.5	1.8205	1209.1	1.0621	27.492
852	99.50454	422.6303	3.6762	38.8151	2.77577	2.39023	2065.1	1.8140	1201.1	1.0550	27.010
860	100.39906	424.4570	3.6502	38.4380	2.76440	2.38044	2058.2	1.8079	1193.5	1.0484	26.564
868	101.2967	426.2778	3.6254	38.0783	2.75352	2.37107	2051.4	1.8019	1186.2	1.0419	26.132
876	102.19228	428.0928	3.6011	37.7403	2.74299	2.36200	2045.2	1.7965	1179.3	1.0359	25.733
884	103.09088	429.9021	3.5777	37.3864	2.73189	2.35244	2038.5	1.7906	1172.0	1.0295	25.313
892	103.99348	431.7049	3.5558	37.0108	2.72037	2.34252	2031.5	1.7844	1164.2	1.0226	24.870
900	104.89209	433.5019	3.5325	36.6584	2.70939	2.33307	2024.8	1.7786	1156.9	1.0162	24.460
908	105.79070	435.2932	3.5083	36.3219	2.69894	2.32407	2018.5	1.7730	1150.0	1.0101	24.074
916	106.68930	437.0792	3.4842	36.0013	2.68894	2.31546	2012.4	1.7677	1143.3	1.0043	23.711
924	107.58791	438.8597	3.4613	35.6982	2.67926	2.30712	2006.7	1.7627	1136.9	0.9984	23.360
932	108.48651	440.6352	3.4407	35.3994	2.66984	2.29901	2001.0	1.7577	1130.6	0.9930	23.020
940	109.38512	442.4058	3.4191	35.0861	2.66056	2.29016	1994.9	1.7523	1123.9	0.9872	22.661
948	110.28373	444.1701	3.3979	34.7736	2.65137	2.28087	1988.3	1.7465	1116.5	0.9812	22.273
956	111.18234	445.9286	3.3766	34.4216	2.64243	2.26372	1976.4	1.7360	1103.3	0.9691	21.866
964	112.08095	447.6826	3.3544	34.0767	2.63366	2.24820	1965.6	1.7266	1091.4	0.9587	20.977
972	112.97956	449.4320	3.3320	33.7491	2.62507	2.23339	1954.5	1.7168	1078.9	0.9476	20.356
980	113.87817	451.1756	3.3092	33.4280	2.61664	2.21922	1943.7	1.7073	1066.8	0.9370	19.760
988	114.77678	452.9126	3.2862	33.1133	2.60836	2.20569	1933.8	1.6986	1055.6	0.9273	19.220
996	115.67539	454.6430	3.2630	32.8050	2.60023	2.19272	1923.8	1.6898	1044.3	0.9173	18.687
1004	116.57400	456.3669	3.2395	32.5031	2.59224	2.18030	1913.8	1.6811	1033.1	0.9074	18.167
1012	117.47261	458.0843	3.2157	32.2076	2.58291	2.16843	1904.5	1.6727	1022.5	0.8981	17.685
1020	118.37122	459.7952	3.1917	31.9185	2.57372	2.15710	1895.7	1.6652	1012.6	0.8894	17.240
1028	119.26983	461.5006	3.1675	31.6357	2.56467	2.14638	1886.2	1.6568	1001.7	0.8812	16.763
1036	120.16844	463.2015	3.1430	31.3592	2.55576	2.13620	1876.9	1.6486	991.05	0.8733	16.301
1044	121.06705	464.8979	3.1182	31.0890	2.54697	2.12655	1868.1	1.6409	981.04	0.8657	15.877
1052	121.96566	466.5898	3.0932	30.8251	2.53830	2.11744	1859.4	1.6333	971.03	0.8584	15.459
1060	122.86427	468.2772	3.0679	30.5675	2.52976	2.10887	1850.7	1.6256	961.01	0.8514	15.049
1068	123.76288	469.9601	3.0423	30.3162	2.52134	2.10084	1842.5	1.6184	951.58	0.8446	14.670
1076	124.66149	471.6385	3.0164	30.0711	2.51303	2.09334	1833.8	1.6118	942.82	0.8381	14.322
1084	125.56010	473.3124	2.9902	29.8322	2.50483	2.08637	1825.0	1.6048	933.58	0.8309	13.962
1092	126.45871	474.9818	2.9637	29.5995	2.49674	2.07992	1815.8	1.5976	924.04	0.8240	13.597
1100	127.35732	476.6467	2.9369	29.3730	2.48876	2.07399	1811.1	1.5908	915.28	0.8174	13.268
1108	128.25593	478.3071	2.9098	29.1527	2.48089	2.06857	1803.8	1.5844	906.52	0.8112	12.943
1116	129.15454	479.9630	2.8824	28.9386	2.47313	2.06368	1796.6	1.5781	898.15	0.8053	12.631
1124	130.05315	481.6144	2.8547	28.7306	2.46547	2.05932	1789.5	1.5719	889.77	0.7996	12.336
1132	130.95176	483.2613	2.8267	28.5287	2.45791	2.05550	1782.2	1.5661	882.07	0.7942	12.063
1140	131.85037	484.9037	2.7984	28.3328	2.45045	2.05212	1774.2	1.5602	874.17	0.7891	11.786
1148	132.74898	486.5416	2.7698	28.1430	2.44309	2.04918	1769.4	1.5542	865.61	0.7842	11.495
1156	133.64759	488.1750	2.7409	27.9592	2.43582	2.04667	1762.5	1.5482	858.00	0.7795	11.237
1164	134.54620	489.8039	2.7117	27.7815	2.42864	2.04450	1756.5	1.5424	850.88	0.7750	11.000
1172	135.44481	491.4283	2.6822	27.6099	2.42155	2.04276	1750.0	1.5366	843.00	0.7707	10.770
1180	136.34342	493.0482	2.6524	27.4444	2.41454	2.04145	1743.2	1.5308	835.00	0.7666	10.540
1188	137.24203	494.6636	2.6223	27.2849	2.40761	2.04057	1736.2	1.5250	827.00	0.7627	10.310
1196	138.14064	496.2745	2.5919	27.1314	2.40076	2.04012	1729.2	1.5192	819.00	0.7589	10.080
1204	139.03925	497.8809	2.5612	26.9839	2.39399	2.04012	1722.2	1.5134	811.00	0.7552	9.850
1212	140.93786	499.4828	2.5302	26.8424	2.38740	2.04057	1715.2	1.5076	803.00	0.7516	9.620
1220	141.83647	501.0802	2.5089	26.7069	2.38089	2.04145	1708.2	1.5018	795.00	0.7481	9.390
1228	142.73508	502.6731	2.4873	26.5774	2.37456	2.04276	1701.2	1.4960	787.00	0.7447	9.160
1236	143.63369	504.2615	2.4654	26.4539	2.36839	2.04450	1694.2	1.4902	779.00	0.7414	8.930
1244	144.53230	505.8454	2.4432	26.3364	2.36230	2.04667	1687.2	1.4844	771.00	0.7381	8.700
1252	145.43091	507.4248	2.4207	26.2249	2.35629	2.04918	1680.2	1.4786	763.00	0.7349	8.470
1260	146.32952	509.0002	2.3979	26.1194	2.35036	2.05212	1673.2	1.4728	755.00	0.7317	8.240
1268	147.22813	510.5716	2.3748	26.0199	2.34450	2.05550	1666.2	1.4670	747.00	0.7286	8.010
1276	148.12674	512.1390	2.3514	25.9264	2.33871	2.05932	1659.2	1.4612	739.00	0.7256	7.780
1284	149.02535	513.7024	2.3277	25.8389	2.33300	2.06368	1652.2	1.4554	731.00	0.7227	7.550
1292	149.92396	515.2618	2.3037	25.7574	2.32746	2.06857	1645.2	1.4496	723.00	0.7198	7.320
1300	150.82257	516.8172	2.2794	25.6819	2.32200	2.07399	1638.2	1.4438	715.00	0.7170	7.090
1308	151.72118	518.3686	2.2548	25.6124	2.31671	2.07992	1631.2	1.4380	707.00	0.7142	6.860
1316	152.61979	519.9160	2.2299	25.5489	2.31150	2.08637	1624.2	1.4322	699.00	0.7115	6.630
1324	153.51840	521.4594	2.2047	25.4914	2.30636	2.09334	1617.2	1.4264	691.00	0.7088	6.400
1332	154.41701	523.0008	2.1792	25.4399	2.30129	2.10084	1610.2	1.4206	683.00	0.7062	6.170
1340	155.31562	524.5392	2.1534	25.3944	2.29629	2.10887	1603.2	1.4148	675.00	0.7037	5.940
1348	156.21423	526.0746	2.1273	25.3549	2.29136	2.11744	1596.2	1.4090	667.00	0.7012	5.710
1356	157.11284	527.6070	2.1009	25.3214	2.28650	2.12655	1589.2	1.4032	659.00	0.6987	5.480
1364	158.01145	529.1364	2.0742	25.2939	2.28171	2.13620	1582.2	1.3974	651.00	0.6963	5.250
1372	158.91006	530.6628	2.0472	25.2724	2.27700	2.14638	1575.2	1.3916	643.00	0.6940	5.020
1380	159.80867	532.1862	2.0200	25.2569	2.27246	2.15710	1568.2	1.3858	635.00	0.6917	4.790
1388	160.70728	533.7066	1.9925	25.2464	2.26800	2.16843	1561.2	1.3800	627.00	0.6895	4.560
1396	161.60589	535.2230	1.9647	25.2409	2.26361	2.18030	1554.2	1.3742	619.00	0.6873	4.330
1404	162.50450	536.7364	1.9366	25.2404	2.25929	2.19272	1547.2	1.3684	611.00	0.6852	4.100
1412	163.40311	538.2468	1.9082	25.2449	2.25503	2.20569	1540.2	1.3626	603.00	0.6831	3.870
1420	164.30172	539.7542	1.8795	25.2544	2.25082	2.21922	1533.2	1.3568	595.00	0.6811	3.640
1428	165.20033	541.2586	1.8505	25.2689	2.24667	2.23339	1526.2	1.3510	587.00	0.6791	3.410
1436	166.09894	542.7590	1.8212	25.2884	2.24258	2.24820	1519.2	1.3452	579.00	0.6772	3.180
1444	167.09755	544.2554	1.7916	25.3129	2.23854	2.26372	1512.2	1.3394	571.00	0.6754	2.950
1452	168.										

Time 13m	Time Microsec	Radius feet	Pressure atmosphere	vac pressure PSI	Density gm/ltu	u - P/ρ	Shock Velocity ft/sec	u/c ₀	Material Velocity ft/sec	u/c ₀	Dynamic pressure psi
1396	159.7566	536.3091	2.5929	23.1031	2.24159	1.93024	1750.3	1.5374	843.46	.74088	10.759
1412	161.5287	539.4053	2.5782	22.8174	2.23052	1.92071	1744.0	1.5319	836.05	.73438	10.517
1428	163.3009	542.4905	2.5546	22.5476	2.22016	1.91179	1738.1	1.5267	829.02	.72820	10.292
1444	165.0730	545.5659	2.5331	22.2938	2.21040	1.90338	1732.6	1.5219	822.88	.72228	10.081
1460	166.8451	548.6314	2.5194	22.0371	2.20048	1.89484	1726.9	1.5169	815.54	.71636	9.8722
1476	168.6172	551.6862	2.5015	21.7775	2.19043	1.88619	1721.1	1.5118	806.61	.70852	9.6132
1492	170.3893	554.7313	2.4847	21.5338	2.18089	1.87797	1715.6	1.5070	802.06	.70452	9.4636
1508	172.1615	557.7669	2.4677	21.2872	2.17142	1.86882	1710.2	1.5022	795.52	.69877	9.2694
1524	173.9336	560.7927	2.4518	21.0566	2.16192	1.86164	1705.0	1.4976	789.26	.69328	9.0844
1540	175.7057	563.8094	2.4358	20.8246	2.15283	1.85381	1699.8	1.4931	782.91	.68770	8.9010
1556	177.4778	566.8174	2.4206	20.6041	2.14412	1.84621	1694.8	1.4887	776.84	.68237	8.7282
1572	179.2499	569.8167	2.4055	20.3851	2.13525	1.83867	1689.9	1.4844	770.87	.67712	8.5588
1588	181.0221	572.8067	2.3900	20.1603	2.12634	1.83100	1684.8	1.4799	764.71	.67171	8.3874
1604	182.7942	575.7884	2.3753	19.9471	2.11789	1.82372	1680.0	1.4757	758.74	.66647	8.2243
1620	184.5663	578.7615	2.3605	19.7469	2.10980	1.81676	1675.4	1.4716	753.25	.66165	8.0748
1636	186.3384	581.7266	2.3473	19.5410	2.10148	1.80959	1670.7	1.4675	747.48	.65658	7.9202
1652	188.1105	584.6827	2.3330	19.3336	2.09303	1.80232	1665.9	1.4633	741.60	.65141	7.7646
1668	189.8827	587.6309	2.3194	19.1363	2.08507	1.79546	1661.4	1.4594	736.12	.64660	7.6212
1684	191.6548	590.5713	2.3065	18.9492	2.07753	1.78897	1657.1	1.4556	730.72	.64185	7.4825
1700	193.4269	593.5041	2.2935	18.7607	2.06968	1.78221	1652.7	1.4517	725.43	.63721	7.3470
1716	195.1990	596.4286	2.2800	18.5644	2.06168	1.77532	1648.2	1.4478	719.85	.63231	7.2065
1732	196.9711	599.3457	2.2673	18.3807	2.05417	1.76855	1643.9	1.4440	714.55	.62765	7.0746
1748	198.7433	602.2556	2.2554	18.2081	2.04702	1.76270	1639.9	1.4405	709.54	.62325	6.9515
1764	200.5154	605.1583	2.2432	18.0311	2.03984	1.75651	1635.8	1.4369	704.44	.61877	6.8280
1780	202.2875	608.0534	2.2312	17.8624	2.03276	1.75042	1629.9	1.4327	700.40	.61522	6.7264
1812	205.8317	613.8674	2.2101	17.5510	2.01965	1.73913	1624.5	1.4269	690.39	.60643	6.4934
1844	209.3760	619.6164	2.1894	17.2515	2.00709	1.72831	1617.4	1.4207	681.62	.59873	6.2902
1876	212.9202	625.3370	2.1696	16.9636	1.99499	1.71789	1610.7	1.4148	673.06	.59121	6.0962
1908	216.4645	631.0337	2.1495	16.6721	1.98249	1.70713	1603.7	1.4087	664.39	.58359	5.9029
1940	220.0087	636.7041	2.1286	16.3870	1.96991	1.69820	1596.4	1.4023	653.25	.57556	5.7050
1972	223.5529	642.3572	2.1099	16.0978	1.95815	1.68617	1590.0	1.3966	647.06	.56837	5.5302
2004	227.0972	647.9753	2.0920	15.8351	1.94705	1.67661	1583.7	1.3911	639.17	.56144	5.3655
2036	230.6414	653.5783	2.0741	15.5760	1.93576	1.66889	1577.4	1.3856	631.08	.55433	5.2002
2068	234.1857	659.1604	2.0561	15.3175	1.92437	1.65708	1571.0	1.3799	622.97	.54723	5.0100
2100	237.7299	664.7174	2.0389	15.0680	1.91368	1.64788	1565.0	1.3747	615.29	.54046	4.8269
2132	241.2741	670.2547	2.0227	14.8359	1.90358	1.63918	1559.4	1.3698	608.07	.53412	4.7477
2164	244.8184	675.7738	2.0062	14.6024	1.89330	1.63034	1553.6	1.3647	600.66	.52761	4.6077
2196	248.3626	681.2694	1.9906	14.3675	1.88291	1.62138	1547.8	1.3596	593.24	.52109	4.4697
2228	251.9069	686.7450	1.9757	14.1427	1.87304	1.61288	1542.2	1.3546	586.02	.51475	4.3388
2260	255.4511	692.2019	1.9607	13.9309	1.86371	1.60485	1536.9	1.3500	579.28	.50853	4.2185
2292	259.9953	697.6406	1.9459	13.7191	1.85440	1.59683	1531.6	1.3453	572.45	.50253	4.0990

130

UNCLASSIFIED

UNCLASSIFIED

Time 50m	Time milliseconds	Radius feet	Pressure atmosphere	over pressure Psi	Density gm/liter	$\eta = \rho/c$	Shock Velocity ft/sec	V/c_0	Material Velocity ft/sec	u/c_0	Dynamic Pressure psi
2324	262.5396	703.0599	1.9318	13.5746	1.84509	1.58881	1526.5	1.3409	565.71	.49691	40198
2356	266.0838	708.4615	1.9182	13.3174	1.83485	1.58123	1521.6	1.3366	559.26	.4925	38743
2388	269.6281	713.8459	1.9055	13.1332	1.82790	1.57401	1517.0	1.3325	553.29	.48600	37745
2420	273.1723	719.2146	1.8931	12.9533	1.81991	1.56713	1512.5	1.3286	547.32	.48076	36775
2452	276.7165	724.5677	1.8806	12.7720	1.81181	1.56016	1507.9	1.3245	541.35	.47557	35816
2484	280.2608	729.9034	1.8684	12.5937	1.80359	1.55308	1503.3	1.3205	535.38	.47027	34871
2516	283.8050	735.2236	1.8565	12.4225	1.79579	1.54636	1508.3	1.3137	529.61	.46520	33976
2548	287.3493	740.5291	1.8453	12.2601	1.78840	1.54000	1497.8	1.3130	524.12	.46038	33138
2580	290.8935	745.8201	1.8341	12.0976	1.78095	1.53318	1490.7	1.3094	518.63	.45556	32312
2612	294.4377	751.0954	1.8229	11.9352	1.77341	1.52709	1486.5	1.3057	513.14	.45074	31499
2644	297.9820	756.3567	1.8121	11.7785	1.76623	1.52091	1482.4	1.3021	507.75	.44600	30715
2676	301.5262	761.6044	1.8019	11.6306	1.75942	1.51504	1478.6	1.2988	502.65	.44152	29986
2708	305.0705	766.8292	1.7916	11.4812	1.75242	1.50902	1474.7	1.2954	497.55	.43704	29263
2740	308.6147	772.0578	1.7810	11.3271	1.74524	1.50292	1470.8	1.2919	492.16	.43231	28518
2772	312.1589	777.2640	1.7710	11.1824	1.73865	1.49716	1467.0	1.2886	487.15	.42791	27833
2804	315.7032	782.4574	1.7617	11.0475	1.73230	1.49169	1463.5	1.2855	482.43	.42376	27196
2836	319.2474	787.6383	1.7527	10.9170	1.72627	1.48650	1460.0	1.2824	477.81	.41970	26585
2868	322.7917	792.8074	1.7437	10.7865	1.72014	1.48122	1456.6	1.2795	473.19	.41564	25980
2900	326.3359	797.9634	1.7345	10.6630	1.71392	1.47586	1453.2	1.2765	468.59	.41159	25384
2932	329.8801	803.1081	1.7259	10.5283	1.70799	1.47076	1449.8	1.2735	464.04	.40761	24810
2964	333.4244	808.2411	1.7176	10.4029	1.70236	1.46591	1446.7	1.2708	459.81	.40389	24279
2996	336.9686	813.3631	1.7097	10.2933	1.69676	1.46109	1443.6	1.2680	455.67	.40025	23764
3028	340.5129	818.4738	1.7022	10.1701	1.69115	1.45626	1440.4	1.2652	451.24	.39666	23227
3060	344.0571	823.5738	1.6955	10.0584	1.68575	1.45161	1437.4	1.2626	447.20	.39321	22741
3092	347.6013	828.6630	1.6860	9.95461	1.68056	1.44714	1434.5	1.2600	443.25	.38985	22272
3124	351.1456	833.7421	1.6788	9.84518	1.67556	1.44283	1431.8	1.2577	439.49	.38604	21831
3156	354.6898	838.8119	1.6715	9.73930	1.67043	1.43841	1428.9	1.2557	435.55	.38258	21376
3188	358.2341	843.8709	1.6637	9.62617	1.66519	1.43390	1425.8	1.2524	431.41	.37894	20905
3220	361.7783	848.9188	1.6567	9.52465	1.66021	1.42961	1423.1	1.2500	427.65	.37564	20481
3252	365.3225	853.9588	1.6498	9.42457	1.65567	1.42543	1420.5	1.2477	423.99	.37243	20087
3284	368.8668	858.9888	1.6433	9.33029	1.65089	1.42159	1417.9	1.2455	420.53	.36939	19694
3316	372.4110	864.0101	1.6366	9.23312	1.64631	1.41764	1415.2	1.2431	416.87	.36617	19298
3348	375.9553	869.0212	1.6301	9.13884	1.64169	1.41367	1412.7	1.2409	413.40	.36313	18926
3380	379.4995	874.0234	1.6236	9.04457	1.63725	1.40984	1410.2	1.2387	409.94	.36009	18560
3412	383.0437	879.0177	1.6172	8.95200	1.63296	1.40615	1407.9	1.2367	406.66	.35720	18215
3444	386.5880	884.0033	1.6115	8.86907	1.62862	1.40241	1405.4	1.2345	403.29	.35424	17867
3476	390.1322	889.9799	1.6052	8.79770	1.62422	1.39867	1402.9	1.2323	399.83	.35121	17516
3508	393.6765	893.9481	1.5992	8.72908	1.61998	1.39497	1400.6	1.2303	396.16	.34833	17184
3540	397.2207	898.9081	1.5935	8.66801	1.61583	1.39148	1398.3	1.2282	393.38	.34554	16868
3572	400.7649	903.8601	1.5880	8.52823	1.61200	1.38810	1396.2	1.2264	390.39	.34291	16572
3604	404.3092	908.8047	1.5823	8.44856	1.60796	1.38462	1393.9	1.2244	387.22	.34013	16264
3636	407.8534	913.7407	1.5765	8.36144	1.60382	1.38106	1391.6	1.2224	383.94	.33725	15947
3668	411.3977	918.6691	1.5709	8.28022	1.59940	1.37768	1389.3	1.2203	380.90	.33458	15658
3700	414.9419	923.5897	1.5657	8.20480	1.59614	1.37444	1387.3	1.2186	377.96	.33200	15380
3732	418.4861	928.5030	1.5605	8.12938	1.59250	1.37131	1385.2	1.2167	375.07	.32946	15111
3764	422.0304	933.4094	1.5552	8.05251	1.58888	1.36819	1383.0	1.2148	372.08	.32683	14838
3796	425.5746	938.3076	1.5505	7.97434	1.58530	1.36511	1381.1	1.2132	369.42	.32429	14592
3828	429.1189	943.1989	1.5455	7.91122	1.58178	1.36208	1379.2	1.2114	366.61	.32203	14341
3860	432.6631	948.0838	1.5407	7.84200	1.57839	1.35916	1377.1	1.2096	363.89	.31964	14098
3892	436.2073	952.9614	1.5359	7.77259	1.57500	1.35624	1375.3	1.2080	361.19	.31726	13857

181

UNCLASSIFIED

Time GMT	Time Milliseconds	Radius feet	Pressure atmosphere	open pressure Psi	Density g/liter	$\eta = \rho \cdot$ c.c.	Shock velocity ft./sec.	v/c_0	material velocity ft./sec.	w/c_0	Dynamic pressure psi
5012	560.2557	1120.000	1.40530	5.91755	1.48152	1.27574	1322.7	1.1618	285.92	.25115	.81697
5024	563.8000	1124.687	1.40540	5.87984	1.47953	1.27403	1321.7	1.1610	284.30	.24973	.80668
5076	567.3442	1129.369	1.40260	5.83923	1.47716	1.27238	1320.4	1.1598	282.63	.24826	.79618
5108	570.8885	1134.047	1.40220	5.80442	1.47576	1.27075	1319.4	1.1589	281.15	.24696	.78687
5140	574.4327	1138.721	1.39750	5.76526	1.47365	1.26857	1318.2	1.1580	279.85	.24549	.77742
5172	577.9769	1143.391	1.39440	5.72030	1.47136	1.26693	1317.0	1.1568	278.55	.24390	.76858
5204	581.5212	1148.057	1.39150	5.67824	1.46918	1.26522	1315.8	1.1558	277.29	.24225	.76037
5236	585.0654	1152.718	1.38860	5.63618	1.46712	1.26334	1314.5	1.1546	276.00	.24068	.75299
5268	588.6097	1157.375	1.38600	5.59847	1.46515	1.26165	1313.4	1.1537	274.80	.23927	.74632
5300	592.1539	1162.029	1.38320	5.55786	1.46318	1.25995	1312.2	1.1526	273.65	.23796	.74032
5332	595.6981	1166.677	1.38080	5.52305	1.46126	1.25830	1311.3	1.1518	272.64	.23683	.73512
5364	602.7566	1175.786	1.37620	5.45633	1.45777	1.25557	1309.3	1.1501	271.31	.23392	.69736
5460	609.8751	1185.240	1.37170	5.39106	1.45441	1.25240	1307.4	1.1484	269.49	.23195	.68114
5524	616.9636	1194.501	1.36730	5.32725	1.45120	1.24963	1305.5	1.1467	267.78	.22907	.66573
5588	624.0521	1203.749	1.36320	5.26778	1.44809	1.24696	1303.8	1.1452	266.22	.22682	.65132
5652	631.1406	1212.965	1.35910	5.20831	1.44490	1.24421	1302.0	1.1437	264.83	.22454	.63881
5716	638.2290	1222.207	1.35480	5.14695	1.44166	1.24142	1300.4	1.1423	263.58	.22213	.62899
5780	645.3175	1231.418	1.35060	5.08503	1.43858	1.23877	1298.5	1.1406	262.27	.21983	.60778
5844	652.4060	1240.617	1.34670	5.02547	1.43566	1.23625	1296.7	1.1390	261.00	.21766	.59463
5908	659.4945	1249.803	1.34300	4.97450	1.43284	1.23382	1295.2	1.1377	260.00	.21561	.58233
5972	666.5829	1258.978	1.33910	4.92124	1.43005	1.23142	1293.4	1.1361	259.02	.21347	.56972
6036	673.6714	1268.141	1.33570	4.86893	1.42725	1.22901	1292.0	1.1349	258.22	.21153	.55831
6100	680.7599	1277.294	1.33200	4.81826	1.42451	1.22665	1290.8	1.1330	257.44	.20944	.54829
6164	687.8484	1286.436	1.32840	4.76805	1.42185	1.22436	1289.5	1.1322	256.87	.20745	.53945
6228	694.9369	1295.568	1.32510	4.71919	1.41925	1.22215	1288.7	1.1309	256.25	.20569	.53244
6292	702.0253	1304.689	1.32170	4.66587	1.41670	1.21992	1288.0	1.1296	255.86	.20366	.51722
6356	709.1138	1313.799	1.31830	4.61656	1.41410	1.21769	1287.6	1.1284	255.66	.20173	.50310
6420	716.2023	1322.800	1.31490	4.56725	1.41157	1.21551	1287.1	1.1271	255.47	.19981	.49269
6484	723.2908	1331.791	1.31150	4.52228	1.40912	1.21340	1286.8	1.1259	255.46	.19804	.48316
6548	730.3793	1340.772	1.30820	4.47587	1.40676	1.21137	1286.4	1.1247	255.40	.19633	.47357
6612	737.4677	1350.743	1.30550	4.43091	1.40437	1.20931	1286.0	1.1235	255.38	.19446	.46428
6676	744.5562	1359.704	1.30230	4.38450	1.40192	1.20720	1285.7	1.1223	255.29	.19262	.45474
6740	751.6447	1368.657	1.29910	4.33809	1.39958	1.20518	1285.3	1.1211	255.22	.19080	.44544
6804	758.7332	1377.601	1.29620	4.29603	1.39732	1.20324	1285.0	1.1199	255.37	.18918	.43720
6868	765.8217	1386.532	1.29340	4.25541	1.39513	1.20135	1284.8	1.1189	255.49	.18753	.42893
6932	772.9101	1395.457	1.29050	4.21335	1.39293	1.19946	1284.6	1.1178	255.57	.18584	.42058
6996	779.9986	1404.373	1.28770	4.17274	1.39075	1.19758	1284.4	1.1165	255.75	.18424	.41272
7060	787.0871	1413.280	1.28490	4.13213	1.38861	1.19574	1284.1	1.1156	255.91	.18263	.40491
7124	794.1756	1422.179	1.28220	4.09297	1.38655	1.19396	1283.9	1.1146	256.13	.18106	.39739
7188	801.2641	1431.070	1.27960	4.05526	1.38455	1.19224	1283.8	1.1136	256.43	.17957	.39031
7252	808.3525	1440.953	1.27700	4.01755	1.38258	1.19046	1283.6	1.1126	256.70	.17805	.38316
7316	815.4410	1449.827	1.27440	3.97974	1.38037	1.18864	1283.4	1.1115	256.84	.17642	.37560
7380	822.5295	1458.693	1.27150	3.93778	1.37834	1.18689	1283.2	1.1105	257.06	.17485	.36840
7444	829.6180	1467.550	1.26900	3.90152	1.37637	1.18520	1283.1	1.1095	257.39	.17338	.36172
7508	836.7065	1476.400	1.26650	3.86526	1.37441	1.18357	1282.0	1.1086	257.74	.17194	.35524
7572	843.7949	1485.242	1.26420	3.83190	1.37267	1.18201	1281.1	1.1077	258.19	.17057	.34915
7636	850.8834	1494.077	1.26170	3.79564	1.37081	1.18041	1280.5	1.1066	258.55	.16913	.34281
7700	857.9719	1502.904	1.25930	3.76084	1.36894	1.17880	1280.8	1.1057	258.93	.16771	.33662
7764	865.0604	1511.723	1.25700	3.72748	1.36714	1.17725	1280.7	1.1047	259.36	.16633	.33067
7828	872.1489	1520.525	1.25470	3.69412	1.36537	1.17574	1280.6	1.1040	259.86	.16500	.32495

Time EOT	Time milliseconds	Radius feet	Pressure atmosphere	over pressure psi	Density g/cm ³	$\eta = \frac{P}{\rho}$ %	shock velocity ft/sec	v/c	material velocity ft/sec	w/c	Dynamic pressure psi
7892	879.2373	1529.741	1.25260	3.66366	1.36368	1.17427	1256.0	1.1033	186.42	.16375	.31968
7956	886.3258	1538.640	1.25030	3.63030	1.36191	1.17275	1254.8	1.1022	184.89	.16240	.31402
8020	893.4143	1547.531	1.24790	3.59849	1.36006	1.17115	1254.0	1.1015	183.24	.16096	.30806
8084	900.5028	1556.416	1.24530	3.56668	1.35829	1.16963	1252.6	1.1003	181.66	.15957	.30236
8148	907.5913	1565.293	1.24350	3.53468	1.35660	1.16817	1252.1	1.0996	180.27	.15825	.29729
8212	914.6797	1574.163	1.24130	3.49977	1.35497	1.16677	1250.9	1.0988	178.99	.15705	.29217
8276	921.7682	1583.028	1.23910	3.46786	1.35319	1.16524	1250.0	1.0980	177.32	.15576	.28702
8340	928.8567	1591.884	1.23660	3.43160	1.35132	1.16363	1248.8	1.0969	175.60	.15424	.28185
8404	935.9452	1600.732	1.23430	3.39524	1.34958	1.16213	1247.7	1.0960	174.05	.15288	.27676
8468	943.0337	1609.573	1.23220	3.35778	1.34793	1.16071	1246.8	1.0952	172.63	.15164	.27195
8532	950.1221	1618.408	1.23020	3.32177	1.34632	1.15935	1245.9	1.0944	171.26	.15043	.26736
8596	957.2106	1627.237	1.22830	3.31122	1.34486	1.15806	1245.2	1.0938	169.94	.14927	.26297
8660	964.2991	1636.060	1.22640	3.28366	1.34345	1.15685	1244.2	1.0929	168.67	.14816	.25882
8724	971.3876	1644.877	1.22460	3.25755	1.34207	1.15566	1243.3	1.0921	167.43	.14707	.25485
8788	978.4761	1653.687	1.22300	3.23235	1.34071	1.15449	1242.7	1.0916	166.32	.14609	.25116
8852	985.5645	1662.493	1.22130	3.20969	1.33940	1.15336	1241.9	1.0909	165.17	.14508	.24767
8916	992.6530	1671.294	1.21970	3.18648	1.33812	1.15226	1241.4	1.0904	164.04	.14409	.24438
8980	999.7415	1680.091	1.21810	3.16328	1.33681	1.15113	1240.5	1.0896	162.94	.14312	.24139
9044	1006.830	1688.882	1.21620	3.13572	1.33548	1.14999	1239.5	1.0888	161.66	.14200	.23842
9108	1013.918	1697.666	1.21460	3.11252	1.33419	1.14888	1238.9	1.0882	160.55	.14113	.23549
9172	1021.007	1706.445	1.21300	3.08931	1.33294	1.14780	1238.2	1.0876	159.64	.14023	.23285
9236	1028.095	1715.220	1.21140	3.06610	1.33172	1.14675	1237.4	1.0869	158.35	.13909	.22982
9300	1035.184	1723.989	1.20990	3.04295	1.33045	1.14566	1236.9	1.0865	157.29	.13816	.22702
9364	1042.272	1732.753	1.20820	3.01969	1.32914	1.14453	1236.2	1.0859	156.12	.13713	.22451
9428	1049.361	1741.513	1.20660	2.99649	1.32789	1.14345	1235.5	1.0852	154.99	.13614	.22216
9492	1056.449	1750.269	1.20500	2.97328	1.32667	1.14240	1234.6	1.0845	153.90	.13518	.21994
9556	1063.538	1759.019	1.20360	2.95297	1.32548	1.14138	1234.2	1.0841	152.89	.13430	.21781
9620	1070.626	1767.764	1.20200	2.92977	1.32431	1.14037	1233.4	1.0834	151.81	.13335	.21582
9684	1077.715	1776.505	1.20050	2.90801	1.32312	1.13934	1232.7	1.0828	150.76	.13243	.21386
9748	1084.803	1785.240	1.19900	2.88626	1.32195	1.13832	1232.0	1.0822	149.73	.13152	.21191
9812	1091.892	1793.971	1.19760	2.86578	1.32083	1.13737	1231.4	1.0816	148.73	.13064	.21008
9876	1098.980	1802.698	1.19620	2.84565	1.31974	1.13643	1230.8	1.0811	147.76	.12978	.20830
9940	1106.069	1811.421	1.19480	2.82534	1.31857	1.13543	1230.1	1.0805	146.78	.12893	.20652
10004	1113.157	1820.242	1.19320	2.80213	1.31737	1.13439	1229.4	1.0799	145.63	.12792	.20486

UNCLASSIFIED

UNCLASSIFIED

Time JEM	Time minutes	Radius feet	Measured alt. depth	Sea pressure Psi	Density g/cm ³	$n = \frac{p}{\rho}$	Horizontal velocity ft/sec	v/c	Material velocity ft/sec	$1/c$	Dynamics feet
10068	1120.246	1828.850	1.1917	2.78038	1.31622	1.13340	1228.7	1.07927	144.61	.12702	.18566
10132	1127.334	1837.557	1.1903	2.76007	1.31511	1.13245	1228.0	1.07866	143.64	.12617	.18303
10196	1134.423	1846.260	1.1890	2.74122	1.31406	1.13154	1227.6	1.07831	142.72	.12536	.18054
10260	1141.511	1854.959	1.1877	2.72236	1.31304	1.13066	1226.9	1.07769	141.79	.12455	.17807
10324	1148.600	1863.654	1.1863	2.70206	1.31199	1.12976	1226.2	1.07708	140.82	.12369	.17548
10388	1155.688	1872.343	1.1850	2.68320	1.31093	1.12885	1225.7	1.07664	139.90	.12289	.17308
10452	1162.777	1881.029	1.1837	2.66435	1.30990	1.12794	1225.2	1.07620	138.98	.12208	.17067
10516	1173.852	1894.595	1.1817	2.63534	1.30836	1.12663	1224.1	1.07523	137.58	.12085	.16705
10580	1184.928	1908.153	1.1797	2.60633	1.30685	1.12533	1223.1	1.07436	136.18	.11962	.16348
10644	1196.004	1921.694	1.1779	2.58023	1.30532	1.12402	1222.5	1.07383	134.89	.11849	.16022
10708	1207.080	1935.228	1.1761	2.55412	1.30388	1.12278	1221.7	1.07313	133.60	.11735	.15698
10772	1218.155	1948.755	1.1743	2.52801	1.30250	1.12159	1220.8	1.07233	132.34	.11625	.15389
10836	1229.231	1962.273	1.1726	2.50391	1.30112	1.12040	1220.2	1.07181	131.12	.11517	.15088
10900	1240.307	1975.781	1.1708	2.47725	1.29974	1.11921	1219.2	1.07130	129.85	.11406	.14783
10964	1251.383	1989.283	1.1692	2.45404	1.29841	1.11807	1218.6	1.07040	128.69	.11304	.14505
11028	1262.458	2002.777	1.1675	2.42939	1.29715	1.11693	1217.9	1.06979	127.48	.11198	.14220
11092	1273.534	2016.259	1.1658	2.40473	1.29578	1.11580	1216.9	1.06891	126.29	.11093	.13940
11156	1284.610	2029.787	1.1642	2.38152	1.29452	1.11472	1216.1	1.06821	125.14	.10992	.13674
11220	1295.686	2043.201	1.1627	2.35977	1.29330	1.11367	1215.5	1.06768	124.06	.10897	.13426
11284	1306.761	2056.640	1.1612	2.33801	1.29217	1.11269	1214.9	1.06715	122.99	.10803	.13184
11348	1317.837	2070.113	1.1600	2.32041	1.29110	1.11177	1214.5	1.06680	122.11	.10726	.12986
11412	1328.913	2083.559	1.1584	2.30030	1.29003	1.11085	1213.8	1.06619	121.11	.10638	.12763
11476	1339.989	2097.000	1.1574	2.28000	1.28896	1.10993	1212.9	1.06540	120.13	.10552	.12547
11540	1351.064	2110.431	1.1559	2.26114	1.28786	1.10898	1212.5	1.06504	119.19	.10469	.12340
11604	1362.140	2123.857	1.1545	2.24284	1.28679	1.10806	1211.8	1.06443	118.18	.10381	.12123
11668	1373.216	2137.276	1.1532	2.22498	1.28573	1.10715	1211.3	1.06399	117.22	.10296	.11916
11732	1384.292	2150.688	1.1519	2.20713	1.28466	1.10623	1210.7	1.06346	116.28	.10214	.11717
11796	1395.367	2164.094	1.1505	2.18822	1.28363	1.10534	1209.9	1.06276	115.30	.10128	.11511
11860	1406.443	2177.493	1.1493	2.16542	1.28263	1.10448	1209.5	1.06241	114.42	.10051	.11328
11924	1417.519	2190.884	1.1490	2.14656	1.28163	1.10362	1208.6	1.06162	113.49	.09968	.11135
11988	1428.595	2204.269	1.1467	2.12771	1.28061	1.10274	1208.0	1.06109	112.55	.09886	.10942
12052	1439.670	2217.646	1.1455	2.11030	1.27964	1.10190	1207.7	1.06083	111.67	.09808	.10764
12116	1450.746	2229.711	1.1443	2.09290	1.27865	1.10105	1207.2	1.06039	110.79	.09731	.10587
12180	1461.822	2244.385	1.1430	2.07404	1.27765	1.10019	1206.4	1.05969	109.87	.09650	.10403
12244	1472.898	2257.743	1.1418	2.05644	1.27670	1.09937	1205.9	1.05925	108.99	.09573	.10230
12308	1483.973	2271.096	1.1407	2.04068	1.27578	1.09858	1205.6	1.05898	108.18	.09502	.10071
12372	1495.049	2284.446	1.1395	2.02328	1.27491	1.09783	1204.9	1.05837	107.31	.09426	.09903
12436	1506.125	2297.789	1.1384	2.01023	1.27409	1.09712	1204.4	1.05793	106.66	.09368	.09777
12500	1517.201	2311.126	1.1375	1.99427	1.27326	1.09641	1203.8	1.05740	105.86	.09298	.09624
12564	1528.276	2324.457	1.1365	1.97977	1.27244	1.09570	1203.5	1.05714	105.13	.09234	.09486
12628	1539.352	2337.784	1.1355	1.96526	1.27161	1.09499	1203.1	1.05679	104.38	.09168	.09345
12692	1550.428	2351.106	1.1344	1.94931	1.27079	1.09428	1202.4	1.05617	103.61	.09101	.09202
12756	1561.504	2364.422	1.1334	1.93481	1.27000	1.09360	1202.0	1.05582	102.87	.09036	.09065
12820	1572.579	2377.732	1.1325	1.92175	1.26918	1.09290	1201.8	1.05565	102.19	.08972	.08940
12884	1583.655	2391.038	1.1314	1.90580	1.26835	1.09218	1201.2	1.05512	101.40	.08906	.08796
12948	1594.731	2404.340	1.1303	1.88985	1.26755	1.09149	1200.5	1.05450	100.61	.08837	.08654
13012	1605.807	2417.635	1.1293	1.87534	1.26673	1.09079	1200.0	1.05406	99.875	.08772	.08523
13076	1616.882	2430.923	1.1283	1.86084	1.26589	1.09006	1199.7	1.05380	99.134	.08707	.08396
13140	1627.958	2444.206	1.1273	1.84633	1.26507	1.08936	1199.4	1.05354	98.383	.08641	.08259
13204	1639.034	2457.488	1.1263	1.83183	1.26428	1.08868	1198.9	1.05310	97.661	.08578	.08133

135

UNCLASSIFIED

Time IBM	Time milliseconds	Radius feet	Pressure atmosphere	core pressure psi	Density gm/ltm	$n = \rho/\rho_0$	Shock Velocity ft/msec	v/c_0	Material Velocity ft/msec	u/c_0	Dynamic pressure psi
20752	2303.579	3247.835	1.08890	1.28929	1.23416	1.06274	1181.3	1.0376	69.751	.061268	.040502
20952	2325.730	3274.002	1.08900	1.29000	1.23344	1.06212	1180.1	1.0372	69.077	.060676	.039700
21152	2347.882	3300.187	1.08910	1.29050	1.23279	1.06156	1180.5	1.0369	68.384	.060068	.038888
21352	2370.033	3326.311	1.08920	1.29100	1.23216	1.06102	1180.1	1.0366	67.854	.059602	.038267
21552	2392.185	3352.454	1.08930	1.29150	1.23154	1.06048	1179.6	1.0361	67.267	.059086	.037588
21752	2414.336	3378.586	1.08940	1.29200	1.23092	1.05995	1179.6	1.0361	66.718	.058604	.036959
21952	2436.488	3404.711	1.089420	1.29222	1.23029	1.05941	1179.4	1.0360	66.170	.058123	.036336
22152	2458.639	3430.834	1.089330	1.29217	1.22965	1.05886	1178.5	1.0352	65.515	.057548	.035602
22352	2480.791	3456.946	1.089260	1.19801	1.22903	1.05832	1178.7	1.0354	64.956	.057057	.034980
22552	2502.942	3483.049	1.089180	1.18641	1.22843	1.05781	1178.0	1.0347	64.369	.056541	.034333
22752	2525.094	3509.148	1.089110	1.17626	1.22781	1.05727	1177.6	1.0344	63.830	.056067	.033743
22952	2547.245	3535.234	1.089030	1.16466	1.22716	1.05671	1177.6	1.0344	63.204	.055518	.033068
23152	2569.397	3561.316	1.089050	1.15305	1.22650	1.05619	1177.0	1.0329	62.598	.054985	.032420
23352	2591.548	3587.392	1.089070	1.14145	1.22588	1.05570	1176.4	1.0321	62.010	.054469	.031799
23552	2613.700	3613.453	1.089020	1.13020	1.22523	1.05522	1176.7	1.0336	61.597	.054106	.031363
23752	2635.851	3639.511	1.089040	1.12259	1.22488	1.05475	1176.7	1.0327	61.019	.053598	.030763
23952	2658.002	3665.522	1.089080	1.11389	1.22436	1.05430	1176.7	1.0327	60.547	.053184	.030277
24152	2680.154	3691.602	1.089100	1.10374	1.22380	1.05382	1176.1	1.0322	60.027	.052727	.029745
24352	2702.304	3717.635	1.089140	1.09359	1.22322	1.05335	1175.4	1.0319	59.478	.052245	.029190
24552	2724.455	3743.659	1.089170	1.08343	1.22269	1.05286	1174.4	1.0316	58.988	.051797	.028679
24752	2746.609	3769.674	1.089200	1.07328	1.22219	1.05243	1173.8	1.0311	58.429	.051323	.028145
24952	2768.760	3795.678	1.089250	1.06403	1.22170	1.05201	1173.7	1.0310	57.834	.050976	.027734
25152	2790.912	3821.674	1.089290	1.05573	1.22122	1.05160	1173.5	1.0308	57.582	.050579	.027313
25352	2813.063	3847.667	1.089230	1.04862	1.22075	1.05119	1173.0	1.0303	57.129	.050181	.026874
25552	2835.215	3873.653	1.089170	1.03992	1.22028	1.05076	1172.8	1.0302	56.667	.049776	.026432
25752	2857.366	3899.632	1.089110	1.03122	1.21972	1.05031	1172.8	1.0302	56.186	.049353	.025973
25952	2879.518	3925.609	1.089050	1.02252	1.21923	1.04988	1172.9	1.0303	55.714	.048938	.025528
26152	2901.669	3951.587	1.089090	1.01382	1.21874	1.04946	1172.8	1.0302	55.242	.048524	.025088
26352	2923.821	3977.566	1.089030	1.00511	1.21827	1.04906	1171.9	1.0294	54.819	.048152	.024695
26552	2945.972	4003.534	1.088980	.997861	1.21783	1.04868	1172.0	1.0295	54.414	.047797	.024323
26752	2968.124	4029.491	1.088920	.989159	1.21740	1.04831	1171.3	1.0289	53.972	.047408	.023921
26952	2990.275	4055.441	1.088970	.981907	1.21700	1.04796	1171.3	1.0289	53.577	.047061	.023564
27152	3012.427	4081.384	1.088930	.976106	1.21664	1.04765	1171.2	1.0288	53.269	.046791	.023287
27352	3034.578	4107.325	1.088900	.968854	1.21625	1.04732	1170.5	1.0282	52.893	.046461	.022953
27552	3056.720	4133.257	1.088840	.963052	1.21587	1.04699	1170.8	1.0284	52.566	.046173	.022662
27752	3078.881	4159.187	1.088800	.955800	1.21546	1.04664	1170.7	1.0283	52.181	.045835	.022324
27952	3101.033	4185.119	1.088830	.947848	1.21502	1.04626	1169.9	1.0276	51.738	.045446	.021939
28152	3123.184	4211.040	1.088880	.939846	1.21463	1.04592	1169.7	1.0274	51.353	.045108	.021607
28352	3145.336	4236.952	1.088940	.931845	1.21423	1.04558	1170.1	1.0278	51.016	.044812	.021317
28552	3167.487	4262.866	1.089000	.923842	1.21384	1.04526	1168.9	1.0267	50.592	.044439	.020957
28752	3189.639	4288.769	1.089030	.919541	1.21349	1.04494	1168.0	1.0268	50.265	.044152	.020681
28952	3211.790	4314.661	1.089000	.913739	1.21313	1.04463	1169.2	1.0270	49.947	.043873	.020444
29152	3233.942	4340.555	1.089050	.906488	1.21279	1.04434	1168.6	1.0265	49.572	.043543	.020103
29352	3256.093	4366.445	1.089120	.901846	1.21248	1.04408	1168.6	1.0265	49.312	.043315	.019888
29552	3278.244	4392.330	1.089180	.896915	1.21218	1.04381	1168.5	1.0264	49.052	.043087	.019674
29752	3300.396	4418.214	1.089240	.891552	1.21182	1.04350	1168.3	1.0262	48.753	.042824	.019429
29952	3322.548	4444.094	1.089300	.883717	1.21143	1.04317	1168.1	1.0260	48.349	.042469	.019102
30152	3344.700	4469.969	1.089370	.877045	1.21106	1.04285	1167.9	1.0259	47.993	.042156	.018816
30352	3366.851	4495.839	1.089440	.870808	1.21071	1.04255	1167.7	1.0257	47.656	.041860	.018547
30552	3389.002	4521.707	1.089500	.865007	1.21036	1.04225	1167.6	1.0256	47.348	.041590	.018303

187

UNCLASSIFIED

Time IBM	Time milliseconds	Radius feet	Pressure atmosphere	air pressure psi	density gm/liter	$\eta = \rho/c_0$	Shock Velocity ft/sec	v/c_0	Material Velocity ft/sec	u/c_0	Dynamic pressure psi
30752	3411.154	4547.570	1.05923	.859060	1.21004	1.04197	1167.5	1.0255	47.021	.041303	.018047
30952	3433.305	4573.430	1.05883	.853259	1.20971	1.04169	1167.3	1.0253	46.712	.041031	.017805
31152	3455.457	4599.288	1.05843	.847457	1.20942	1.04144	1167.1	1.0252	46.404	.040761	.017567
31352	3477.608	4625.141	1.05815	.843396	1.20916	1.04121	1166.9	1.0250	46.183	.040567	.017397
31552	3499.760	4650.991	1.05781	.838465	1.20888	1.04097	1166.8	1.0249	45.923	.040338	.017197
31752	3521.911	4676.836	1.05747	.833533	1.20860	1.04073	1166.6	1.0247	45.663	.040110	.016999
31952	3544.063	4702.678	1.05713	.828602	1.20827	1.04045	1166.4	1.0246	45.393	.039873	.016794
32152	3566.214	4728.516	1.05663	.821350	1.20791	1.04014	1166.1	1.0243	45.008	.039534	.016505
32352	3589.366	4754.348	1.05620	.815114	1.20758	1.03985	1165.9	1.0241	44.681	.039247	.016262
32552	3610.517	4780.175	1.05580	.809312	1.20725	1.03957	1165.7	1.0239	44.363	.038968	.016027
32752	3632.669	4805.998	1.05539	.803365	1.20694	1.03930	1165.6	1.0238	44.046	.038689	.015794
32952	3654.820	4831.817	1.05503	.798144	1.20663	1.03903	1165.3	1.0236	43.766	.038443	.015590
33152	3676.972	4857.631	1.05466	.792778	1.20632	1.03877	1165.1	1.0234	43.487	.038198	.015388
33352	3699.123	4883.441	1.05429	.787411	1.20602	1.03851	1164.9	1.0232	43.198	.037945	.015181
33552	3721.275	4909.246	1.05392	.782045	1.20572	1.03825	1164.7	1.0231	42.900	.037683	.014968
33752	3743.426	4935.047	1.05357	.776969	1.20543	1.03800	1164.6	1.0230	42.630	.037446	.014777
33952	3765.578	4960.843	1.05323	.772037	1.20515	1.03776	1164.4	1.0228	42.370	.037217	.014593
34152	3787.729	4986.636	1.05288	.766961	1.20487	1.03752	1164.2	1.0226	42.101	.036981	.014406
34352	3809.881	5012.428	1.05252	.761740	1.20458	1.03727	1164.0	1.0224	41.822	.036736	.014212
34552	3832.032	5038.213	1.05219	.756953	1.20430	1.03703	1163.9	1.0224	41.562	.036508	.014033
34752	3854.184	5063.994	1.05184	.751877	1.20404	1.03680	1163.6	1.0221	41.292	.036270	.013847
34952	3876.335	5089.770	1.05151	.747091	1.20376	1.03656	1163.5	1.0220	41.032	.036042	.013671
35152	3898.487	5115.542	1.05118	.742304	1.20349	1.03633	1163.4	1.0219	40.772	.035814	.013495
35352	3920.638	5141.312	1.05087	.737808	1.20323	1.03611	1163.2	1.0217	40.532	.035603	.013334
35552	3942.790	5167.080	1.05055	.733167	1.20297	1.03588	1163.0	1.0216	40.291	.035391	.013173
35752	3964.941	5192.842	1.05023	.728526	1.20271	1.03566	1162.9	1.0215	40.041	.035171	.013007
35952	3987.093	5218.601	1.04992	.724030	1.20246	1.03544	1162.6	1.0212	39.800	.034960	.012848
36152	4009.244	5244.356	1.04962	.719679	1.20221	1.03523	1162.5	1.0211	39.559	.034748	.012690
36352	4031.396	5270.108	1.04930	.715037	1.20196	1.03501	1162.4	1.0210	39.280	.034503	.012509
36552	4053.547	5295.857	1.04901	.710831	1.20171	1.03480	1162.2	1.0209	39.088	.034334	.012385
36952	4097.850	5347.341	1.04840	.701984	1.20123	1.03438	1161.9	1.0206	38.606	.033911	.012076
37352	4142.153	5398.810	1.04782	.693572	1.20076	1.03398	1161.6	1.0203	38.154	.033514	.011791
37752	4186.456	5450.266	1.04726	.685450	1.20030	1.03358	1161.3	1.0201	37.720	.033133	.011520
38152	4230.759	5501.710	1.04671	.677472	1.19986	1.03320	1161.0	1.0198	37.287	.032752	.011252

UNCLASSIFIED

UNCLASSIFIED

Time IBM	Time milliseconds	Radius feet	Pressure atmosphere	ambient psi	Density gm/liter	$\eta = \%$	Shock Velocity ft/sec	ν/c_0	Material Velocity ft/sec	μ/c_0	Dynamic Pressure psi
38352	4275.062	5553.141	1.04618	.669785	1.19941	1.03282	1160.7	1.0195	36.873	.032389	.01100
38952	4319.365	5604.557	1.04566	.662244	1.19898	1.03245	1160.4	1.0193	36.469	.032024	.010757
39352	4363.668	5655.962	1.04515	.654847	1.19857	1.03209	1160.2	1.0191	36.074	.031687	.010520
39752	4407.971	5707.354	1.04463	.647305	1.19816	1.03174	1159.8	1.0188	35.670	.031332	.010283
40152	4452.274	5758.755	1.04416	.640488	1.19775	1.03139	1159.4	1.0184	35.294	.030922	.010064
40552	4496.577	5810.103	1.04365	.633091	1.19734	1.03103	1159.1	1.0181	34.900	.030556	.0098374
40952	4540.880	5861.460	1.04317	.626129	1.19694	1.03069	1158.8	1.0179	34.524	.030225	.0096230
41352	4585.183	5912.808	1.04268	.619022	1.19656	1.03036	1158.6	1.0177	34.189	.029987	.0094067
41752	4629.486	5964.143	1.04223	.612495	1.19619	1.03004	1158.4	1.0175	33.783	.029785	.0092091
42152	4673.789	6015.467	1.04178	.605969	1.19581	1.02972	1158.2	1.0173	33.427	.0296362	.0090131
42552	4718.092	6066.781	1.04135	.599732	1.19545	1.02941	1157.9	1.0171	33.090	.0295066	.0088295
42952	4762.395	6118.088	1.0409	.593205	1.19511	1.02911	1157.8	1.0170	32.743	.0294761	.0086428
43352	4806.698	6169.385	1.0405	.587404	1.19477	1.02882	1157.6	1.0168	32.435	.0294490	.0084782
43752	4851.001	6220.674	1.0401	.581602	1.19443	1.02853	1157.4	1.0166	32.098	.0294194	.0083306
44152	4895.304	6271.954	1.0397	.575801	1.19411	1.02825	1157.2	1.0165	31.790	.0293824	.0081802
44552	4939.607	6323.226	1.0393	.570999	1.19377	1.02796	1156.9	1.0162	31.491	.0293661	.0079853
44952	4983.910	6374.488	1.0389	.564998	1.19346	1.02769	1156.7	1.0160	31.164	.029374	.0078115
45352	5028.213	6425.739	1.0385	.558396	1.19314	1.02742	1156.5	1.0159	30.875	.0293720	.0076719
45752	5072.516	6476.980	1.0382	.552405	1.19285	1.02717	1156.2	1.0156	30.577	.0293858	.0075226
46152	5116.819	6528.212	1.0378	.548244	1.19257	1.02693	1156.1	1.0155	30.307	.029421	.0073885
46552	5161.122	6579.432	1.0375	.543893	1.19227	1.02667	1155.9	1.0153	30.057	.029448	.0072658
46952	5205.425	6630.643	1.0371	.538091	1.19197	1.02641	1155.7	1.0152	29.768	.0294770	.0071249
47352	5249.728	6681.844	1.0367	.532289	1.19165	1.02616	1155.5	1.0150	29.460	.029544	.0068714
47752	5294.031	6733.046	1.0364	.527938	1.19139	1.02591	1155.3	1.0148	29.190	.0296671	.0066474
48152	5338.334	6784.236	1.0361	.523587	1.19112	1.02568	1155.1	1.0146	28.931	.0298413	.0063852
48552	5382.637	6835.418	1.0357	.517786	1.19084	1.02544	1155.0	1.0145	28.691	.029985	.0061660
48952	5426.940	6886.589	1.0354	.513435	1.19056	1.02520	1154.8	1.0144	28.420	.029964	.0059850
49352	5471.243	6937.754	1.0351	.509053	1.19027	1.02495	1154.6	1.0142	28.131	.029970	.0058357
49752	5515.546	6988.912	1.0345	.500381	1.18998	1.02470	1154.3	1.0139	27.869	.0299201	.0056671
50152	5559.849	7040.061	1.0343	.497480	1.18971	1.02446	1154.2	1.0138	27.544	.0299194	.0056082
50552	5604.152	7091.199	1.0340	.493129	1.18945	1.02424	1154.0	1.0137	27.323	.0299272	.0055989
50952	5648.455	7142.330	1.0337	.488778	1.18921	1.02403	1153.9	1.0136	27.063	.0299386	.0055875
51352	5692.758	7193.453	1.0334	.484427	1.18896	1.02382	1153.7	1.0134	26.851	.0299486	.0055782
51752	5737.061	7244.571	1.0331	.480076	1.18874	1.02363	1153.6	1.0133	26.620	.0299583	.0055692
52152	5781.364	7295.682	1.0329	.477175	1.18851	1.02345	1153.4	1.0131	26.408	.0299686	.0055596
52552	5825.667	7346.784	1.0326	.472824	1.18828	1.02323	1153.3	1.0131	26.187	.0299702	.0055465
52952	5869.970	7397.891	1.0323	.468473	1.18804	1.02303	1153.2	1.0131	25.975	.0299716	.0055309
53352	5914.273	7448.981	1.0320	.464122	1.18782	1.02284	1152.8	1.0126	25.724	.0299725	.0055169
53752	5958.576	7500.073	1.0318	.460211	1.18760	1.02265	1152.7	1.0128	25.542	.0299736	.0055263
54152	6002.879	7551.151	1.0315	.456870	1.18738	1.02246	1152.6	1.0128	25.330	.0299750	.0055139
54552	6047.182	7602.226	1.0313	.453969	1.18719	1.02229	1152.2	1.0125	25.128	.0299782	.0055056
54952	6091.485	7653.293	1.0310	.449618	1.18696	1.02210	1152.1	1.0124	24.926	.0299895	.0054974
55352	6135.788	7704.351	1.0308	.446717	1.18677	1.02193	1152.1	1.0123	24.733	.0299925	.0054869
55752	6180.091	7755.405	1.0305	.442366	1.18657	1.02176	1152.2	1.0121	24.540	.0299956	.0054820
56152	6224.394	7806.452	1.0303	.439465	1.18638	1.02160	1152.2	1.0121	24.357	.0299975	.0054749
56552	6268.697	7857.493	1.0300	.435114	1.18619	1.02143	1152.0	1.0119	24.165	.0299926	.0054672
56952	6312.900	7908.530	1.0298	.432213	1.18599	1.02126	1151.9	1.0118	23.992	.0299974	.0054604
57352	6357.203	7959.561	1.0296	.429312	1.18580	1.02110	1151.7	1.0116	23.809	.0299914	.0054534
57752	6401.506	8010.584	1.0293	.424961	1.18561	1.02093	1151.8	1.0117	23.607	.0299936	.0054456
58152	6445.809	8061.604	1.0291	.422061	1.18542	1.02077	1151.6	1.0116	23.424	.0299975	.0054382

139

UNCLASSIFIED

14-00000-1

